

EUMETSAT Satellite Application Facility on Climate Monitoring

The EUMETSAT
Network of
Satellite
Application
Facilities



CM SAF

Climate Monitoring

Scientific Validation Report

Top of Atmosphere Radiation

MVIRI/SEVIRI Data Record

CM-Product identifier: CM-23311, CM-23341

Reference Number:

SAF/CM/RMIB/VAL/MET_TOA

Version:

1.1

Date:

5 October 2016

	Scientific Validation Report TOA Radiation MVIRI/SEVIRI Data Record	Doc.No.: SAF/CM/RMIB/VAL/MET_TOA
		Issue: 1.1
		Date: 05 October 2016

Document Signature Table

	Name	Function	Signature	Date
Author	Manon Urbain Nicolas Clerbaux Alessandro Ipe Florian Tornow	CM SAF Scientists		05.10.2016
Editor				
Approval	Rainer Hollmann	Science Manager		
Release	Martin Werscheck	Project Manager		

Distribution List

Internal Distribution	
Name	No. Copies
DWD Archive	1

External Distribution		
Company	Name	No. Copies
PUBLIC		1

Document Change Record

Issue/ Revision	Date	DCN No.	Changed Pages/Paragraphs
1.0	31.08.2016	SAF/CM/RMIB/VAL/MET_TOA	Initial issue
1.1	05.10.2016	SAF/CM/RMIB/VAL/MET_TOA	Update following DRR 2.6

	Scientific Validation Report TOA Radiation MVIRI/SEVIRI Data Record	Doc.No.: SAF/CM/RMIB/VAL/MET_TOA Issue: 1.1 Date: 05 October 2016
---	--	---

Applicable documents

Reference	Title	Code
AD 1	CM SAF CDOP2 Project Plan	SAF/CM/DWD/PP/1.6
AD 2	CM SAF Product Requirement Document	SAF/CM/DWD/PRD/2.8

Reference documents

Reference	Title	Code
RD 1	Requirements Review 2.6 document. TOA Radiation – TCDR MVIRI/SEVIRI Edition 1 data sets, version 3.0	SAF/CM/RMIB/GERB/RR2.6
RD 2	TOA Radiation MVIRI/SEVIRI Dataset Generation Capability Description Document, version 1.1	SAF/CM/RMIB/DGCDD/MET_TOA
RD 3	TOA Radiation MVIRI/SEVIRI Data Record Algorithm Theoretical Basis Document, version 1.3	SAF/CM/RMIB/ATBD/MET_TOA
RD 4	TOA Radiation MVIRI/SEVIRI Data Record Product User Manual, version 1.1	SAF/CM/RMIB/PUM/MET_TOA
RD 5	GERB Dataset Product User Manual, version 3.0	SAF/CM/RMIB/PUM/GERB_DS

	Scientific Validation Report TOA Radiation MVIRI/SEVIRI Data Record	Doc.No.: SAF/CM/RMIB/VAL/MET_TOA Issue: 1.1 Date: 05 October 2016
---	--	---

Table of Contents

1	THE EUMETSAT SAF ON CLIMATE MONITORING (CM SAF)	12
2	INTRODUCTION	14
2.1	TOA radiative fluxes in CM SAF	14
2.2	Summary of user requirements	15
2.3	Summary of processing system	17
3	VALIDATION METHODOLOGY	19
3.1	Data records used for evaluation	19
3.1.1	CERES EBAF Edition2.8	19
3.1.2	CERES SYN1deg-Day, Edition3A	20
3.1.3	CERES SYN1deg-M3Hour, Edition3A	20
3.1.4	HIRS OLR CDR - Daily, Version 1.2	20
3.1.5	HIRS OLR CDR - Monthly, Version 2.7	21
3.1.6	ERBS WFOV-CERES, Version 2	21
3.1.7	ISCCP FD data record	22
3.2	Sources of error	22
3.2.1	Stability of the data records	22
3.2.2	Accuracy (processing error)	23
3.2.3	Effect of missing input data	23
3.3	Statistical measures	23
3.3.1	Bias	24
3.3.2	RMS difference	24
3.3.3	Mean ratio	25
3.3.4	Regional comparison	25
4	VALIDATION OF TRS PRODUCTS	27
4.1	Radiometric stability of TRS products	27
4.1.1	Stability wrt CERES EBAF	27
4.1.2	Stability wrt CERES SYN1deg-Day	27
4.1.3	Stability wrt CERES SYN1deg-M3Hour	28
4.1.4	Stability wrt ERBS WFOV-CERES	29
4.1.5	Stability wrt ISCCP FD	29
4.1.6	Stability of FOV-averaged clear-sky TRS fluxes	30
4.1.7	Stability of FOV-averaged all-sky TRS fluxes	32

	Scientific Validation Report TOA Radiation MVIRI/SEVIRI Data Record	Doc.No.: SAF/CM/RMIB/VAL/MET_TOA Issue: 1.1 Date: 05 October 2016
---	--	---

4.1.8	Discussion of TRS stability results and absolute level.....	34
4.2	Accuracy of monthly mean TRS products.....	35
4.2.1	Comparison with CERES EBAF	35
4.2.2	Comparison with ERBS WFOV-CERES.....	38
4.2.3	Comparison with ISCCP FD.....	39
4.2.4	Effect of missing data	39
4.2.5	Discussion.....	40
4.3	Accuracy of daily mean TRS products.....	40
4.3.1	Comparison with CERES SYN1deg-Day	40
4.3.2	Effect of missing data	43
4.3.3	Discussion.....	44
4.4	Accuracy of monthly mean diurnal cycle TRS products.....	44
4.4.1	Comparison with CERES SYN1deg-M3hour.....	44
4.4.2	Effect of missing data	47
4.4.3	Discussion.....	48
5	VALIDATION OF TET PRODUCTS	49
5.1	Radiometric stability of the TET products	49
5.1.1	Stability wrt CERES EBAF	49
5.1.2	Stability wrt CERES SYN1deg-Day.....	49
5.1.3	Stability wrt CERES SYN1deg-M3hour.....	50
5.1.4	Stability wrt HIRS OLR CDR – Daily	51
5.1.5	Stability wrt HIRS OLR CDR – Monthly.....	51
5.1.6	Stability wrt ERBS WFOV-CERES – Monthly.....	52
5.1.7	Stability wrt ISCCP FD	53
5.1.8	Stability of FOV-averaged TET fluxes	53
5.1.9	Discussion of TET stability results and absolute level	55
5.2	Accuracy of the monthly mean TET products.....	56
5.2.1	Comparison with CERES EBAF	56
5.2.2	Comparison with HIRS OLR CDR	58
5.2.3	Effect of missing data	61
5.2.4	Discussion.....	62
5.3	Accuracy of the daily mean TET products.....	62
5.3.1	Comparison with CERES SYN1deg-Day	62
5.3.2	Comparison with HIRS OLR CDR - Daily.....	65
5.3.3	Effect of missing data	66
5.3.4	Discussion.....	67

	Scientific Validation Report TOA Radiation MVIRI/SEVIRI Data Record	Doc.No.: SAF/CM/RMIB/VAL/MET_TOA Issue: 1.1 Date: 05 October 2016
---	--	---

5.4	Accuracy of the monthly mean diurnal cycle TET products.....	67
5.4.1	Comparison with CERES SYN1deg-M3Hour	67
5.4.2	Effect of missing data	69
5.4.3	Discussion	70
6	SUMMARY OF THE ERRORS	71
7	CONCLUSION.....	72
8	REFERENCES	73
9	GLOSSARY	75

	Scientific Validation Report TOA Radiation MVIRI/SEVIRI Data Record	Doc.No.: SAF/CM/RMIB/VAL/MET_TOA Issue: 1.1 Date: 05 October 2016
---	--	---

List of Tables

Table 1: Stability requirements for CM-23311 and CM-23341 from [RD1].....16

Table 2: Accuracy requirements for CM-23311 and CM-23341 and for the monthly mean (MM), the daily mean (DM) and the monthly mean diurnal Cycle (MMDC) from [RD1].16

Table 3 : Main characteristics of the data records used for validation.19

Table 4 : Averaged biases (in $W.m^{-2}$) of the MM TRS products per satellite.....35

Table 5: Increase of the RMS error of the CM SAF - SYN1deg-M3Hour TRS comparison as a function of the number of missing days and intercept values for each 3-hours time interval.48

Table 6 : Averaged biases (in $W.m^{-2}$) of the MM TET products per satellite.55

Table 7: Increase of the RMS error of the CM SAF - SYN1deg-M3Hour TET comparison as a function of the number of missing days and intercept values, for each 3-hours time interval.70

Table 8: Errors affecting the monthly mean, daily mean and monthly mean diurnal cycle products in CM-23311 (TRS) and CM-23341 (TET).71

	Scientific Validation Report TOA Radiation MVIRI/SEVIRI Data Record	Doc.No.: SAF/CM/RMIB/VAL/MET_TOA Issue: 1.1 Date: 05 October 2016
---	--	---

List of Figures

Figure 1: Schematic diagram of the Earth Radiation Budget (from Wild et al., 2013). Numbers indicate best estimates or the magnitudes of the globally averaged energy balance components together with their uncertainty ranges, representing present day climate conditions at the beginning of the twenty first century. Units are $W \cdot m^{-2}$ 14

Figure 2: Processing flowchart17

Figure 3: Example of regional comparison between a product *D* and a reference *R*.26

Figure 4: Time series of the bias between CM SAF MM and CERES EBAF TRS products. The red dotted line gives the mean bias over the time series.27

Figure 5: Time series of the bias between CM SAF DM and CERES SYN1deg-Day TRS products. The red dotted line gives the mean bias over the time series.28

Figure 6: Time series of the bias between CM SAF MMDC and CERES SYN1deg-M3Hour TRS products.28

Figure 7: Time series of the bias between CM SAF MM and ERBS WFOV-CERES (or DEEP-C) TRS products. The red dotted line gives the mean bias over the time series.29

Figure 8: Time series of the bias between CM SAF MM and ISCCP FD TRS products. The red dotted line gives the mean bias over the time series.29

Figure 9 : Time series of averaged CS TRS fluxes according to various surface types.30

Figure 10: Time series of anomalies for the averaged CS TRS fluxes according to various surface types. The anomalies are obtained by subtracting the average TRS flux (straight lines) from the time series. An additional shift of $-20 W/m^2$, $-10 W/m^2$, $0 W/m^2$, $+10 W/m^2$, $+20 W/m^2$ is done to improve the readability of the graph.31

Figure 11: Time series of CS TRS fluxes averaged over the whole Meteosat disk.31

Figure 12: Time series of anomalies for the CS TRS fluxes averaged over the whole Meteosat disk. The anomalies are obtained by subtracting the average TRS flux (straight line) from the time series.32

Figure 13: Time series of averaged TRS fluxes according to various surface types.32

Figure 14: Time series of anomalies for the averaged TRS fluxes according to various surface types. The anomalies are obtained by subtracting the average TRS flux (straight lines) from the time series. An additional shift of $-40 W/m^2$, $-20 W/m^2$, $0 W/m^2$, $+20 W/m^2$, $+40 W/m^2$ is done to improve the readability of the graph.33

Figure 15: Time series of TRS fluxes averaged over the whole Meteosat disk.33

Figure 16: Time series of anomalies for the TRS fluxes averaged over the whole Meteosat disk. The anomalies are obtained by subtracting the average TRS flux (straight line) from the time series.34

Figure 17: Time series of the RMS difference (bias corrected) between CM SAF MM and CERES EBAF TRS products. The red dotted line gives the mean RMS over the time series. Dark violet dots are for MFG data while purple dots are for MSG data. The optimal, target and threshold accuracies are indicated in black dotted lines.36

Figure 18: Comparison of CM SAF MM and CERES EBAF TRS products for April 2006 (MFG7). Upper panels show the CM SAF (left) and CERES EBAF (right) products. Bottom images show the difference (left) and the ratio (right) of these products.37

	Scientific Validation Report TOA Radiation MVIRI/SEVIRI Data Record	Doc.No.: SAF/CM/RMIB/VAL/MET_TOA Issue: 1.1 Date: 05 October 2016
---	--	---

Figure 19: Comparison of CM SAF MM and CERES EBAF TRS products for December 2008 (MSG2). Upper panels show the CM SAF (left) and CERES EBAF-TOA (right) products. Bottom images show the difference (left) and the ratio (right) of these products. ...38

Figure 20: Time series of the RMS difference (bias corrected) between CM SAF MM and ERBS WFOV-CERES TRS products. The optimal, target and threshold accuracies are indicated in black dotted lines.....39

Figure 21 : Time series of the RMS difference (bias corrected) between CM SAF MM and ISCCP FD TRS products. The optimal, target and threshold accuracies are indicated in black dotted lines.....39

Figure 22: Bias (left) and RMS (right) of the CM SAF - EBAF comparison as a function of the number of days without Meteosat TRS observations.40

Figure 23: Time series of the RMS difference (bias corrected) between CM SAF DM and CERES SYN1deg-Day TRS products. The optimal and target accuracies are indicated in black dotted lines (threshold at 16 W/m² is out of the figure).41

Figure 24: Comparison of CM SAF DM and CERES SYN1deg-Day TRS products for the 26th June 2008 (MSG2). Upper panels show the CM SAF (left) and CERES SYN1deg-Day (right) products. Bottom images show the difference (left) and the ratio (right) of these products.42

Figure 25: Comparison of CM SAF DM and CERES SYN1deg-Day TRS products for the 13th March 2002 (MFG7). Upper panels show the CM SAF (left) and CERES SYN1deg-Day (right) products. Bottom images show the difference (left) and the ratio (right) of these products.43

Figure 26: Bias (left) and RMS (right, bias corrected) of the CM SAF - CERES SYN1deg-Day comparison as a function of the number of repeat cycles of acquisition without Meteosat TRS observations.....44

Figure 27: Time series of the RMS difference (bias corrected) between CM SAF MMDC and CERES SYN1deg-M3Hour TRS products. The optimal, target and threshold accuracies are indicated in black dotted lines.....45

Figure 28: Comparison of CM SAF MMDC and CERES SYN1deg-M3Hour TRS products for November 2004 (MFG7) at 12 UTC. Upper panels show the CM SAF (left) and CERES SYN1deg-M3Hour (right) products. Bottom images show the difference (left) and the ratio (right) of these products.....46

Figure 29: Comparison of CM SAF MMDC and CERES SYN1deg-M3Hour TRS products for December 2008 (MSG2) at 12 UTC. Upper panels show the CM SAF (left) and CERES SYN1deg-M3Hour (right) products. Bottom images show the difference (left) and the ratio (right) of these products.....47

Figure 30: Bias (left) and RMS (bias-corrected, right) of the CM SAF - SYN1deg-M3Hour comparison as a function of the number of days without Meteosat TRS observations.48

Figure 31: Time series of the bias between CM SAF MM and CERES EBAF TET products. The red dotted line gives the mean bias over the time series.....49

Figure 32: Time series of the bias between CM SAF DM and CERES SYN1deg-Day TET products. The red dotted line gives the mean bias over the time series.....50

Figure 33: Time series of the bias between CM SAF MMDC and CERES SYN1deg-M3Hour TET products.50

	Scientific Validation Report TOA Radiation MVIRI/SEVIRI Data Record	Doc.No.: SAF/CM/RMIB/VAL/MET_TOA Issue: 1.1 Date: 05 October 2016
---	--	---

Figure 34: Time series of the bias between CM SAF TET DM and HIRS OLR CDR - Daily products. The red dotted line gives the mean bias over the time series. MET-2 and -3 data, displayed in red, use the EUMETSAT operational calibration.51

Figure 35: Time series of the bias between CM SAF TET MM and HIRS OLR CDR – Monthly products. The red dotted line gives the mean bias over the time series. MET-2 and -3 data, displayed in red, use the EUMETSAT operational calibration.52

Figure 36: Time series of the bias between CM SAF MM and ERBS WFOV-CERES (or DEEP-C) TET products. The red dotted line gives the mean bias over the time series. MET-2 and -3 data, displayed in red, use the EUMETSAT operational calibration.52

Figure 37: Time series of the bias between CM SAF MM and ISCCP FD TET products. The red dotted line gives the mean bias over the time series. MET-2 and -3 data, displayed in red, use the EUMETSAT operational calibration.53

Figure 38: Time series of averaged TET fluxes according to various surface types.54

Figure 39: Time series of anomalies for the averaged TET fluxes according to various surface types. The anomalies are obtained by subtracting the average TET flux (straight lines) from the time series. An additional shift of -40 W/m^2 , -20 W/m^2 , 0 W/m^2 , $+20 \text{ W/m}^2$, $+40 \text{ W/m}^2$ is done to improve the readability of the graph.54

Figure 40: Time series of TET fluxes averaged over the whole Meteosat disk.54

Figure 41: Time series of anomalies for the TET fluxes averaged over the whole Meteosat disk. The anomalies are obtained by subtracting the average TET flux (straight line) from the time series.55

Figure 42: Time series of the RMS difference (bias corrected) between CM SAF MM and CERES EBAF TET products. The red dotted line gives the mean RMS over the time series. The optimal, target and threshold accuracies are indicated in black dotted lines.56

Figure 43: Comparison of CM SAF MM and CERES EBAF TET products for December 2006 (MSG1). Upper panels show the CM SAF (left) and CERES EBAF (right) products. Bottom images show the difference (left) and the ratio (right) of these products.57

Figure 44: Comparison of CM SAF MM and CERES EBAF TET products for June 2001 (MFG7). Upper panels show the CM SAF (left) and CERES EBAF (right) products. Bottom images show the difference (left) and the ratio (right) of these products.58

Figure 45: Time series of the RMS difference (bias corrected) between CM SAF MM TET and HIRS OLR CDR - Monthly products. The red dotted line gives the mean RMS over the time series. The optimal, target and threshold accuracies are indicated in black dotted lines.59

Figure 46: Comparison of CM SAF MM TET and HIRS OLR CDR - Monthly products for August 1997 (MFG6). Upper panels show the CM SAF (left) and HIRS OLR CDR (right) products. Bottom images show the difference (left) and the ratio (right) of these products. ..60

Figure 47: Comparison of CM SAF MM TET and HIRS OLR CDR - Monthly products for April 1986 (MFG2). Upper panels show the CM SAF (left) and HIRS OLR CDR (right) products. Bottom images show the difference (left) and the ratio (right) of these products. ..61

Figure 48: Bias (left) and RMS difference (right) of the CM SAF - EBAF comparison as a function of the number of days without Meteosat TET observations.62

Figure 49: Time series of the RMS difference (bias corrected) between CM SAF DM and CERES SYN1deg-Day TET products. The red dotted line gives the mean RMS over the time series. The optimal, target and threshold accuracies are indicated in black dotted lines.63

	Scientific Validation Report TOA Radiation MVIRI/SEVIRI Data Record	Doc.No.: SAF/CM/RMIB/VAL/MET_TOA Issue: 1.1 Date: 05 October 2016
---	--	---

Figure 50: Comparison of CM SAF DM and CERES SYN1deg-Day TET products for the 10th July 2014 (MSG3). Upper panels show the CM SAF (left) and CERES SYN1deg-Day (right) products. Bottom images show the difference (left) and the ratio (right) of these products.64

Figure 51: Comparison of CM SAF DM and CERES SYN1deg-Day TET products for the 13th March 2002 (MFG7). Upper panels show the CM SAF (left) and CERES SYN1deg-Day (right) products. Bottom images show the difference (left) and the ratio (right) of these products.65

Figure 52: Time series of the RMS difference (bias corrected) between CM SAF DM and HIRS OLR CDR - Daily products. The red dotted line gives the mean RMS over the time series.66

Figure 53: Bias (left) and RMS (right, bias corrected) of the CM SAF - SYN1deg-Day comparison as a function of the number of repeat cycles of acquisition without Meteosat TET observations.66

Figure 54: Time series of the RMS difference (bias corrected) between CM SAF MMDC and CERES SYN1deg-M3Hour TET products. The target and threshold accuracies are indicated in black dotted lines.67

Figure 55: Comparison of CM SAF MMDC and CERES SYN1deg-M3Hour TET products for November 2004 (MSG1) at [12-15] UTC. Upper panels show the CM SAF (left) and CERES SYN1deg-M3Hour (right) products. Bottom images show the difference (left) and the ratio (right) of these products.68

Figure 56: Comparison of CM SAF MMDC and CERES SYN1deg-M3Hour TET products for June 2001 (MFG7) at [12-15] UTC. Upper panels show the CM SAF (left) and CERES SYN1deg-M3Hour (right) products. Bottom images show the difference (left) and the ratio (right) of these products.69

Figure 57: Bias (left) and RMS difference (right, bias corrected) of the CM SAF - SYN1deg-M3Hour comparison as a function of the number of days without Meteosat TET observations.70

	Scientific Validation Report TOA Radiation MVIRI/SEVIRI Data Record	Doc.No.: SAF/CM/RMIB/VAL/MET_TOA Issue: 1.1 Date: 05 October 2016
---	--	---

1 The EUMETSAT SAF on Climate Monitoring (CM SAF)

The importance of climate monitoring with satellites was recognized in 2000 by EUMETSAT Member States when they amended the EUMETSAT Convention to affirm that the EUMETSAT mandate is also to “contribute to the operational monitoring of the climate and the detection of global climatic changes”. Following this, EUMETSAT established within its Satellite Application Facility (SAF) network a dedicated centre, the SAF on Climate Monitoring (CM SAF, <http://www.cmsaf.eu>).

The consortium of CM SAF currently comprises the Deutscher Wetterdienst (DWD) as host institute, and the partners from the Royal Meteorological Institute of Belgium (RMIB), the Finnish Meteorological Institute (FMI), the Royal Meteorological Institute of the Netherlands (KNMI), the Swedish Meteorological and Hydrological Institute (SMHI), the Meteorological Service of Switzerland (MeteoSwiss), and the Meteorological Service of the United Kingdom (UK MetOffice). Since the beginning in 1999, the EUMETSAT Satellite Application Facility on Climate Monitoring (CM SAF) has developed and will continue to develop capabilities for a sustained generation and provision of Climate Data Records (CDR’s) derived from operational meteorological satellites.

In particular, the generation of long-term data records is pursued. The ultimate aim is to make the resulting data records suitable for the analysis of climate variability and potentially the detection of climate trends. CM SAF works in close collaboration with the EUMETSAT Central Facility and liaises with other satellite operators to advance the availability, quality and usability of Fundamental Climate Data Records (FCDRs) as defined by the Global Climate Observing System (GCOS). As a major task the CM SAF utilizes FCDRs to produce records of Essential Climate Variables (ECVs) as defined by GCOS. Thematically, the focus of CM SAF is on ECVs associated with the global energy and water cycle.

Another essential task of CM SAF is to produce data records that can serve applications related to the Global Framework of Climate Services initiated by the WMO World Climate Conference-3 in 2009. CM SAF is supporting climate services at national meteorological and hydrological services (NMHSs) with long-term data records but also with data records produced close to real time that can be used to prepare monthly/annual updates of the state of the climate. Both types of products together allow for a consistent description of mean values, anomalies, variability and potential trends for the chosen ECVs. CM SAF ECV data records also serve the improvement of climate models both at global and regional scale.

As an essential partner in the related international frameworks, in particular WMO SCOPE-CM (Sustained COordinated Processing of Environmental satellite data for Climate Monitoring), the CM SAF - together with the EUMETSAT Central Facility, assumes the role as main implementer of EUMETSAT’s commitments in support to global climate monitoring. This is achieved through:

- Application of highest standards and guidelines as lined out by GCOS for the satellite data processing,
- Processing of satellite data within a true international collaboration benefiting from developments at international level and pollinating the partnership with own ideas and standards,
- Intensive validation and improvement of the CM SAF climate data records,

	Scientific Validation Report TOA Radiation MVIRI/SEVIRI Data Record	Doc.No.: SAF/CM/RMIB/VAL/MET_TOA Issue: 1.1 Date: 05 October 2016
---	--	---

- Taking a major role in data record assessments performed by research organisations such as WCRP (World Climate Research Program). This role provides the CM SAF with deep contacts to research organizations that form a substantial user group for the CM SAF CDRs,
- Maintaining and providing an operational and sustained infrastructure that can serve the community within the transition of mature CDR products from the research community into operational environments.

A catalogue of all available CM SAF products is accessible via the CM SAF webpage, <http://www.cmsaf.eu/>. Here, detailed information about product ordering, add-on tools, sample programs and documentation is provided.

	Scientific Validation Report TOA Radiation MVIRI/SEVIRI Data Record	Doc.No.: SAF/CM/RMIB/VAL/MET_TOA Issue: 1.1 Date: 05 October 2016
---	--	---

2 Introduction

2.1 TOA radiative fluxes in CM SAF

At the Top-Of-Atmosphere (TOA), the following radiative fluxes are defined: the TOA Incoming Solar (TIS), the TOA Reflected Solar (TRS) and the TOA Emitted Thermal (TET).

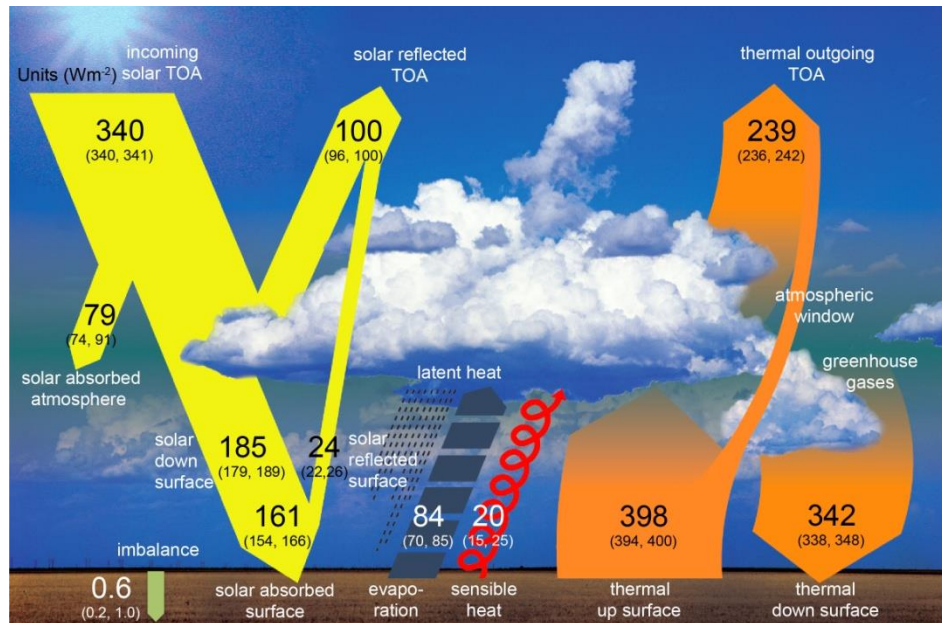


Figure 1: Schematic diagram of the Earth Radiation Budget (from Wild et al., 2013). Numbers indicate best estimates or the magnitudes of the globally averaged energy balance components together with their uncertainty ranges, representing present day climate conditions at the beginning of the twenty first century. Units are $W.m^{-2}$.

These three components of the Earth Radiation Budget (ERB) are the driver of the climate on our planet. In the frame of climate monitoring, the continuous monitoring of these fluxes is of prime importance to understand climate variability and change. The nature of these quantities, which are defined at TOA, makes the use of satellite observations especially useful.

Over the Meteosat Field Of View (FOV), broadband observations of the TRS and TET are available since 2004 from the Geostationary Earth Radiation Budget (GERB; Harries et al., 2005) instruments on the Meteosat Second Generation (MSG) satellites. The instruments' observations are processed by the GERB team, a consortium including institutions in Germany, the United Kingdom and Belgium. Currently, GERB Edition-1 instantaneous fluxes are generated (Dewitte et al., 2008) and made available to the user community. Within CM SAF, the GERB instantaneous fluxes have been daily and monthly averaged, as well as monthly averaged of the hourly integrated values. These data records have been released in 2013, with product identifier CM-113 (TRS) and CM-115 (TET).

Meteosat observations from around 0° longitude¹ are however available since 1982 and have been used to derive a data record of surface radiation in CM SAF. Given the overlap

¹ This is the nominal position of the Meteosat satellites. The operational one might be slightly different as for Meteosat-8 which was located at 3.5° West.

	Scientific Validation Report TOA Radiation MVIRI/SEVIRI Data Record	Doc.No.: SAF/CM/RMIB/VAL/MET_TOA Issue: 1.1 Date: 05 October 2016
---	--	---

between the Meteosat Visible and InfraRed Imager (MVIRI) and GERB in the period 2004-2006, empirical narrowband (NB) to broadband (BB) regressions can be derived to “unfilter” the MVIRI channel observations, making the estimation of instantaneous fluxes from 1982 to 2006 possible. From 2004 onward, this estimation can be built on the MVIRI-like visible (VIS), water vapour (WV) and infrared (IR) channels simulated from the NB channels of the Spinning Enhanced Visible and InfraRed Imager (SEVIRI, Schmetz et al., 2002). This opens the door to the generation of a homogeneous data record covering more than 30 years. Consequently, it is proposed to use the Meteosat first and second generations’ observations to construct long geostationary-based data records of TRS and TET radiative fluxes. These two data records are generated with the following CM SAF identifiers:

CM SAF identifier	Content
CM-23311	TOA Reflected Solar radiative flux All Sky (TRS_AS)
CM-23341	TOA Emitted Thermal radiative flux All Sky (TET_AS)

After brief summaries of the user requirements (section 2.2) and of the processing system (section 2.3), the validation methodology is presented in section 3. Then, sections 4 and 5 provide the detailed validations of the TRS and TET products respectively. In view of providing the relevant information to the users (through the Product User Manual [RD4]), a summary table is given in section 6. Then sections 7, 8 and 9, provide conclusions, references and acronyms.

2.2 Summary of user requirements

[RD1] discusses the application areas and user requirements for the MVIRI/SEVIRI data record products. Table 1 summarizes the requirements in terms of stability and Table 2 in terms of accuracy. Table 2 also summarizes the accuracy of the CM-113 and CM-115 products (from [RD5]) as well as documented accuracies of the Clouds and the Earth’s Radiant Energy System (CERES; Wielicki et al., 1996) products.

The stability refers to the maximum acceptable change (max-min) of the systematic error over a period of 10 years. Changes of systematic error are primarily caused by switches from one instrument to another and instrumental drift. Stability requirements are only defined for the monthly mean products but, as it will be shown in this document, they also characterise the daily mean and monthly mean diurnal cycle products. Evidence will also be provided that stability requirements are met over most of the scene types.

Table 1: Stability requirements for CM-23311 and CM-23341 from [RD1].

Products	Threshold	Target	Optimal
TRS all sky MM	4 W/m ² /dec	0.6 W/m ² /dec	0.3 W/m ² /dec
TET all sky MM	4 W/m ² /dec	0.6 W/m ² /dec	0.3 W/m ² /dec ²

Table 2: Accuracy requirements for CM-23311 and CM-23341 and for the monthly mean (MM), the daily mean (DM) and the monthly mean diurnal Cycle (MMDC) from [RD1].

Products		Threshold	Target	Optimal	CM-113 and CM-115 accuracy	CERES accuracy	Remarks	
TRS	CM-23311	MM	8 W/m ²	4 W/m ²	2 W/m ²	3.0 W/m ²	Requirements referring to error: - at 1 standard deviation (RMS error) - at 1° x 1° scale - taking only VZA<60° - does not include error (bias) due to the absolute calibration.	
		DM	16W/m ²	8 W/m ²	4 W/m ²	5.5 W/m ²		7.8 W/m ²
		MMDC	16W/m ²	8 W/m ²	4 W/m ²	12.8W/m ²		16.7 W/m ² (3-hour)
TET	CM-23341	MM	4 W/m ²	2 W/m ²	1 W/m ²	2.0 W/m ²		2.0 W/m ²
		DM	8 W/m ²	4 W/m ²	2 W/m ²	3.6 W/m ²		1.9 W/m ²
		MMDC	8 W/m ²	4 W/m ²	2 W/m ²	3.1 W/m ²		3.1 W/m ² (3-hour)

² The new GCOS requirement for TET is 0.2W.m⁻²/decade.

	Scientific Validation Report TOA Radiation MVIRI/SEVIRI Data Record	Doc.No.: SAF/CM/RMIB/VAL/MET_TOA Issue: 1.1 Date: 05 October 2016
---	--	---

2.3 Summary of processing system

Figure 2 provides a sketch of the processing into its 4 main processing steps and outlines its main inputs and outputs. Further details on the implemented algorithm are available in the Algorithm Theoretical Basis Document [RD3]. Details on the processing system are given in the Dataset Generation Capability Description Document [RD2]. Finally, details on the product content and format are given in the Product User Manual [RD4].

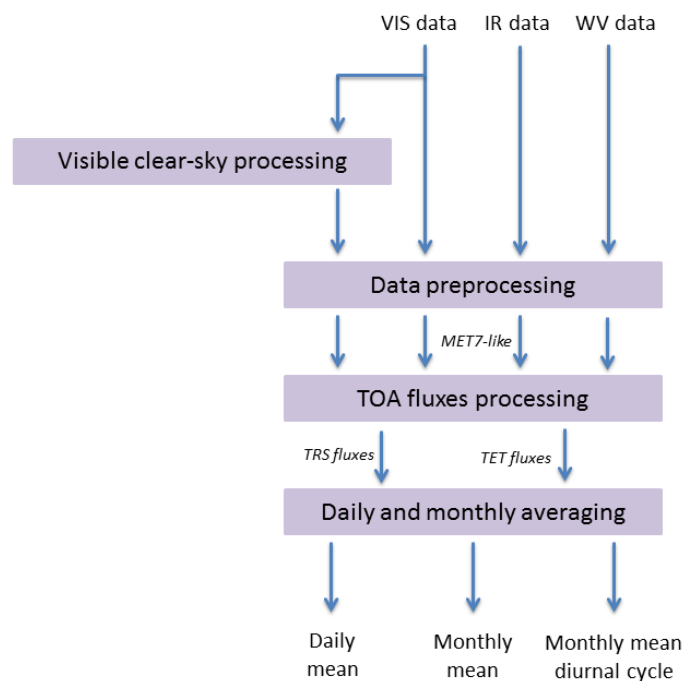


Figure 2: Processing flowchart

- The “**Visible clear-sky processing**” subsystem aims at generating the clear-sky (CS) VIS data that are needed to process the TOA fluxes. In those images, the cloud effect has been filtered by image processing techniques, based on a series of input VIS images covering a period of 61 days around the day of interest. The CS VIS estimates are an important input for cloud detection and characterization.
- The “**Data preprocessing**” subsystem performs several corrections of the input VIS, WV and IR data such as calibration, ageing correction, stripes’ interpolation and conversion to equivalent Meteosat-7 (“MET7-like”) observations. This preprocessing step is needed as the Meteosat observations are not yet available as Fundamental Climate Data Record (FCDR). In the future, it can be expected that a FCDR will be provided by EUMETSAT.
- In the “**TOA fluxes processing**”, the TRS and TET instantaneous radiative fluxes are generated at the time of the imager acquisition from the MET7-like observations through various stages: a scene identification (performed only during daytime, i.e. for Solar Zenith Angle (SZA) < 80°), NB to BB relations to “unfilter” the MET7-like radiances, and ADMs to convert BB radiances into fluxes. The TOA fluxes are generated on a geostationary grid at the full resolution, i.e.: (2.5 km)², (5 km)² and (3 km)² at sub-satellite point respectively for the visible MVIRI, the thermal MVIRI and the SEVIRI channels.

	Scientific Validation Report TOA Radiation MVIRI/SEVIRI Data Record	Doc.No.: SAF/CM/RMIB/VAL/MET_TOA Issue: 1.1 Date: 05 October 2016
---	--	---

- Finally, the “**Daily and monthly averaging**” subsystem performs the averaging of the TRS and TET fluxes in hourly boxes, from which the daily mean, monthly mean and monthly mean diurnal cycle are estimated. A maximum of 3 hours of successive missing data is accepted in the daily averaging; otherwise the daily mean is not issued. A minimum number of 15 days is required to process the monthly mean and monthly mean diurnal cycle. The seasonal change in insolation during the month is also taken into account in the monthly averaging. The data are finally re-gridded from the geostationary grid onto a common regular grid with a spatial resolution of $(0.05^\circ)^2$. This re-gridding is performed for consistency with other CM SAF products (e.g. CLAAS and SARAH) and also to ease the use of the product.

It should be noted that data from MFG7 (last of the Meteosat First Generation) and MSG1 (first of the Meteosat Second Generation) have both been processed during the overlap period (February 2004 – June 2006). This will be used to check that the error characteristics are consistent over the 2 generations of Meteosat satellites.

	Scientific Validation Report TOA Radiation MVIRI/SEVIRI Data Record	Doc.No.: SAF/CM/RMIB/VAL/MET_TOA
		Issue: 1.1
		Date: 05 October 2016

3 Validation methodology

3.1 Data records used for evaluation

Given the absence of “Ground Truth” observations for the TOA fluxes, the validations mostly rely on intercomparisons with other satellite-based data. The GERB data records are not used for validation as they share a large part of the data processing (and observation conditions). Instead, data from polar satellites observations (e.g. from CERES and HIRS) are preferred. These data records are described in the following subsections and summarized in Table 3.

Table 3 : Main characteristics of the data records used for validation.

Source	Version	Variable	Temporal resolution	Spatial resolution	Period
CERES EBAF	2.8	TRS TET	MM	1° x 1°	March 2000 onward
CERES SYN1deg-Day	3A	TRS TET	DM	1° x 1°	March 2000 onward
CERES SYN1deg-M3Hour	3A	TRS TET	MMDC in 3-hourly intervals	1° x 1°	March 2000 onward
HIRS OLR CDR - Monthly	2.7	TET	MM	2.5° x 2.5°	1979 onward
HIRS OLR CDR - Daily	1.2	TET	DM	1° x 1°	Jan. 1979 to Dec. 2013
Univ. Reading ERBS WFOV-CERES (DEEP-C)	2	TRS TET	MM	0.7° x 0.7°	Jan. 1985 to May 2015
ISCCP FD	-	TRS TET	MM and MMDC	2.5° x 2.5°	July 1983 to Dec. 2004

3.1.1 CERES EBAF Edition2.8

The CERES Energy Balanced and Filled (EBAF) Ed2.8 data record (Loeb et al., 2009; Loeb et al., 2012) provides state-of-the-art estimates of monthly mean TRS and TET fluxes at a 1°x1° latitude-longitude resolution from March 2000 onward. The EBAF Ed2.8 data record is featured by: (i) the use of both Terra and Aqua satellites, (ii) the use of geostationary satellites for an improved diurnal modelling, and (iii) a small adaptation of the shortwave (SW) and longwave (LW) calibration to be consistent with our current understanding of the Earth imbalance. Prior to July 2002, uncertainties are slightly larger since only Terra observations are used. In Ed2.8, the impact of geostationary instrument artefacts is significantly reduced compared to earlier versions. It should be noted that the EBAF Ed2.8

	Scientific Validation Report TOA Radiation MVIRI/SEVIRI Data Record	Doc.No.: SAF/CM/RMIB/VAL/MET_TOA Issue: 1.1 Date: 05 October 2016
---	--	---

TOA fluxes are provided at the same reference level than the MVIRI/SEVIRI data record, i.e. 20 km.

The CERES EBAF data record is mainly used to evaluate the accuracy of the CM SAF monthly mean products. It does not cover the full time period of the data record but there is still overlap with the MFG and MSG eras. The intercomparisons provide information on the accuracy at 1° spatial resolution which is the spatial scale chosen for the accuracy requirements (see [RD1] and also section 2.2).

3.1.2 CERES SYN1deg-Day, Edition3A

The CERES SYN1deg-day products provide the state-of-the-art estimates of the daily mean TRS and TET fluxes. The CERES SYN1deg products consist in CERES-observed, geostationary enhanced and temporally interpolated TOA radiative fluxes. 3-hourly TOA fluxes and cloud properties from geostationary imagers are used for an improved modelling of the diurnal variability between CERES observations (Doelling et al., 2006). Indeed, the CERES instruments on-board Terra and Aqua satellites are in sun-synchronous orbits thus limiting the diurnal sampling. However GEO-derived fluxes show artefacts over certain regions and are therefore normalized at Terra or Aqua observation times to remain consistent with the CERES instrument calibration (Doelling et al., 2013). Data are available from March 2000 to present (combined Terra and Aqua from July 2002 onward). The flux reference level of the CERES SYN1deg-Day products is the same as for the EBAF Ed2.8 products, i.e. 20 km.

This data is mainly used to evaluate the accuracy of the CM SAF daily mean products.

3.1.3 CERES SYN1deg-M3Hour, Edition3A

The Monthly 3-Hourly Averaged Synoptic Radiative Fluxes and Clouds (SYN1deg-M3Hour) products are part of the CERES SYN1deg products. Therefore, they share the same basic characteristics as the CERES SYN1deg-Day products described previously but instead of being daily means, the CERES SYN1deg-M3Hour products are monthly mean of the TOA fluxes in 3-hourly intervals: 00-03 GMT, 03-06 GMT, ..., 21-24 GMT.

This data is mainly used to evaluate the accuracy of the CM SAF monthly mean diurnal cycle products. The monthly 1-hourly TRS and TET fluxes (diurnal cycle) from the MVIRI/SEVIRI data records were averaged over these time intervals to allow the comparison with the CERES SYN1deg-M3Hour fluxes.

3.1.4 HIRS OLR CDR - Daily, Version 1.2

The NOAA National Centers for Environmental Information (NCEI, was National Climate Data Center, NCDC) provides a high quality Climate Data Record (CDR) of Outgoing Longwave Radiation (OLR) (Lee, 2014; Lee et al., 2014). Level-1b all-sky data from the High-resolution Infrared Radiation Sounder (HIRS) instrument are the main input into the daily OLR record. The data record is produced by applying a combination of statistical techniques, including OLR regression, instrument ambient temperature prediction coefficients and inter-satellite bias corrections. The HIRS OLR CDR – Daily data record is featured by: (i) a global coverage, (ii) a 1°x1° equal-angle grid resolution, (iii) a temporal coverage from the 1st January 1979 to the 31st December 2013 (the data from 2014 onward are available through <http://olr.umd.edu/> but have not been used in this work). The OLR estimated from imagers' radiance observations on-board operational geostationary satellites (via Gridsat CDR and GSIP OLR product) is incorporated to allow an accurate temporal integration of the daily mean OLR. Since polar areas (about 60° polewards) are not covered by geostationary observations, only HIRS observations are used to derive the daily OLR in

	Scientific Validation Report TOA Radiation MVIRI/SEVIRI Data Record	Doc.No.: SAF/CM/RMIB/VAL/MET_TOA Issue: 1.1 Date: 05 October 2016
---	--	---

these regions. The HIRS OLR estimation technique has been vigorously validated against the Earth Radiation Budget Experiment (ERBE) and CERES data (see Ellingson et al., 1994; Lee et al., 2007). It can achieve an accuracy of about 4 to 8 W.m⁻² for various instrument types, with biases within the respective radiometric accuracy of the reference instruments.

As it covers the full data record extend, this data is the main reference to address the stability of the daily mean TET products. It is also used to check that the accuracy estimated over the CERES era (thus from 2000 onward) remains valid in the early part of the data record.

3.1.5 HIRS OLR CDR - Monthly, Version 2.7

The HIRS OLR CDR – Monthly data record share the same basic characteristics as the HIRS OLR CDR – Daily data record, described previously. The data record uses the Level-1b HIRS data as main input and is produced by applying the same combination of statistical techniques. However, the monthly mean OLR time series is generated on a 2.5°x2.5° equal-angle grid. In addition, the monthly OLR CDR is estimated from the HIRS all-sky radiance observations directly and does not use geostationary observations.

Currently, the official NCEI release of the monthly OLR CDR is version 2.2. However, this version is known to have artificial trend and discontinuities mainly caused by inconsistent regression models used for the OLR retrieval across the HIRS instruments (pers. comm. Hai-Tien Lee). This inconsistency between the OLR regression models cause misleading inter-satellite calibration and thus introduce discontinuities between HIRS instruments. New sets of regression models were thus generated and helped to improve the accuracy of inter-satellite calibration in the HIRS monthly OLR CDR version 2.7 (as well as the daily OLR CDR version 1.2). This version 2.7 of the monthly OLR CDR is expected to be officially released by NCEI at the end of 2016 and should then replace the current official version 2.2. However, it was decided to validate the MVIRI/SEVIRI data record based on the version 2.7 of the HIRS monthly OLR CDR.

This data is the main reference to address the stability of the monthly mean TET products.

3.1.6 ERBS WFOV-CERES, Version 2

In the frame of the Diagnosing Earth's Energy Pathways in the Climate system (DEEP-C) consortium, the Earth Radiation Budget Satellite (ERBS) wide field of view (WFOV) data record developed by Wielicki et al. (2002) has been updated and extended from January 1985 to May 2015 using CERES Edition 2.8 data (Allan et al., 2014; Wong et al., 2006; Minnis et al., 1993). The ERBS WFOV non-scanning instrument provides a stable, near-global record of radiative fluxes at a 10°x10° spatial resolution covering the time period 1985-1999. Based on this data record, the reconstructed ERBS WFOV-CERES (or DEEP-C) data record combines satellite data, atmospheric reanalyses and climate model simulations to generate an extended time series of updated TOA radiative fluxes. Monthly observations of TOA radiation from the CERES instruments on-board the Terra and Aqua satellites are central to this reconstruction. Radiative fluxes simulated by the European Centre for Medium-range Weather Forecasts interim reanalysis (ERA-Interim) are used to provide estimates of regional changes in radiative fluxes. Therefore, this approach combines the quality of the CERES data, the stability of the WFOV measurements, and the realistic circulation changes depicted by ERA-Interim. However, regional errors relating to systematic model biases and inadequate representation of tropospheric aerosols are likely to remain.

In short, the homogenization strategy of the data record is featured as follows: (i) CERES data are used from March 2000 onward; (ii) reconstructed monthly mean radiative fluxes are used prior to March 2000. The fluxes reconstruction is performed as follows (see Allan et al., 2014 and supporting information for details): (i) a repeating monthly mean seasonal cycle

	Scientific Validation Report TOA Radiation MVIRI/SEVIRI Data Record	Doc.No.: SAF/CM/RMIB/VAL/MET_TOA Issue: 1.1 Date: 05 October 2016
---	--	---

from 2001-2005 CERES data is prescribed at each grid point; (ii) using ERAI data, deseasonalised radiative flux anomalies (relative to 2001-2005) are computed at each grid point, and these spatial anomalies are added to (1); and (3) a globally uniform adjustment is applied to the radiative fluxes such that 60°S-60°N mean deseasonalised anomalies match the WFOV time series.

This data is used to address the stability of the monthly mean products in the early part of the data record, especially for the TRS products which are not covered by the HIRS OLR CDR.

3.1.7 ISCCP FD data record

In the International Satellite Cloud Climatology Project (ISCCP) FD data record (Zhang et al., 2004), the upwelling and downwelling SW and LW radiative fluxes have been calculated at TOA (defined to be at a height of 100 km) using a complete radiative transfer model from the GISS Global Climate Modelling (GCM) program (revised) with improved observations of the physical properties of the surface, atmosphere and clouds based on the ISCCP data records. In the last version, the most important changes are the introduction of a better treatment of ice clouds, revision of the aerosol climatology, accounting for diurnal variations of surface skin/air temperatures and the cloud-radiative effects on them, revision of the water vapour profiles used, and refinement of the land surface albedos and emissivities (Zhang et al., 2004). The ISCCP FD data record consists of 3-hourly data covering the whole globe on a 280 km equal-area global grid. The monthly mean of the FD variables were directly downloaded from the ISCCP web page (<http://isccp.giss.nasa.gov/pub/data/FC/>) under the native ISCCP file format. Data are available from July 1983 to December 2004 on a 2.5° equal-area grid. Comparisons of monthly regional mean values from ISCCP FD with the ERBE, CERES and the Baseline Surface Radiation Network (BSRN) values suggested uncertainties of 5-10 W.m⁻² at TOA.

The all-sky upwelling SW and LW TOA fluxes were selected to compare with the MVIRI/SEVIRI TRS and TET monthly mean fluxes, including the diurnal cycle. This data is used as additional indicator for the stability of the CM SAF products in the early part of the data record.

3.2 Sources of error

Three sources of error can be identified as affecting the data records.

3.2.1 Stability of the data records

A first source of error is introduced by the temporal stability and consistency of the MVIRI and SEVIRI instruments used as primary inputs for the data records. The stability of the resulting data record is evaluated as the (max – min) variability of the systematic error over a period of 10 years (decade). The systematic error (i.e. the absolute calibration error) is also shortly discussed.

The stability is addressed by building time series of overall bias between the CM SAF products and several other reference data records (CERES, HIRS ...). Using different references allows attributing observed stability problems (e.g. drift, jumps) to one of these sources.

As additional information about the stability, time series of fluxes averaged over the FOV are also presented (thus without using reference data record). This is a useful tool but it relies on the assumption that the cloudiness, surface albedo, aerosol content, etc., do not vary significantly over the data record extend.

	Scientific Validation Report TOA Radiation MVIRI/SEVIRI Data Record	Doc.No.: SAF/CM/RMIB/VAL/MET_TOA Issue: 1.1 Date: 05 October 2016
---	--	---

3.2.2 Accuracy (processing error)

The second source of error comes from the processing of the MVIRI and SEVIRI observations into TOA fluxes. This includes the conversion to equivalent Meteosat-7 (“MET7-like”) observations, the conversion to instantaneous radiative fluxes and finally the daily and monthly averaging of these fluxes (see [RD3] for details). To quantify this error, the CM SAF products are compared with similar products derived from the CERES instruments at a 1° spatial scale. CERES is considered as the best reference data to address the accuracy, especially for the monthly mean and monthly mean diurnal cycle products which are based on a collection of CERES measurements taken from varying observation directions. This reduces significantly the radiance-to-flux error in the CERES monthly means.

In practice, the CM SAF products are first regridded on the same 1°x1° lat-lon grid as used for the CERES products. Then, the root mean squared (RMS, bias corrected) of the difference with the CERES products is evaluated over the area 50°S-50°N and 50°W-50°E. It is interesting to look at the time series of the processing error, to check the consistency over the data record extend, in particular to check that the errors obtained with MFG and MSG are consistent.

3.2.3 Effect of missing input data

Finally, an additional error is sometimes introduced by missing input MVIRI or SEVIRI images. Data gaps of up to 3 successive hours are filled by temporal interpolation of the instantaneous fluxes and this can be the source of additional error in the final daily mean (DM) products. When a gap is longer than 3 hours, the full day is discarded and no DM product is provided. This day is not used in the monthly averaging which is in turn the source of error in the monthly mean products (“sampling problem”).

For the DM products, a day with complete coverage (48 MVIRI or 96 SEVIRI observations), the 23rd June 2006, is selected as reference and the DM product is computed by simulating missing input data. Comparison with the reference product provides an idea of the error level (bias and RMS).

For the monthly means and the monthly mean diurnal cycles, the effect of missing days on the final products is considered. Therefore, all the months with one or several missing days are selected within the full data record and the RMS of the differences with respect to the CERES products (EBAF for the monthly means and SYN1deg-M3Hour for the diurnal cycles) are computed for each of these months. The RMS error is therefore obtained as a function of the number of missing days as input.

3.3 Statistical measures

Several statistical measures are used to evaluate the quality of the MVIRI/SEVIRI data records and are briefly described in the following subsections. These statistical measures are the commonly used bias and RMS, but also the mean ratio between the CM SAF data record (denoted here as D) and a reference data record (denoted as R). Regional comparisons are also performed (at pixel level) in order to isolate potential regional patterns or artefacts within the data records.

To allow the comparison, D and R must be at the same resolution. In practice, the grid of R is used (e.g. the 1°x1° lat-lon grid for CERES or HIRS daily). The products are provided until a VZA of 80° but the quality is estimated over the 50°-50° lat-lon region which includes the VZA<60° region. In the following equations, the individual pixels are denoted as k and N is their total number.

	Scientific Validation Report TOA Radiation MVIRI/SEVIRI Data Record	Doc.No.: SAF/CM/RMIB/VAL/MET_TOA Issue: 1.1 Date: 05 October 2016
---	--	---

3.3.1 Bias

The bias features the mean difference between two data records. It is computed as the arithmetic mean of the differences between corresponding pixel values from both data records.

$$\mu = \frac{1}{N} \sum_{k=1}^N (D_k - R_k) = \bar{D} - \bar{R}$$

In practice, a positive bias indicates that the CM SAF fluxes are higher than the reference while negative bias indicates the opposite. The bias can be computed for each time step which results in time series useful to address the stability of the products.

3.3.2 RMS difference

The RMS difference is a measure to evaluate the accuracy of a data record compared to the reference. It is computed as:

$$RMS = \sqrt{\frac{1}{N} \sum_{k=1}^N (D_k - R_k)^2}$$

This RMS can however be affected by a systematic difference (bias) between D and R . For this reason it is often preferred to correct the systematic bias before computing the RMS of the difference:

$$RMS (bias\ corrected) = \sqrt{\frac{1}{N} \sum_{k=1}^N ((D_k - R_k) - (\bar{D} - \bar{R}))^2}$$

This RMS is often qualified as “bias-corrected”. The two RMS differences are linked by the following relation:

$$RMS (bias\ corrected)^2 = RMS^2 - \mu^2$$

In this work, the RMS (bias corrected) is used as an indicator for the accuracy. The resulting value is however affected by the reference’s error and by possible correlation of the errors. The reference’s error makes the RMS an overestimation of the CM SAF accuracy. On the other hand, correlation of the errors can make the RMS an underestimation of the accuracy. This is why it is important to:

- use high quality references for R (e.g. the CERES data which are based on BB observations).
- use references with the lowest possible correlation of errors with D . This explains why the CERES data are preferred to the GERB data records (CM-113 and CM-115) for validation. Indeed, the GERB and the MVIRI/SEVIRI data records share many important characteristics (e.g. the viewing direction and the ADMs) making the errors highly correlated. On the other hand, error correlation is minimized using polar satellite observations which have totally different spatial, temporal and directional samplings.

	Scientific Validation Report TOA Radiation MVIRI/SEVIRI Data Record	Doc.No.: SAF/CM/RMIB/VAL/MET_TOA Issue: 1.1 Date: 05 October 2016
---	--	---

3.3.3 Mean ratio

To extract a single value for the ratio over the FOV (for instance to create time series) the ratio of the arithmetic means of D and R is estimated (and not the average of the pixel level ratio).

$$MR = \frac{\frac{1}{N} \sum_{k=1}^N D_k}{\frac{1}{N} \sum_{k=1}^N R_k}$$

3.3.4 Regional comparison

In addition to the previous quantitative estimators, an analysis of the regional patterns of the difference ($D - R$) and the ratio (D/R) with respect to the reference data record is done at pixel level. The image of the difference depicts the regional differences between both data records and allows isolating the areas with the highest differences. The image of the ratio is useful when comparing solar fluxes which can exhibit large variations, e.g. due to solar insolation and surface albedo. In this document, both these images are not corrected for the bias.

As illustrated on Figure 3, the regional comparison contains 4 panels: the top left and right show the TOA fluxes in D and R (using the same colorbar to ease the comparison) while the bottom left and right panels show the difference ($D - R$), in $W.m^{-2}$, and the ratio (D/R), unitless. These images cover the region defined by 70° in latitude and longitude (grid used for the products, [RD4]). The region defined by 50° in latitude and longitude, shown in black on the difference image, is used to evaluate the bias and RMS error.

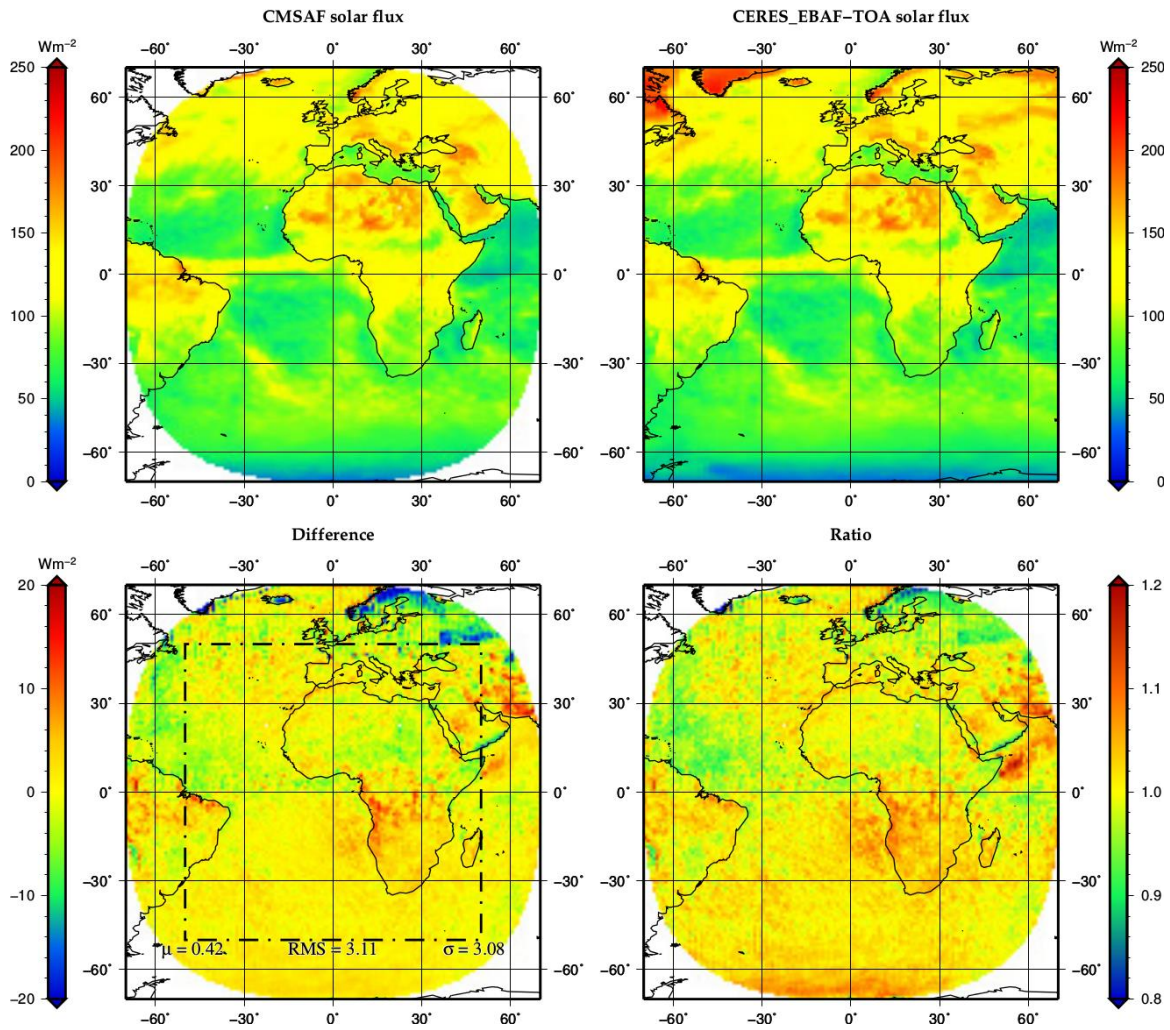


Figure 3: Example of regional comparison between a product D and a reference R .

	Scientific Validation Report TOA Radiation MVIRI/SEVIRI Data Record	Doc.No.: SAF/CM/RMIB/VAL/MET_TOA Issue: 1.1 Date: 05 October 2016
---	--	---

4 Validation of TRS Products

This section presents the validation activities of the TRS products while the TET products are addressed in section 5. The temporal stability of the products is first discussed in section 4.1. Then, sections 4.2 to 4.4 present the validations of the monthly mean (MM), daily mean (DM) and monthly mean diurnal cycle (MMDC) products. The effect of missing data is also quantified in these 3 sections.

4.1 Radiometric stability of TRS products

4.1.1 Stability wrt CERES EBAF

The radiometric stability of the TRS MM products has been investigated by computing the bias against the CERES EBAF products for each month from March 2000 to March 2015, as shown in Figure 4. The mean bias over the whole time series (about -0.1 W/m^2) is indicated by the red dotted line. The threshold requirements for stability, i.e. $4 \text{ W/m}^2/\text{decade}$, are indicated by the 2 black dotted lines at $\pm 2 \text{ W/m}^2$ wrt to the mean bias.

As it can be seen, MFG data (dark violet dots) and MSG data (purple dots) agree quite well during the overlap period (2004-2006) suggesting that the merging of both generations does not introduce significant discontinuities in the TRS data record. In general, a good stability in time is observed with a limited change between satellites and generations of instruments. The MSG era however suggests a slight downward trend over the period 2006-2015.

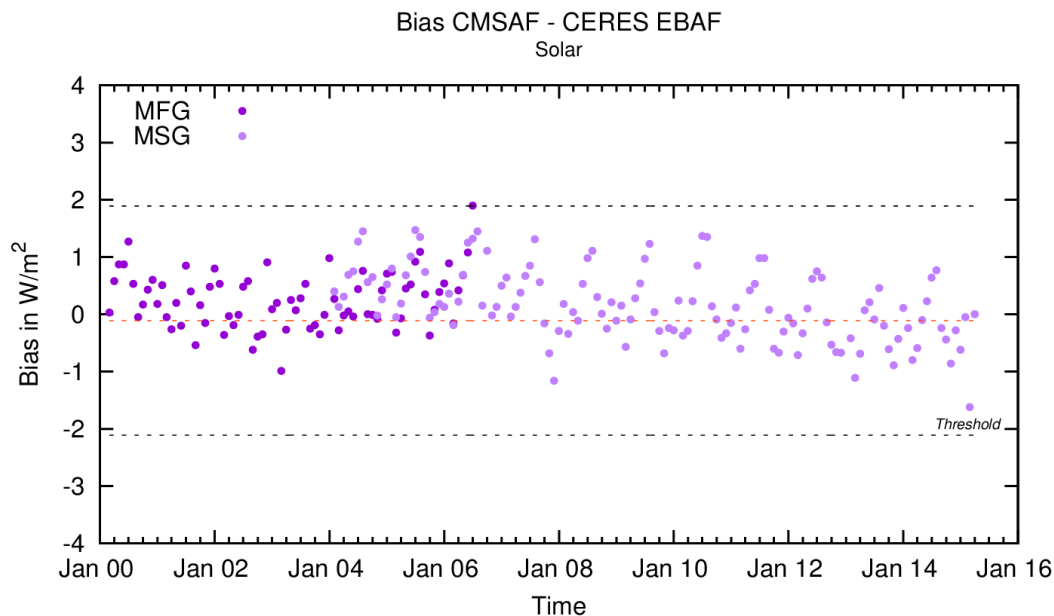


Figure 4: Time series of the bias between CM SAF MM and CERES EBAF TRS products. The red dotted line gives the mean bias over the time series.

4.1.2 Stability wrt CERES SYN1deg-Day

Figure 5 shows the time series of the bias between the DM TRS products and the CERES SYN1deg-Day products. The mean bias over the whole time series is about 1.6 W.m^{-2} (red dotted line). As wrt EBAF, no obvious stability problem (jump) is observed, at least over the covered 2000-2015 period, except for a slight downward trend for MSG over the period 2006-2015.

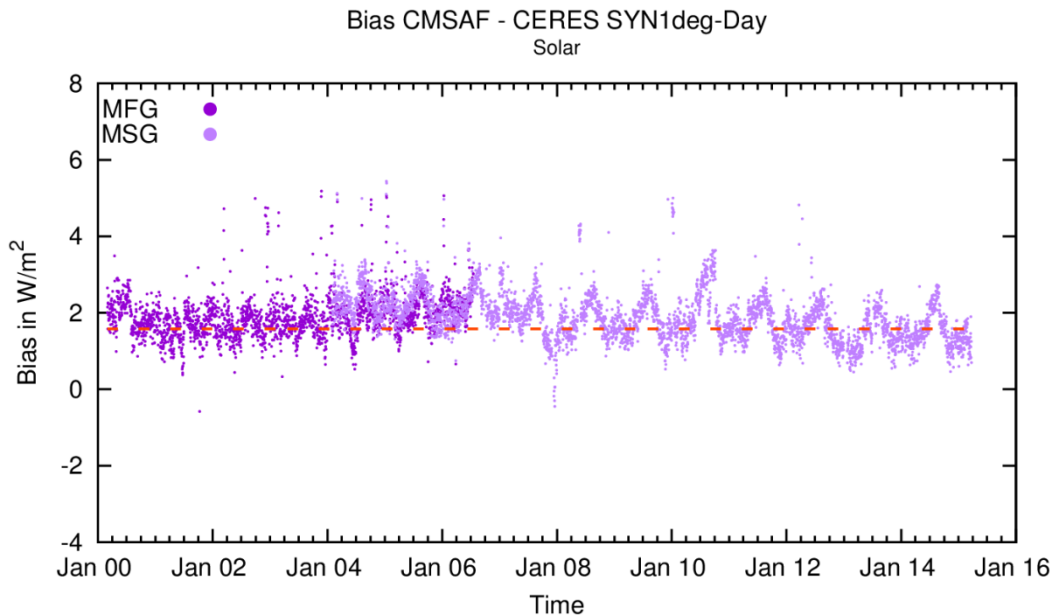


Figure 5: Time series of the bias between CM SAF DM and CERES SYN1deg-Day TRS products. The red dotted line gives the mean bias over the time series.

The outliers visible on Figure 5 are attributed to missing data, e.g. during Meteosat decontaminations. Note that missing images affect not only the CM SAF but also the CERES SYN products.

4.1.3 Stability wrt CERES SYN1deg-M3Hour

The radiometric stability of the TRS MMDC products has been investigated by comparison with the CERES SYN1deg-M3Hour products. Time series of the bias between both products are shown in Figure 6 for the various 3-hourly intervals (which are referred to by the start of the interval). Logically, the biases are higher for the intervals close to midday than those close to midnight.

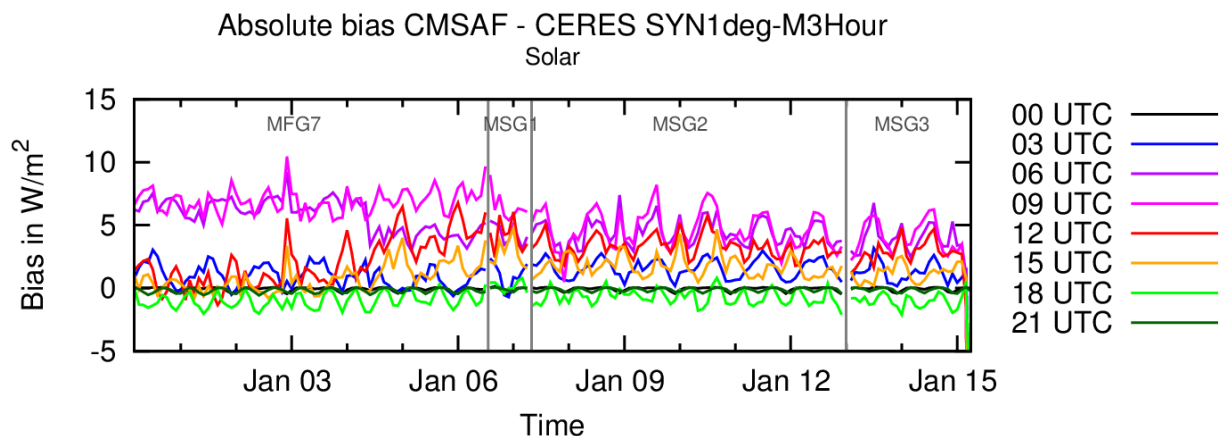


Figure 6: Time series of the bias between CM SAF MMDC and CERES SYN1deg-M3Hour TRS products.

In general, a good stability in time is observed without sharp transitions. However for MFG7, the 06 UTC time interval shows a slight decrease around June 2004 while the 12 UTC and 15 UTC time intervals are increasing. Those variations can be attributed to the switch between MFG and MSG (June 2004 for CERES and July 2006 for CM SAF). For all the satellites, the morning/early afternoon time intervals (06 UTC, 09 UTC and 12 UTC) show the

	Scientific Validation Report TOA Radiation MVIRI/SEVIRI Data Record	Doc.No.: SAF/CM/RMIB/VAL/MET_TOA Issue: 1.1 Date: 05 October 2016
---	--	---

highest biases. It should be noted that isolated high biases, such as the peak value for December 2002 in the MFG7 time series or the sharp decrease at the end of the MSG3 time series (March 2015), are due to high numbers of missing days within the MDC.

4.1.4 Stability wrt ERBS WFOV-CERES

To extend the analysis of the stability before 2000, Figure 7 shows the time series of the MM bias wrt the ERBS WFOV-CERES (or DEEP-C) data record. In general, the stability threshold of $4 \text{ W/m}^2/\text{decade}$ is fulfilled except for the MFG4 period for which about half of the months lie out of the threshold requirements. However, Table 4 shows that the average bias for MFG4 agrees with the other satellites within this threshold.

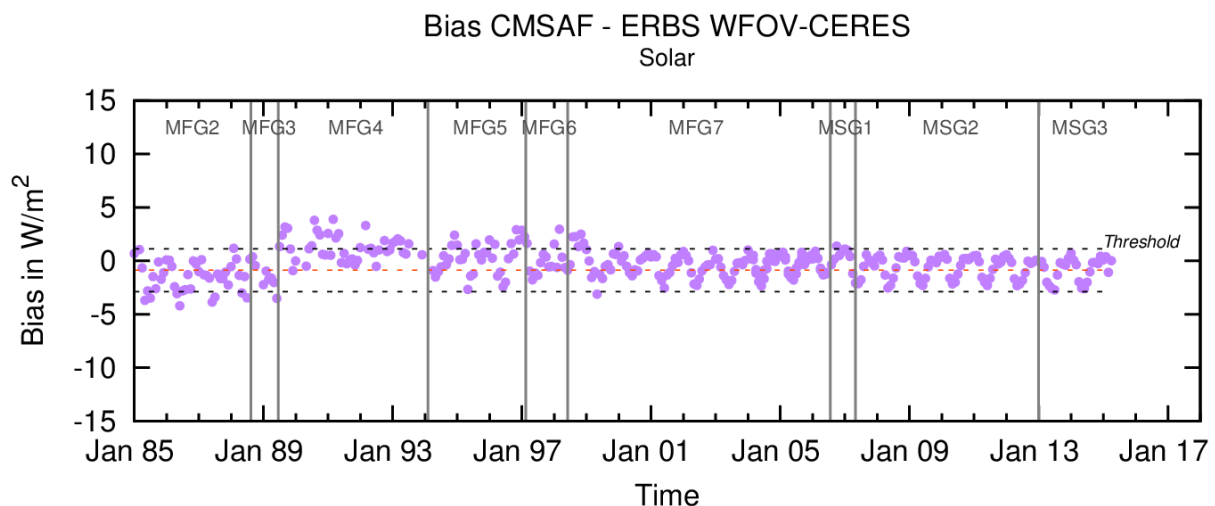


Figure 7: Time series of the bias between CM SAF MM and ERBS WFOV-CERES (or DEEP-C) TRS products. The red dotted line gives the mean bias over the time series.

4.1.5 Stability wrt ISCCP FD

Figure 8 shows the time series of the bias wrt the ISCCP FD data record from July 1983 to December 2004. Validation has been performed at the spatial resolution of the ISCCP FD data record ($2.5^\circ \times 2.5^\circ$). The bias wrt ISCCP shows a much higher variability than what is observed with CERES or the ERBS-WFOV-CERES data record.

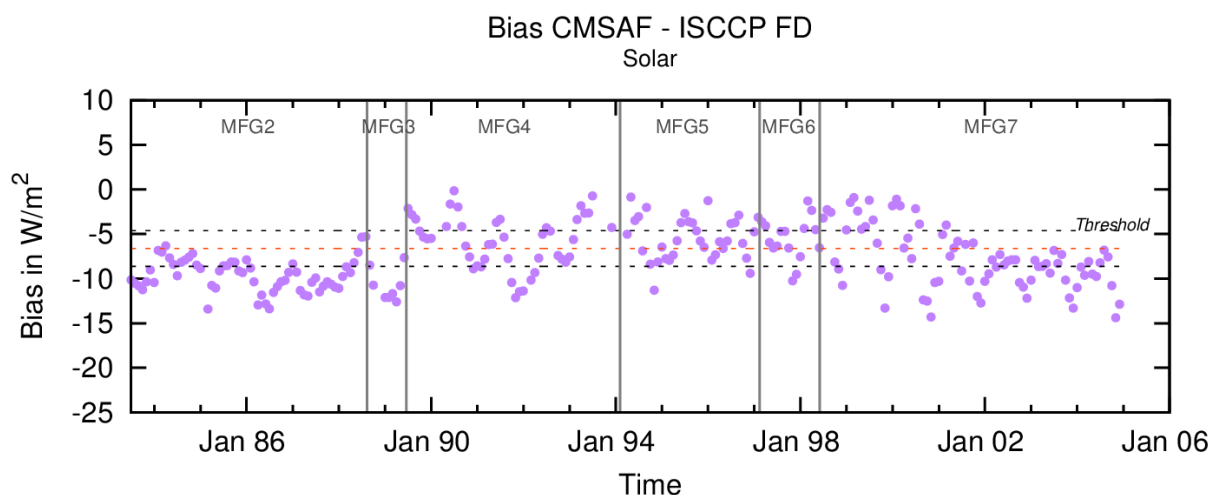


Figure 8: Time series of the bias between CM SAF MM and ISCCP FD TRS products. The red dotted line gives the mean bias over the time series.

4.1.6 Stability of FOV-averaged clear-sky TRS fluxes

This section addresses the stability of the TRS products based on the processing of CS TRS fluxes. These CS fluxes have been obtained from the VIS CS images (see [RD3]) as input of the TOA fluxes processing. The time series stability for the 12 UTC repeat cycle of acquisition is investigated on 5 different surface types as well as all surface together. Figure 9 shows the time series of the CS TRS instantaneous fluxes at 12 UTC over the whole data record and averaged over 5 surface types, while Figure 10 shows the anomalies for these time series. A fixed surface type map compiled from AVHRR data in the frame of the International Geosphere Biosphere Program (IGBP) (Loveland et al., 2000; Townshend, 1994) is used to separate out the pixels into 6 classes: ocean, bright and dark desert, bright and dark vegetation and ice/snow. However, the instantaneous fluxes from the MVIRI/SEVIRI data record retrieved over ice and snow should not be considered. Indeed, the TOA processing (in particular the scene identification) is highly unreliable over these surfaces since their VIS reflectances are too close to those of clouds. Therefore, the snow/ice class is not presented here but are well present in the data record. Furthermore, it should be noted that the displayed time series have been deseasonalised to remove the seasonal cycle (e.g. due to solar insolation).

In general, a good stability in time is observed for each surface type with a limited change between satellites and generations of instruments. However, MFG3 and MFG4 seem to have a slightly higher variability than the other satellites. It is worth considering here that the fluxes are instantaneous fluxes at the maximum illumination of the Meteosat FOV (12 UTC). The observed variability will be decreased by a factor of ~2.5 in the daily and monthly means. In addition, a large jump of about 5 W/m² is apparent on Figure 10 between MFG and MSG eras for dark desert surfaces (magenta curve). For this scene type, which is very infrequent in the FOV, the conversion from MSG channels to the MET7-like VIS channel is quite imperfect.

The use of CS fluxes allows being independent of change in cloudiness but the time series may still suffer of natural changes in aerosol content and surface albedo. The effect of the Mount Pinatubo eruption in 1991 is well visible with increase of the TRS flux over dark surfaces (ocean, dark vegetation) and decrease over bright surfaces (bright desert). The decrease over bright surfaces indicates that the absorption from volcanic aerosols is not negligible.

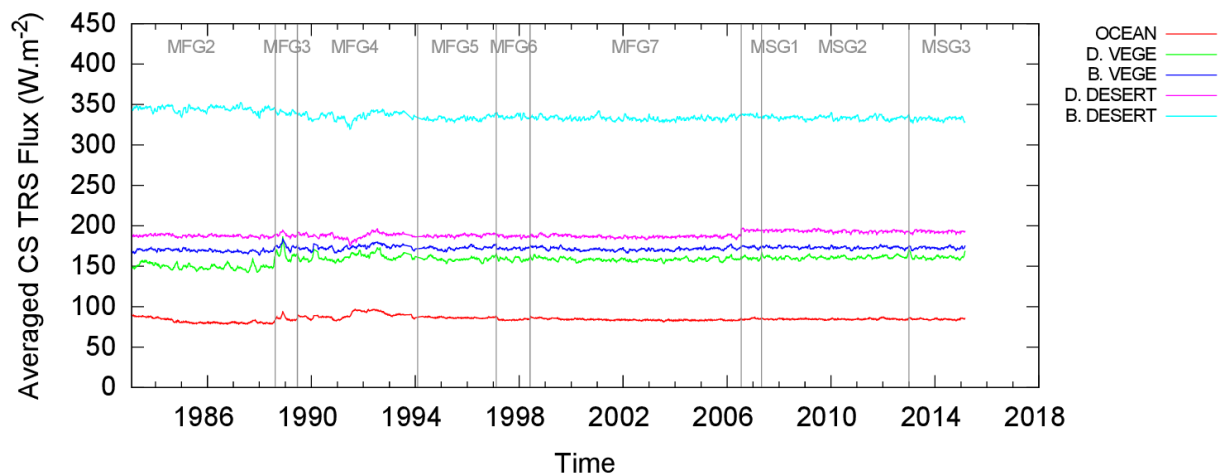


Figure 9 : Time series of averaged CS TRS fluxes according to various surface types.

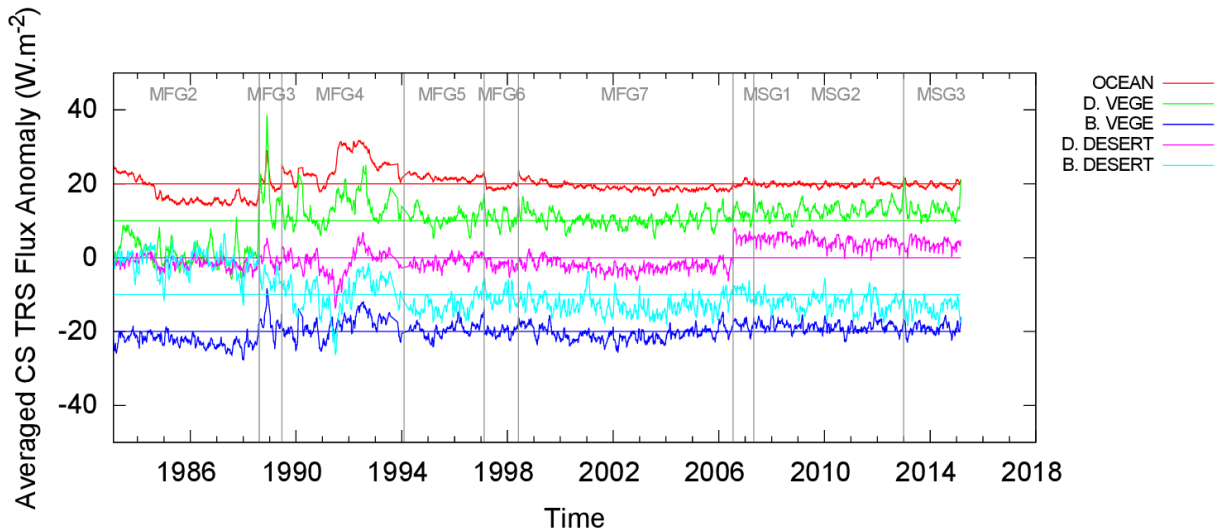


Figure 10: Time series of anomalies for the averaged CS TRS fluxes according to various surface types. The anomalies are obtained by subtracting the average TRS flux (straight lines) from the time series. An additional shift of -20 W/m^2 , -10 W/m^2 , 0 W/m^2 , $+10 \text{ W/m}^2$, $+20 \text{ W/m}^2$ is done to improve the readability of the graph.

Figures 11 and 12 show the time series of the CS TRS instantaneous fluxes, and its anomalies, at 12 UTC without any surface type distinction. Again, the time series has first been deseasonalised before investigating its stability in time. In general, a good stability is observed with a limited change between satellites and generations of instruments. However, a slight decrease in time of the CS TRS fluxes averaged over the whole Meteosat disk is visible, in particular for the MSG era. This is consistent with the observed downward trend in the comparisons with CERES EBAF (see Figure 4) and SYN1deg-Day (see Figure 5).

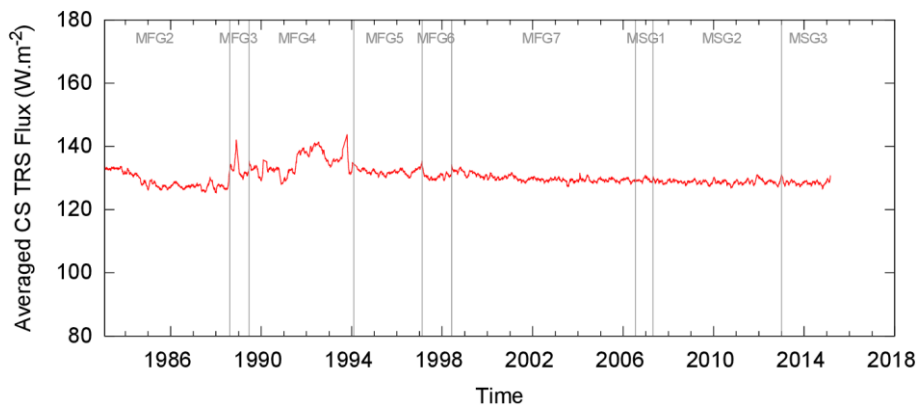


Figure 11: Time series of CS TRS fluxes averaged over the whole Meteosat disk.

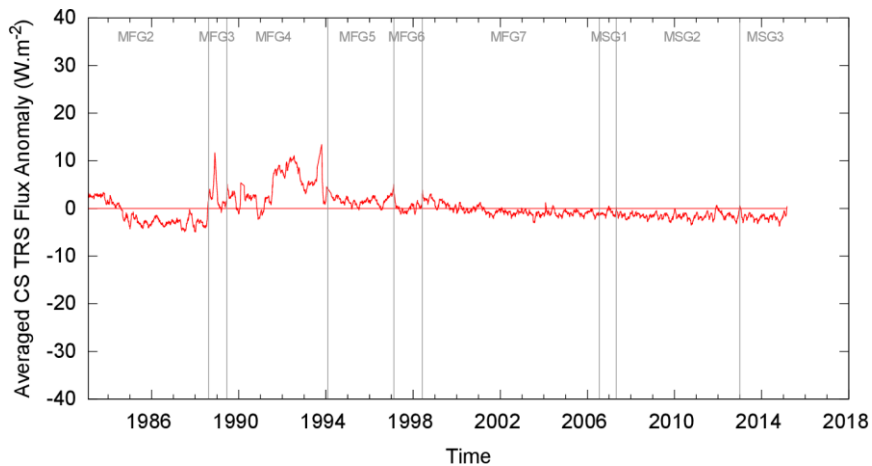


Figure 12: Time series of anomalies for the CS TRS fluxes averaged over the whole Meteosat disk. The anomalies are obtained by subtracting the average TRS flux (straight line) from the time series.

4.1.7 Stability of FOV-averaged all-sky TRS fluxes

Figures 13 and 14 show the time series of the TRS instantaneous all-sky fluxes, and anomalies, at 12 UTC averaged over the 5 previously mentioned surface types. It should be noted that the displayed time series have first been deseasonalised to remove the seasonal cycle and then been locally smoothed to reduce the variations due to rapid changes in the cloud cover. The applied smoothing procedure consists in taking the local mean from inside a moving window of 60 days. Such a span allows removing the effect of clouds while keeping the main natural variations in the time series. In general, a good stability in time is observed for each surface type with a limited change between satellites and generations of instruments. Unlike the CS TRS fluxes, the all-sky TRS fluxes do not seem to have a particularly higher variability for MFG3 and MFG4 than other satellites. On the other hand, MFG2 and MFG3 seem to have a smaller absolute level of the TRS fluxes over dark vegetation than the others.

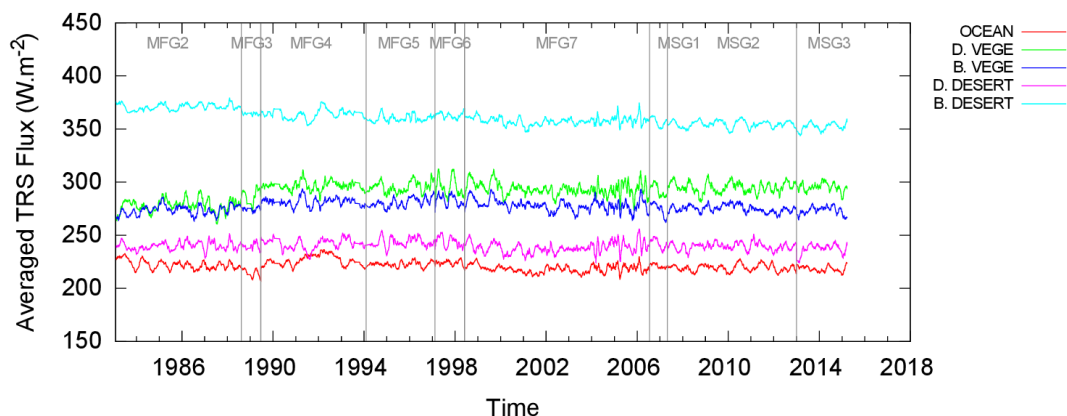


Figure 13: Time series of averaged TRS fluxes according to various surface types.

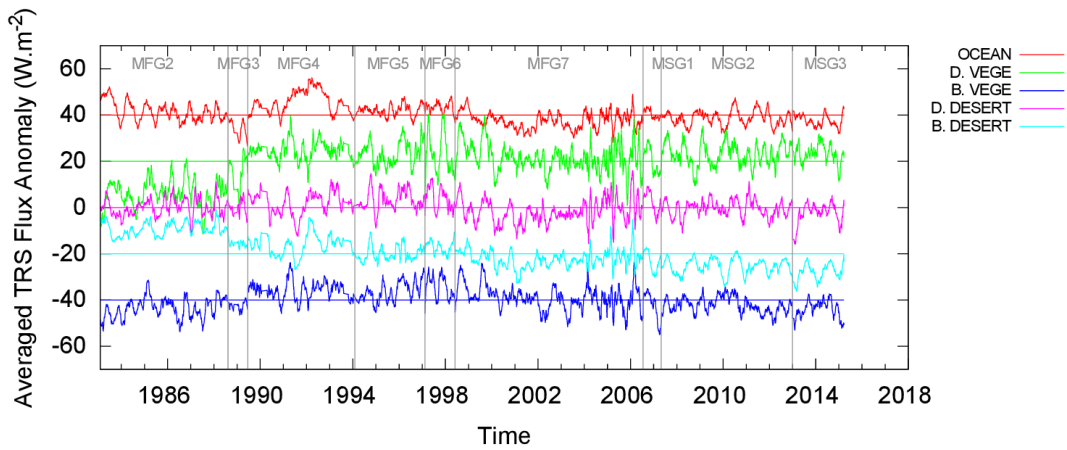


Figure 14: Time series of anomalies for the averaged TRS fluxes according to various surface types. The anomalies are obtained by subtracting the average TRS flux (straight lines) from the time series. An additional shift of -40 W/m^2 , -20 W/m^2 , 0 W/m^2 , $+20 \text{ W/m}^2$, $+40 \text{ W/m}^2$ is done to improve the readability of the graph.

Figures 15 and 16 show the time series of the TRS instantaneous all-sky fluxes, and anomalies, at 12 UTC without any surface type distinction. Again, the time series has first been deseasonalised and locally smoothed over a moving window of 60 days before investigating its stability in time. In general, a good stability is observed. Figure 16 suggests a slight decrease in time of the TRS fluxes averaged over the whole Meteosat disk.

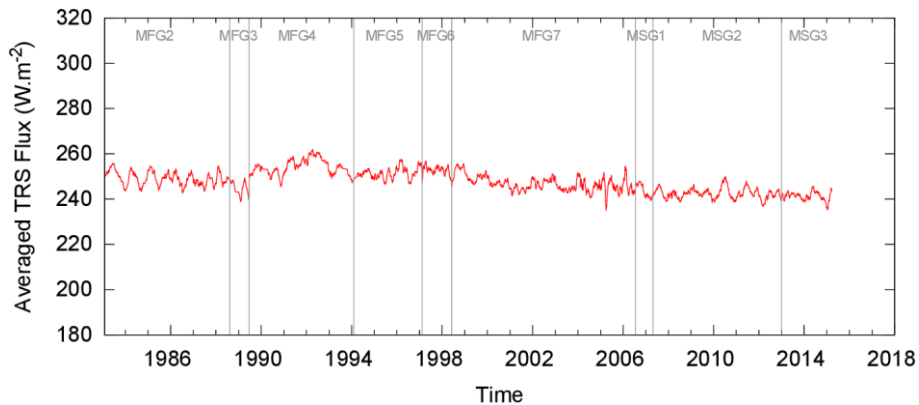


Figure 15: Time series of TRS fluxes averaged over the whole Meteosat disk.

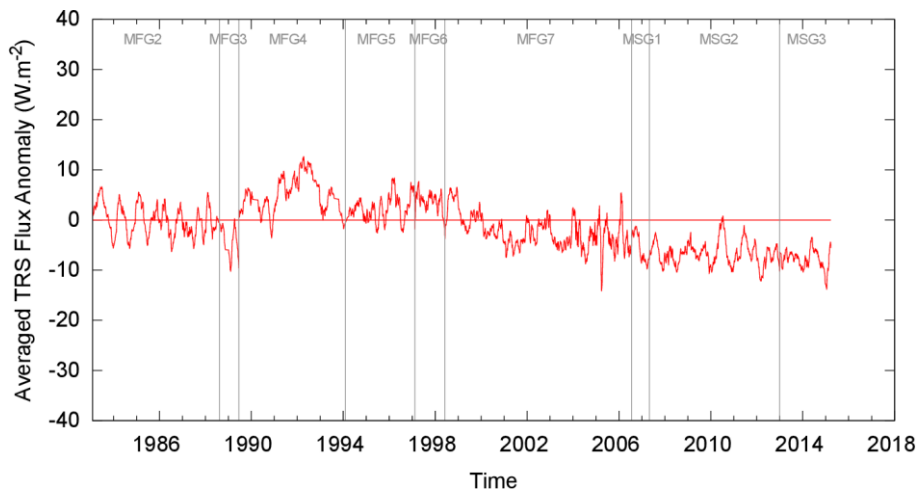


Figure 16: Time series of anomalies for the TRS fluxes averaged over the whole Meteosat disk. The anomalies are obtained by subtracting the average TRS flux (straight line) from the time series.

4.1.8 Discussion of TRS stability results and absolute level

From the (somewhat contradicting) results presented before, it is not possible to provide a single value that would represent the stability of the TRS products over the full data record extend. It is however obvious that the stability is far from the optimal and target requirements (0.3 and 0.6 W/m²/decade, resp.). On the other hand, most of the results agree with a stability better than the threshold value of 4 W/m²/decade for the MM. The main argument to support this is the good long term consistency with the ERBS WFOV-CERES data record (see Figure 7). Since the ERBS/CERES reconstruction is itself inhomogeneous, it is expected that the stability is better than reflected by this comparison. From the time series of CS fluxes anomalies (see Figure 10) it is expected that the threshold requirement of 4 W/m²/decade will be met not only in all-sky but also over most of the surface types in CS conditions.

Table 4 gives a summary of the averaged biases, expressed in W.m⁻², of the MM TRS products per satellite wrt to several data records. The last line gives the (max –min) values. The 4 W/m²/decade threshold is fulfilled except with respect to the ISCCP FD data record and in the all-sky anomaly.

	Scientific Validation Report TOA Radiation MVIRI/SEVIRI Data Record	Doc.No.: SAF/CM/RMIB/VAL/MET_TOA
		Issue: 1.1
		Date: 05 October 2016

Table 4 : Averaged biases (in $W.m^{-2}$) of the MM TRS products per satellite.


	CERES EBAF	ERBS WFOV CERES	ISCCP FD	Averaged CS flux anomaly (divided by 2.5)	Averaged all-sky flux anomaly (divided by 2.5)
MFG2	-	-1.5	-9.7	-0.6	0.7
MFG3	-	-1.3	-10.2	0.8	-0.9
MFG4	-	1.3	-5.8	1.8	2.8
MFG5	-	0.2	-5.5	0.6	1.6
MFG6	-	0.1	-5.3	0.1	2.2
MFG7	0.3	-0.8	-7.8	-0.2	-0.4
MSG1	0.5	-1.1	-	-0.4	-1.6
MSG2	0.1	-0.6	-	-0.6	-1.9
MSG3	-0.3	-0.8	-	-0.7	-2.4
(max-min)	0.8	2.8	4.9	2.5	5.2

Concerning the absolute level of the systematic error, the CM SAF TRS data agree closely with the CERES EBAF data record (the average bias is about $-0.1 W.m^{-2}$). A higher averaged bias is observed wrt the CERES SYN1deg-Day products (about $1.6 W.m^{-2}$) while in general a negative bias is observed wrt ISCCP FD ($-6.6 W.m^{-2}$) and wrt ERBS WFOV–CERES ($-0.9 W.m^{-2}$) records. The relative bias of $1.7 W.m^{-2}$ between EBAF Ed2.8 and SYN1deg E3A inferred from our comparisons is consistent with the early EBAF adjustment of $1.7 W.m^{-2}$ for SW TOA flux compared to SRBAVG-GEO Ed2D_rev1 reported in Loeb et al., 2009.

4.2 Accuracy of monthly mean TRS products

4.2.1 Comparison with CERES EBAF

To estimate the overall accuracy of the MVIRI/SEVIRI MM TRS products, the RMS difference (bias corrected) wrt CERES EBAF has been computed. As it can be seen in Figure 17, the RMS difference is clearly better after the addition of Aqua in the EBAF product in July 2002. Considering only this period and removing the outlier points (sampling problem due to missing input data), the accuracy can be estimated at $3.6 W.m^{-2}$.

	Scientific Validation Report TOA Radiation MVIRI/SEVIRI Data Record	Doc.No.: SAF/CM/RMIB/VAL/MET_TOA Issue: 1.1 Date: 05 October 2016
---	--	---

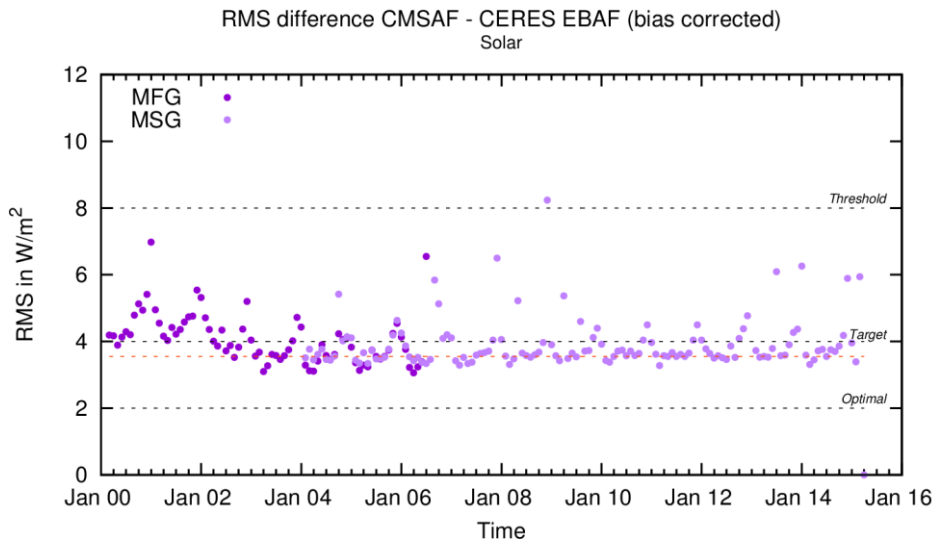


Figure 17: Time series of the RMS difference (bias corrected) between CM SAF MM and CERES EBAF TRS products. The red dotted line gives the mean RMS over the time series. Dark violet dots are for MFG data while purple dots are for MSG data. The optimal, target and threshold accuracies are indicated in black dotted lines.

Figures 18 and 19 show the comparison between CM SAF MM and CERES EBAF TRS products for the best and the worst months in terms of bias-corrected RMS difference, respectively April 2006 and December 2008. Mean values, RMS (bias not corrected) and sigma (RMS bias corrected) computed in the region between 50°S, 50°N, 50°E and 50°W (which approximately corresponds to VZA<60°), are also provided in the figures.

The image of the difference on Figure 18 (bottom left panel) do not show obvious regional problem. The RMS difference (bias corrected) is about 3.1 W/m² and is consistent with the 4 W/m² target accuracy. On the other hand, Figure 19 shows a huge RMS difference (8.2 W/m²) for December 2008, a month featured by 9 missing days due to SEVIRI instrument decontamination.

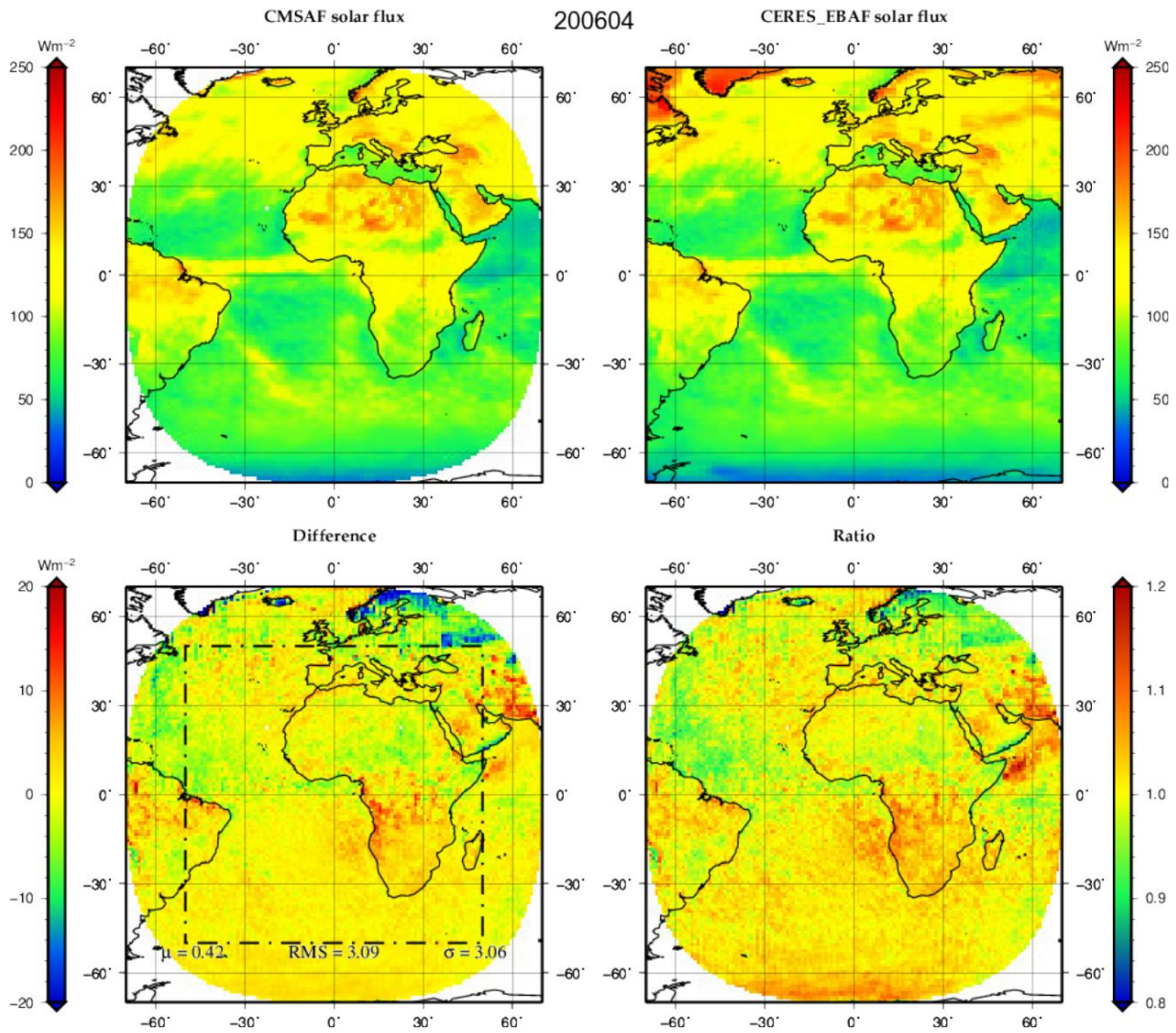


Figure 18: Comparison of CM SAF MM and CERES EBAF TRS products for April 2006 (MFG7). Upper panels show the CM SAF (left) and CERES EBAF (right) products. Bottom images show the difference (left) and the ratio (right) of these products.

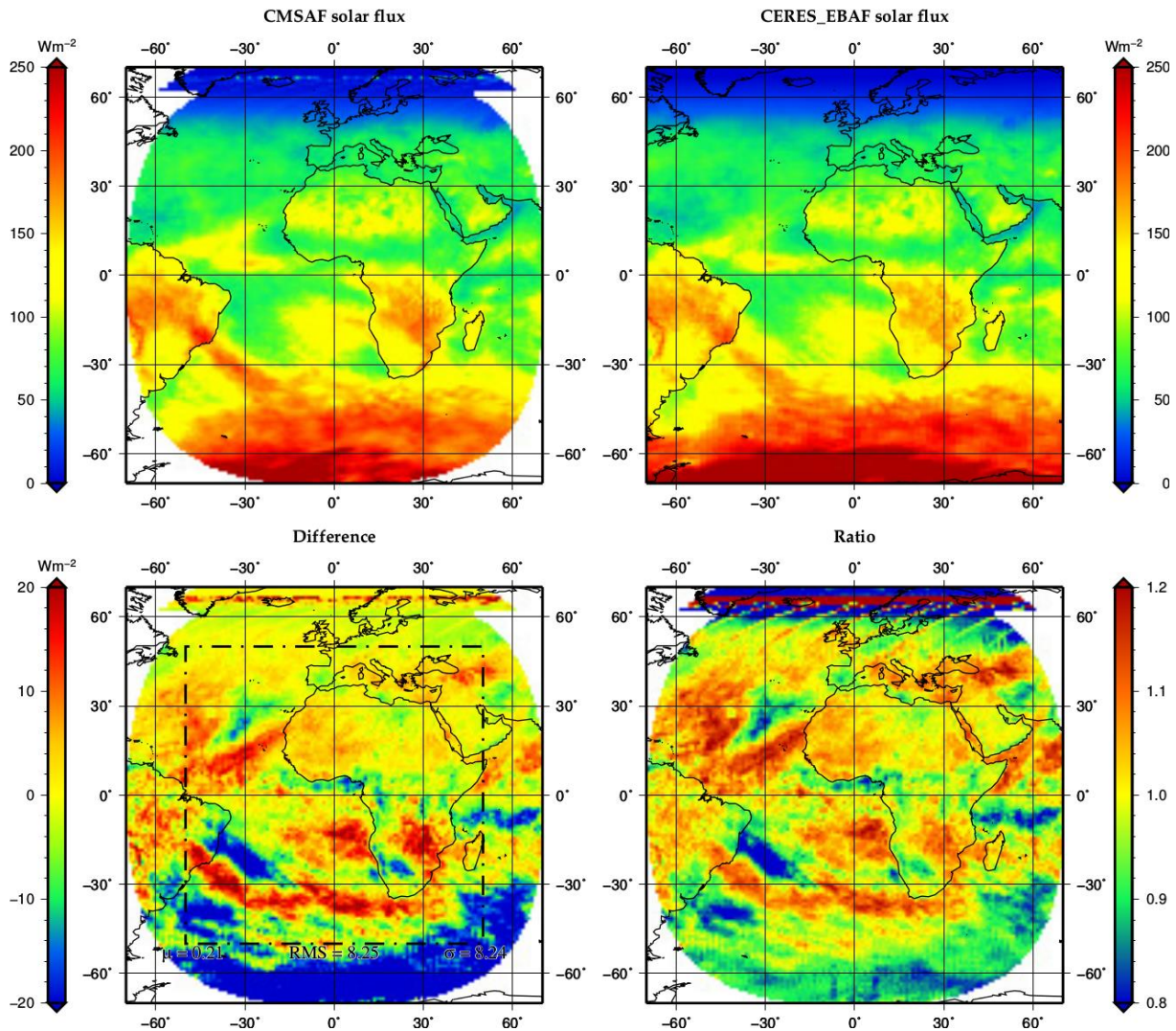


Figure 19: Comparison of CM SAF MM and CERES EBAF TRS products for December 2008 (MSG2). Upper panels show the CM SAF (left) and CERES EBAF-TOA (right) products. Bottom images show the difference (left) and the ratio (right) of these products.

4.2.2 Comparison with ERBS WFOV-CERES

Figure 20 shows the temporal evolution of the RMS difference with respect to the ERBS WFOV-CERES data record. The RMS is about 10 W/m² during the pre-CERES period, when the ERA interim is tuned using the ERBS-WFOV data. During the CERES period, the RMS is about 6 W/m² which is less good than the direct comparison with EBAF data.

RMS difference CMSAF - ERBS WFOV-CERES (bias corrected)
Solar

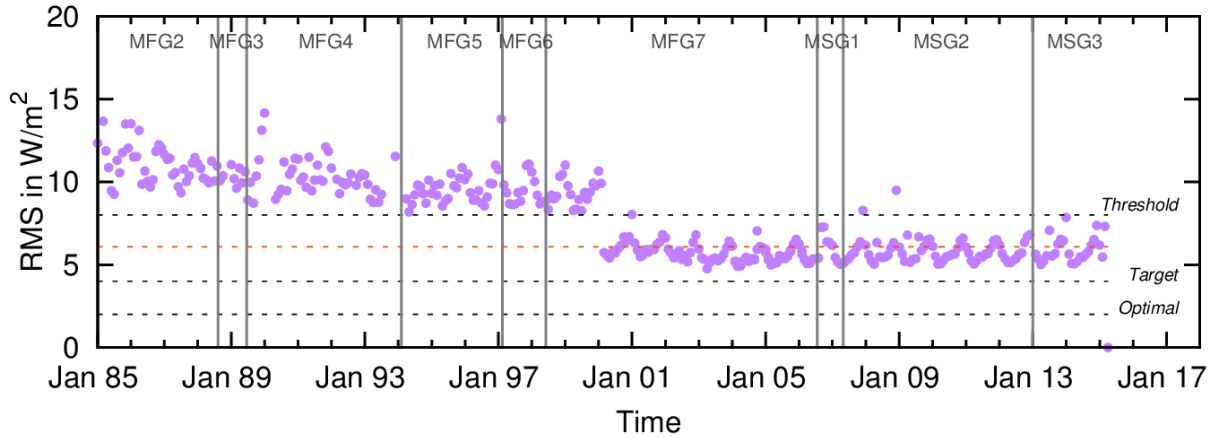


Figure 20: Time series of the RMS difference (bias corrected) between CM SAF MM and ERBS WFOV-CERES TRS products. The optimal, target and threshold accuracies are indicated in black dotted lines.

4.2.3 Comparison with ISCCP FD

Figure 21 shows the time series of the RMS difference (bias corrected) with respect to the ISCCP FD data record. Generally, the RMS lies between 6 and 8 W/m^2 , except for the months with missing data. These highest levels of RMS difference (with respect to the comparison with CERES EBAF) can be attributed to the FD data record. Still the graph is interesting as it does not exhibit significant change of RMS difference over the extended period.

RMS difference CMSAF - ISCCP FD (bias corrected)
Solar

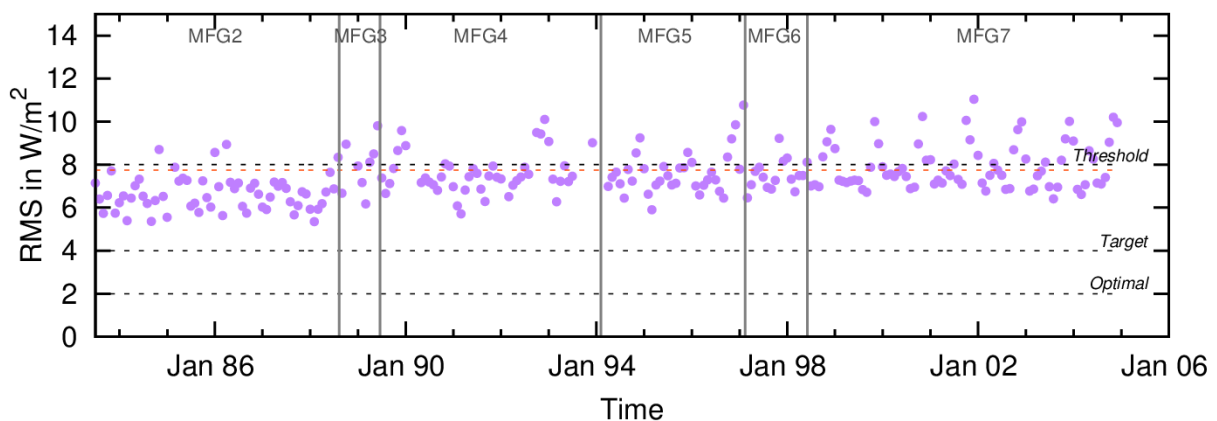


Figure 21 : Time series of the RMS difference (bias corrected) between CM SAF MM and ISCCP FD TRS products. The optimal, target and threshold accuracies are indicated in black dotted lines.

4.2.4 Effect of missing data

Figure 22 shows the bias (left panel) and the RMS difference (right panel, bias-corrected) of the CM SAF - EBAF comparison as a function of the number of days without Meteosat TRS observations during the month, for instance due to decontamination or satellite failure. As expected the bias does not present dependency on the number of missing days while the

RMS shows a clear increase. The increase of RMS error in the monthly mean TRS product due to missing data is estimated to $0.3 \text{ W/m}^2/\text{day}$. The intercept is consistent with 3.6 W/m^2 accuracy already mentioned.

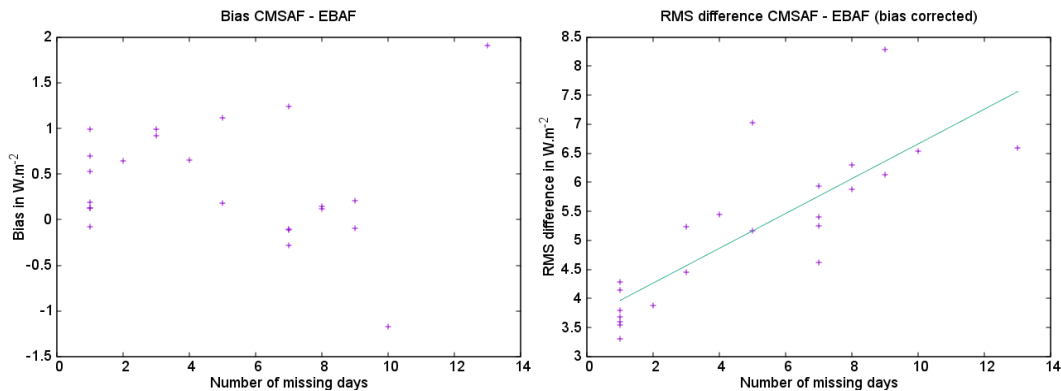


Figure 22: Bias (left) and RMS (right) of the CM SAF - EBAF comparison as a function of the number of days without Meteosat TRS observations.

4.2.5 Discussion

The accuracy on the MM TRS products is estimated at 3.6 W/m^2 , as well for the MFG as for the MSG era. This accuracy is consistent with the one of the MM TRS products in the GERB data record (estimated at 3.0 W/m^2 , [RD 5]), given the need of the additional NB to BB step in the MVIRI/SEVIRI data records. The 3.6 W/m^2 value, and the $0.3 \text{ W/m}^2/\text{day}$ increase in case of missing input, are reported in Table 8, in the summary.

4.3 Accuracy of daily mean TRS products

4.3.1 Comparison with CERES SYN1deg-Day

The RMS difference (bias corrected) with respect to CERES SYN1deg-Day for each day from March 2000 to March 2015 is shown in Figure 23. As for the MM products, the data before July 2002 (pre-Aqua) have slightly higher RMS. Discarding this period, a RMS difference of 6.5 W/m^2 is observed which lies within the target accuracy of 8 W.m^{-2} for this product. Looking at the MFG/MSG overlap period (2004-2006) shows that the error characteristics are not dependent on whether MVIRI or SEVIRI is used as input.

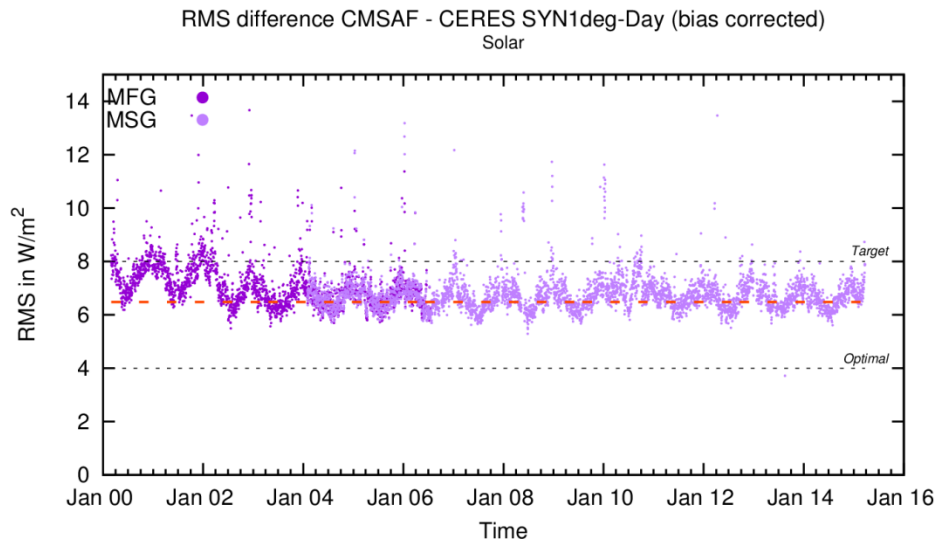


Figure 23: Time series of the RMS difference (bias corrected) between CM SAF DM and CERES SYN1deg-Day TRS products. The optimal and target accuracies are indicated in black dotted lines (threshold at 16 W/m² is out of the figure).

Obviously, a part of the 6.5 W/m² RMS difference can be attributed to error in the SYN1deg-Day product. Under the assumption of uncorrelated errors and assuming a similar level of error for both DM products, they would have an accuracy of about 4.6 W/m². Assuming a twice better accuracy for CERES SYN1deg-Day (thanks to the BB observations, the better scene identification using MODIS, ...), the observed RMS difference would be explained by a 5.8 W/m² and 2.9 W/m² RMS errors for the CM SAF and SYN1deg-Day products, respectively. It is decided not to rely on such assumptions and instead adopt the 6.5 W/m² as (an upper limit of) the CM SAF DM accuracy.

Figures 24 and 25 show the intercomparisons of the products for the best and the worst days of the data record in terms of RMS difference, respectively the 26th June 2008 and the 13th March 2002. For a “good day” (Figure 24) the image of the difference does not exhibit obvious regional patterns. On the other hand, Figure 25 shows obvious artefacts, in this case affecting the CERES SYN1deg-Day product.

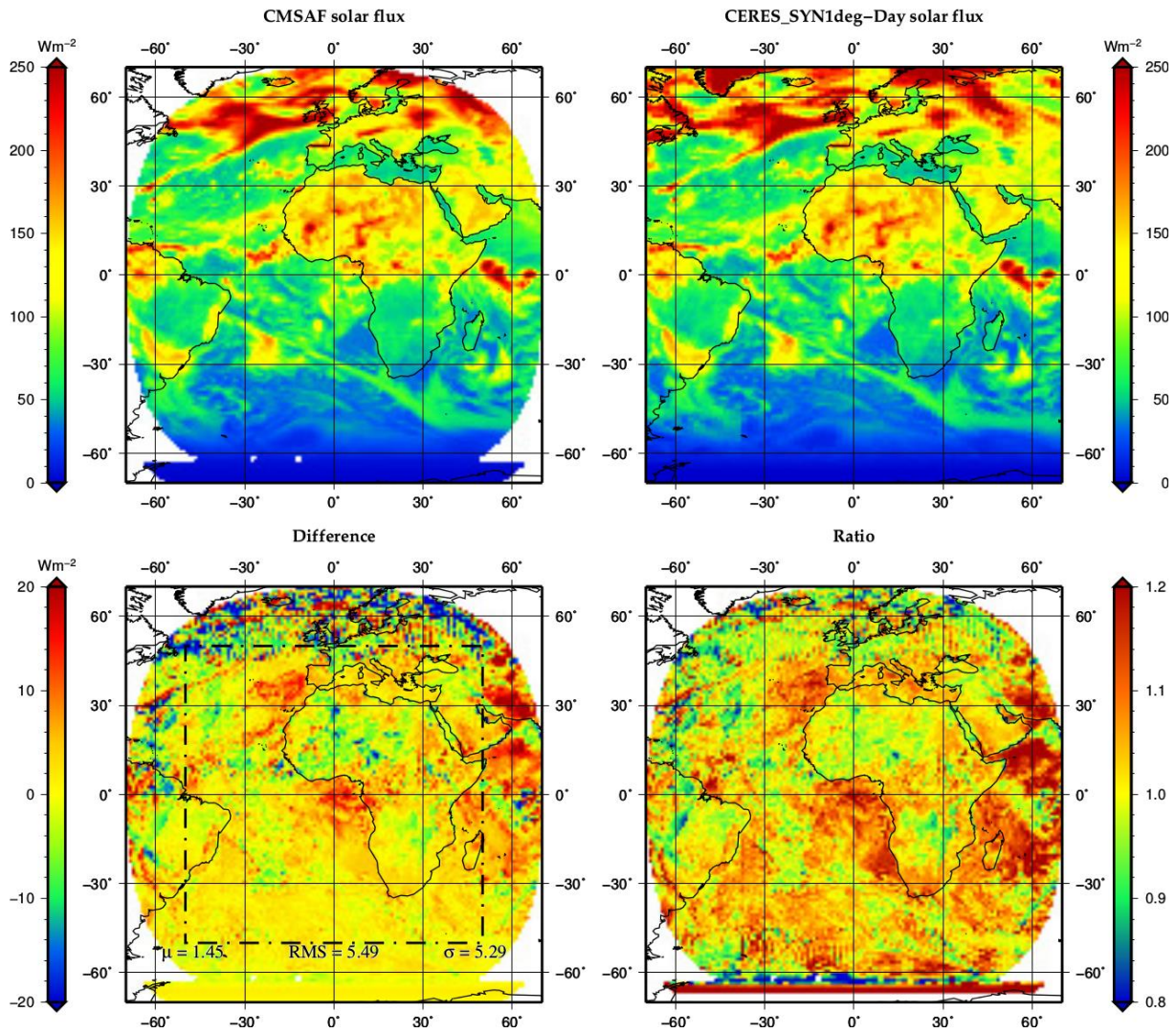


Figure 24: Comparison of CM SAF DM and CERES SYN1deg-Day TRS products for the 26th June 2008 (MSG2). Upper panels show the CM SAF (left) and CERES SYN1deg-Day (right) products. Bottom images show the difference (left) and the ratio (right) of these products.

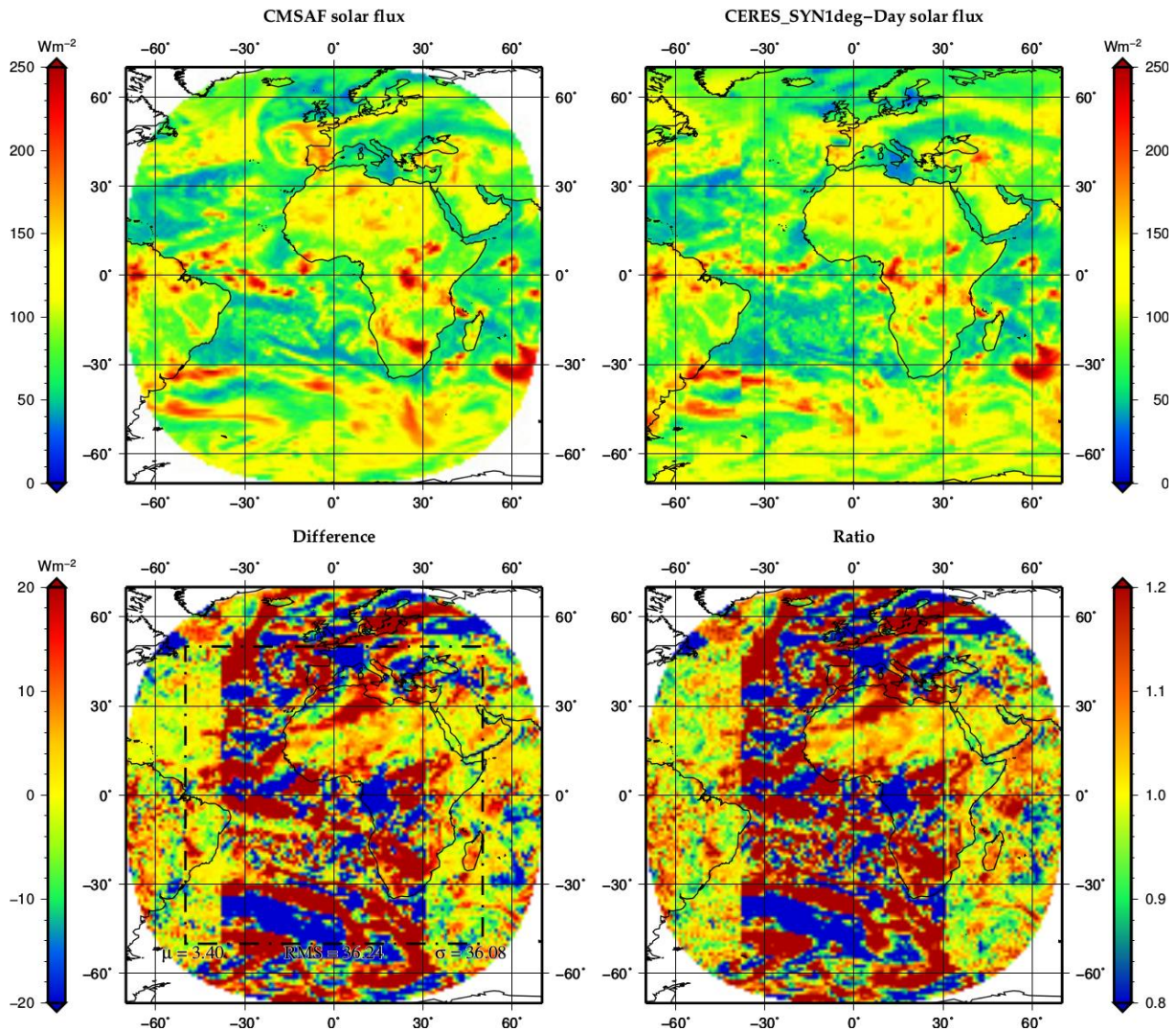


Figure 25: Comparison of CM SAF DM and CERES SYN1deg-Day TRS products for the 13th March 2002 (MFG7). Upper panels show the CM SAF (left) and CERES SYN1deg-Day (right) products. Bottom images show the difference (left) and the ratio (right) of these products.

4.3.2 Effect of missing data

The methodology described in section 3.2.3 is followed to quantify the (additional) error that can affect the daily mean when some input Meteosat images are missing. Figure 26 shows the bias (left panel) and RMS (right panel, bias corrected) of the differences with respect to the CERES SYN1deg-Day products as a function of the number of missing MVIRI images. It should be noted that the days with more than 5 (MVIRI) or 11 (SEVIRI) successive missing images were not considered because the interpolation of missing data can not exceed 3 hours in the daily processing. No DM product is issued in these cases.

	Scientific Validation Report TOA Radiation MVIRI/SEVIRI Data Record	Doc.No.: SAF/CM/RMIB/VAL/MET_TOA Issue: 1.1 Date: 05 October 2016
---	--	---

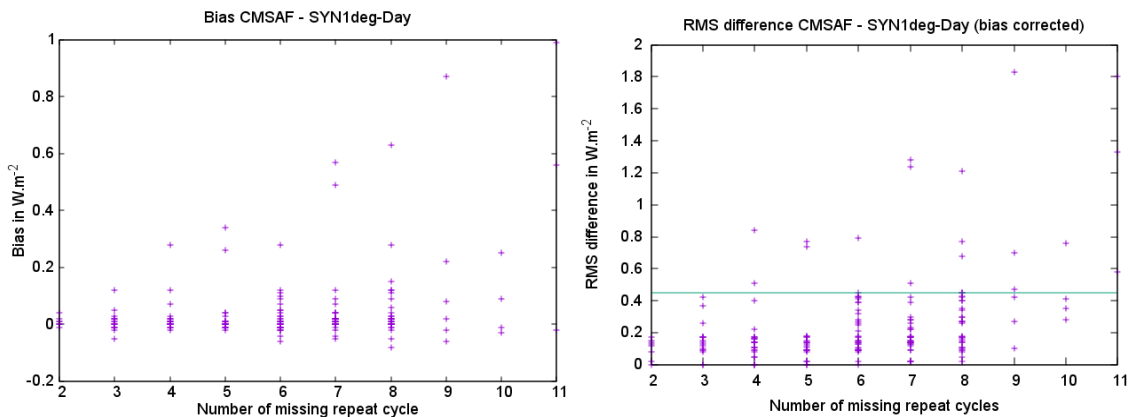


Figure 26: Bias (left) and RMS (right, bias corrected) of the CM SAF - CERES SYN1deg-Day comparison as a function of the number of repeat cycles of acquisition without Meteosat TRS observations.

Although a value of 0.9 W/m^2 is reported for a particular day with 9 missing images, the bias remains in general small. The RMS error does not show an obvious dependency on the number of missing images. The error is probably highly dependent on the timing of the missing observations: (i) missing images during the night have less impact on the DM TRS product than during the day and (ii) a large number of short gaps is more accurately interpolated than a long gap. For a large majority (0.9 percentile) of the days with missing input data, the RMS errors are of the order or lower than 0.5 W/m^2 and it is proposed to report this value as representative of the effect of missing data on the DM TRS. Obviously, most of the days in the data record are based on a complete set of input data and are not affected by this error.

4.3.3 Discussion

The accuracy on the DM TRS is estimated at 6.5 W/m^2 , as well for the MFG as for the MSG era. This accuracy is consistent with the one of the DM TRS products in the GERB data record (estimated at 5.5 W/m^2 , [RD 5]), given the need of the additional NB to BB step in the MVIRI/SEVIRI data records. The 6.5 W/m^2 value, and the 0.5 W/m^2 increase in case of missing input, are reported in Table 8, in the summary.

4.4 Accuracy of monthly mean diurnal cycle TRS products

4.4.1 Comparison with CERES SYN1deg-M3hour

The overall accuracy of the CM SAF MMDC products is estimated by computing the RMS difference (bias corrected) against the CERES SYN1deg-M3Hour products for each monthly diurnal cycle, in 3-hours intervals, from March 2000 to March 2015. As it can be seen in Figure 27, the overall mean RMS difference for each time interval lies under the threshold accuracy of 16 W.m^{-2} . This threshold is exceeded only occasionally for specific months. Obviously, the magnitude of the error is higher for the daytime intervals (e.g. 09 and 12 UTC) than during the night. In the worst cases, for the two most illuminated intervals of 09 UTC (i.e. the 3-hours interval [09-12] UTC) and 12 UTC (i.e. the 3-hours interval [12-15] UTC), the overall mean RMS error is estimated at about 11 W.m^{-2} . The time series shows that the error characteristics remain stable during the 2000 – 2015 period and are similar for the MFG and MSG satellites.

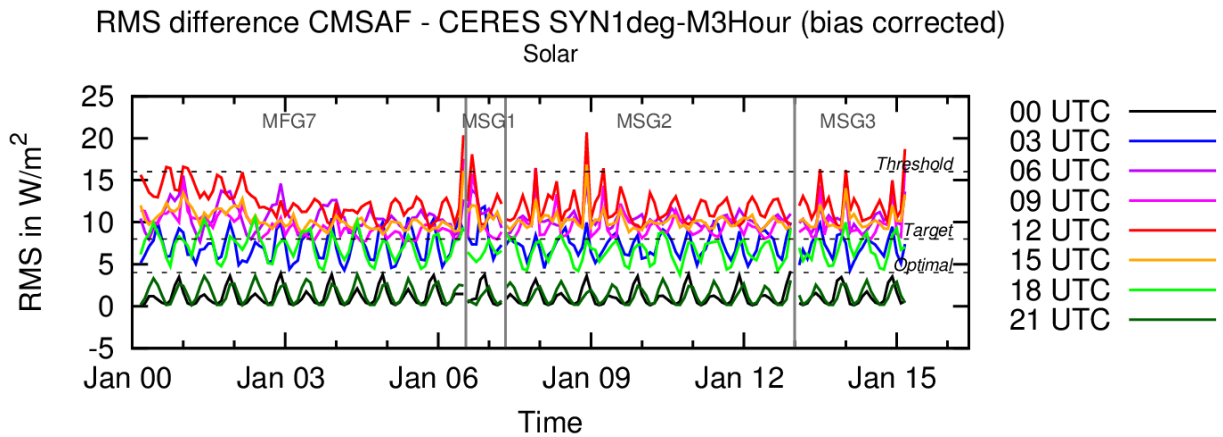


Figure 27: Time series of the RMS difference (bias corrected) between CM SAF MMDC and CERES SYN1deg-M3Hour TRS products. The optimal, target and threshold accuracies are indicated in black dotted lines.

Figures 28 and 29 show the 12 UTC (i.e. the 3-hours interval [12-15] UTC) comparison for the best and the worst months in terms of RMS difference, respectively November 2004 and December 2008. Figure 28 shows some localized errors along the East coast of the African continent. The bias-corrected RMS difference of $9.1 W/m^2$ is slightly above the $8 W/m^2$ target accuracy but is consistent with the $16 W/m^2$ threshold. Figure 29 shows an RMS error of $20.67 W/m^2$ resulting from 9 missing days during the month of December 2008.

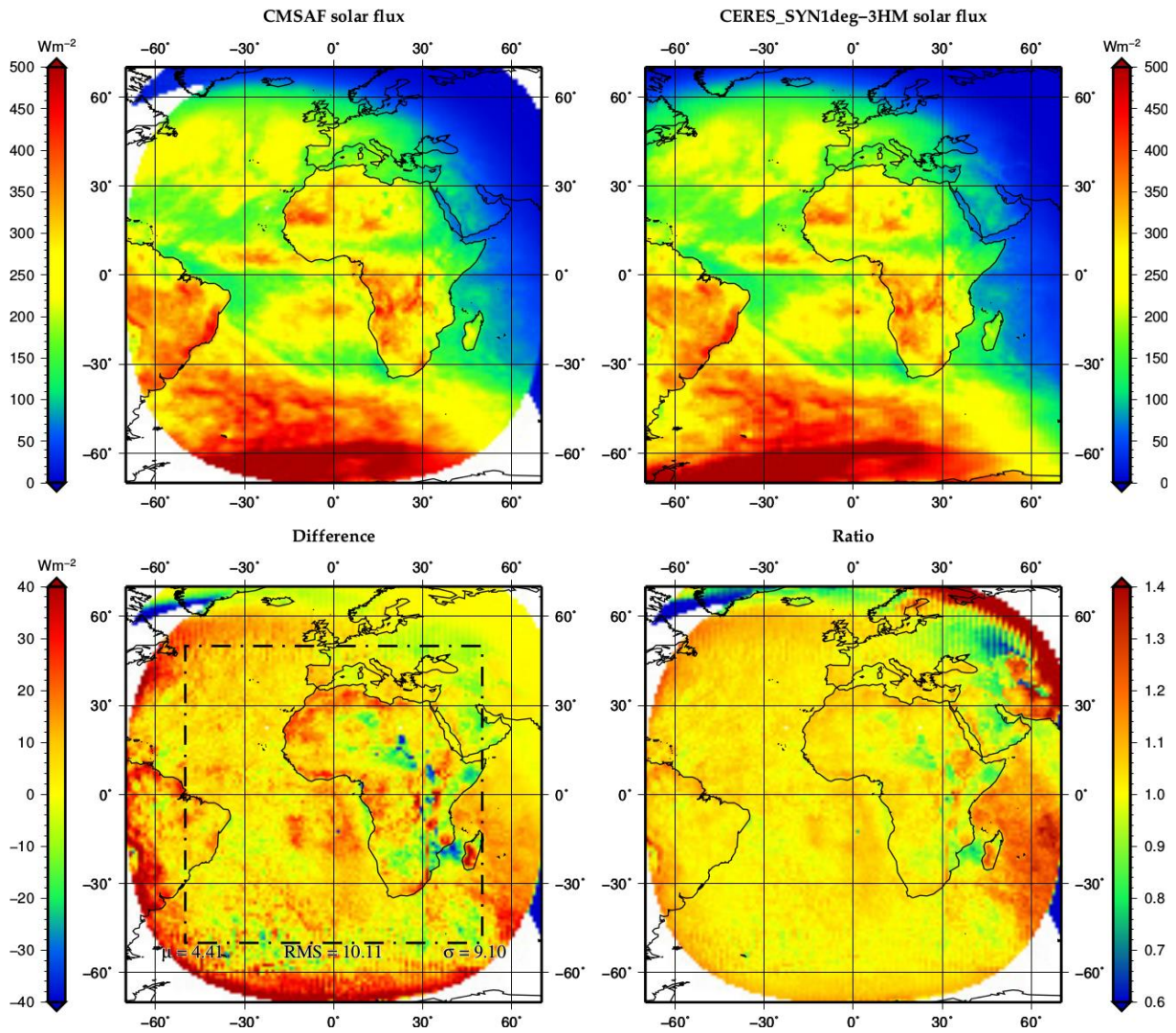


Figure 28: Comparison of CM SAF MDC and CERES SYN1deg-M3Hour TRS products for November 2004 (MFG7) at 12 UTC. Upper panels show the CM SAF (left) and CERES SYN1deg-M3Hour (right) products. Bottom images show the difference (left) and the ratio (right) of these products.

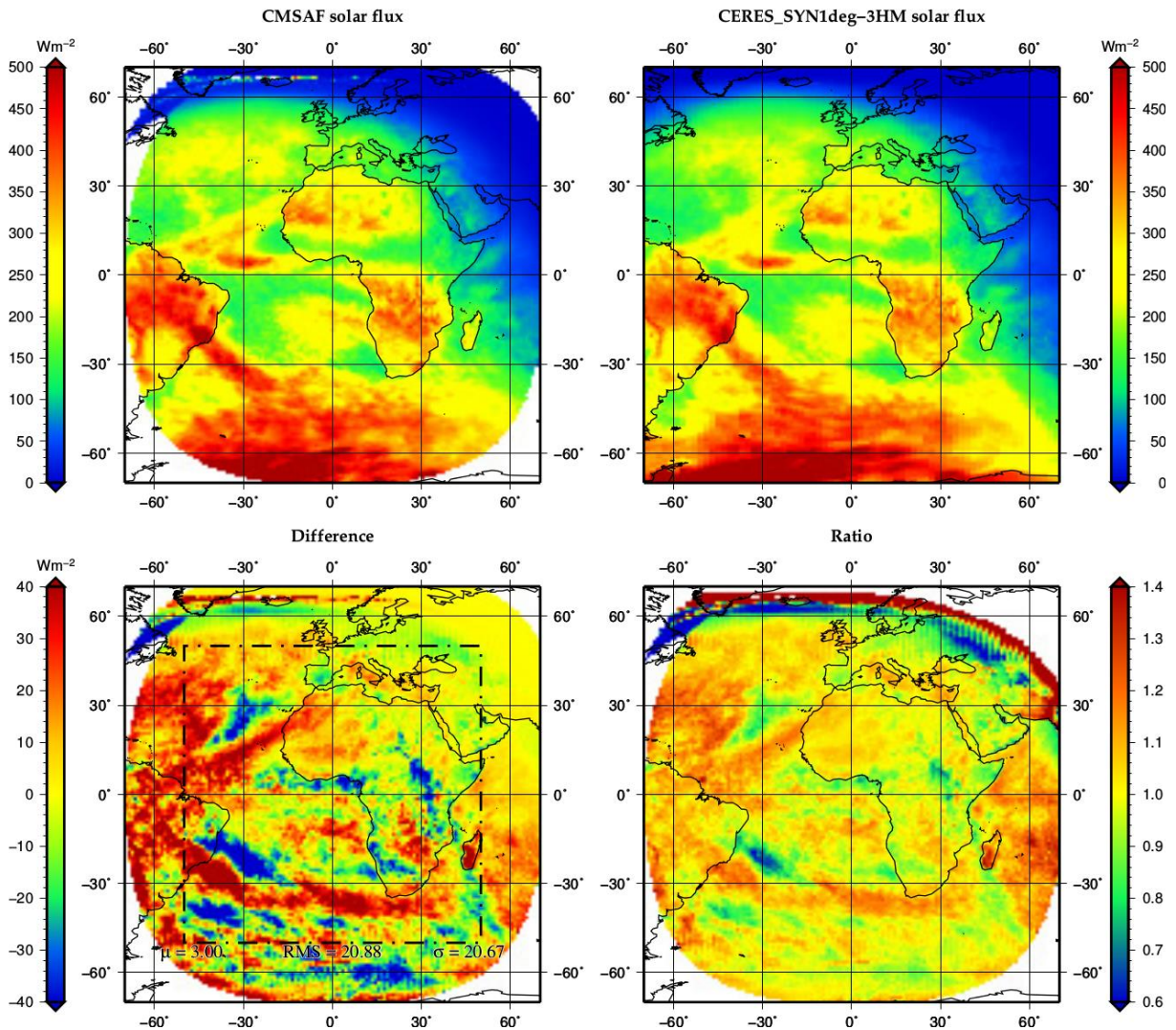


Figure 29: Comparison of CM SAF MDC and CERES SYN1deg-M3Hour TRS products for December 2008 (MSG2) at 12 UTC. Upper panels show the CM SAF (left) and CERES SYN1deg-M3Hour (right) products. Bottom images show the difference (left) and the ratio (right) of these products.

4.4.2 Effect of missing data

Figure 30 shows the bias (left panel) and the RMS difference (right panel, bias corrected) of the CM SAF - SYN1deg-M3Hour comparison as a function of the number of days without Meteosat TRS observations within the month (for instance due to decontamination or satellite failure). The various monthly 3-hourly averaged fluxes are shown in different colours. The biases in the diurnal cycle products are in general positive and are higher for the day time intervals (up to $6 \text{ W}\cdot\text{m}^{-2}$ for 09 and 12 UTC) and close to 0 for the night time. As for the MM products, it is difficult to explain the bias as a function of the number of days without observations (see left panel). Therefore, only the bias-corrected RMS are kept as indication of the error. As observed in the right panel, the RMS difference between the products increases more or less linearly with the number of missing days within the month. The slopes and intercepts for each time interval are reported in Table 5. In the worst cases, for the two most illuminated intervals of 09 and 12 UTC, the RMS error is in average $11 + 0.7 N_{\text{day}} \text{ W}\cdot\text{m}^{-2}$.

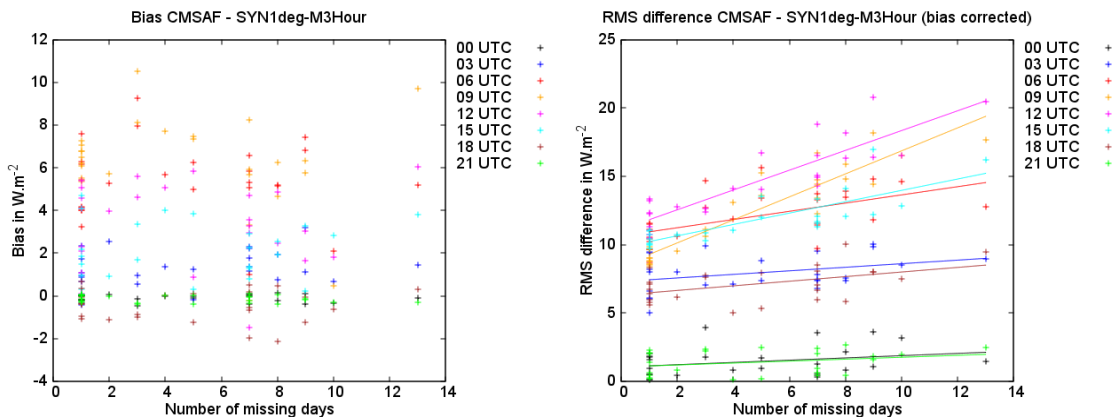


Figure 30: Bias (left) and RMS (bias-corrected, right) of the CM SAF - SYN1deg-M3Hour comparison as a function of the number of days without Meteosat TRS observations.

Table 5: Increase of the RMS error of the CM SAF - SYN1deg-M3Hour TRS comparison as a function of the number of missing days and intercept values for each 3-hours time interval.

3-hourly interval	RMS error increase (W/m ² /day)	Intercept (W/m ²)
00 UTC	0.1	1.1
03 UTC	0.1	7.3
06 UTC	0.3	10.6
09 UTC	0.8	8.4
12 UTC	0.7	11.1
15 UTC	0.4	9.8
18 UTC	0.2	6.3
21 UTC	0.1	1.1

4.4.3 Discussion

The accuracy on MMDC TRS products is estimated at about $11.0 + 0.7 N_{\text{day}}$ W/m² both for the MFG and MSG eras. These numbers, which refer to the intervals with the highest TRS fluxes (around 12 UTC), are reported in Table 8, in the summary.

It should be noted that this accuracy is not the one of the products at full spatial (0.05° lat-lon) and temporal (1-hourly interval) resolution but instead of the products when averaged in 1° spatial grid boxes and 3-hourly intervals.

	Scientific Validation Report TOA Radiation MVIRI/SEVIRI Data Record	Doc.No.: SAF/CM/RMIB/VAL/MET_TOA Issue: 1.1 Date: 05 October 2016
---	--	---

5 Validation of TET Products

5.1 Radiometric stability of the TET products

5.1.1 Stability wrt CERES EBAF

The radiometric stability of the TET MM products is first addressed by computing the bias against CERES EBAF for each month from March 2000 to March 2015, see Figure 31. The mean bias over the whole time series is indicated by the red dotted line at -4.9 W/m^2 and the black dotted lines on both sides at $\pm 2 \text{ W/m}^2$ indicate the threshold requirements of $4 \text{ W/m}^2/\text{decade}$ for stability. The MFG and MSG data are plotted respectively in dark violet and purple and show a close agreement in the overlap period. In general, a good stability in time is observed with a limited change between satellites and generations of instruments. The bias varies more or less continuously without sharp transitions and is consistent with the stability threshold of $4 \text{ W/m}^2/\text{decade}$. The thermal flux during the MSG2 period (from May 2007 to December 2012) appears slightly higher than the rest of the time series.

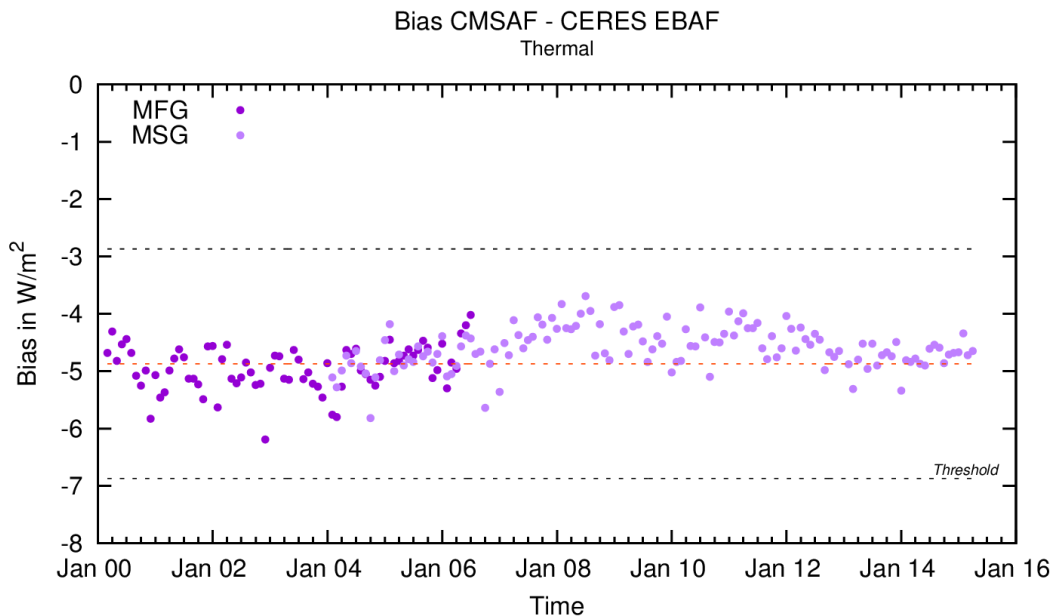


Figure 31: Time series of the bias between CM SAF MM and CERES EBAF TET products. The red dotted line gives the mean bias over the time series.

5.1.2 Stability wrt CERES SYN1deg-Day

Figure 32 shows the time series of the bias of the DM TET products against the CERES SYN1deg-Day products. The mean bias over the whole time series, indicated by the red dotted line, is -4.3 W/m^2 .

Significant changes of the bias are observed for some short periods of one or several days (“outliers”). Even if the use of the MVIRI recalibration using HIRS has significantly improved the overall stability of the time series, some discontinuities still remain and are reflected by occasional abnormally high/low thermal fluxes for several consecutive days. These peaks are due to sudden changes of the instrument gain level which are not fully taken into account in the current version of the MVIRI recalibration. Some outliers are also attributed to the SYN1deg-Day processing (see for instance Figure 51 and the discussion in section 5.3.1).

The apparent increase of the bias after July 2002 is explained by the addition of Aqua in the SYN1deg-Day products.

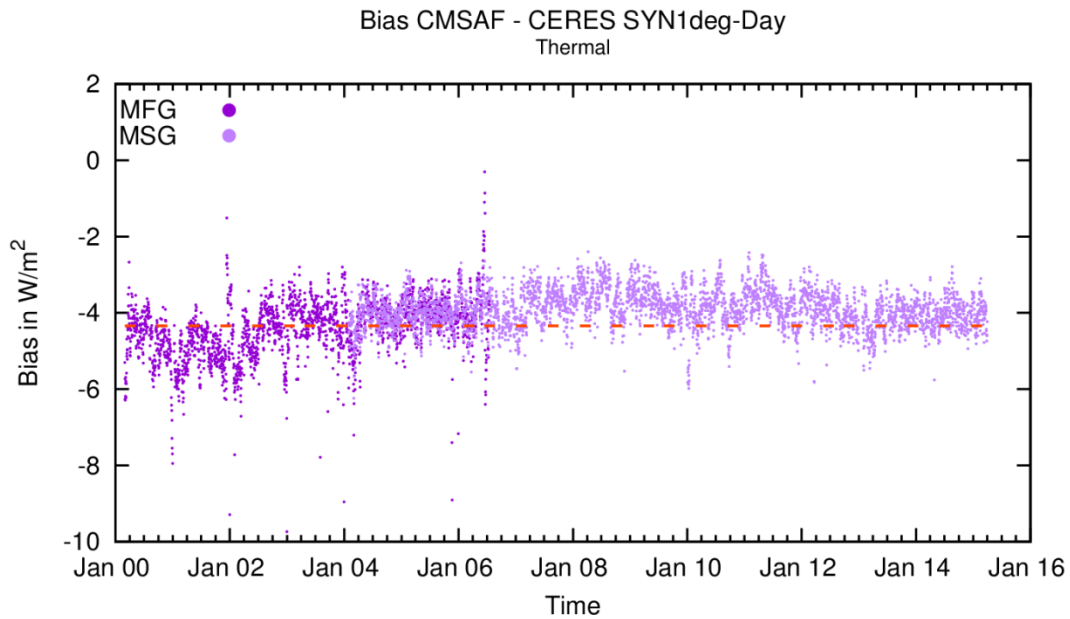


Figure 32: Time series of the bias between CM SAF DM and CERES SYN1deg-Day TET products. The red dotted line gives the mean bias over the time series.

5.1.3 Stability wrt CERES SYN1deg-M3hour

The radiometric stability of the TET MMDC products is investigated by comparing with the CERES SYN1deg-M3Hour products. Time series of the bias between both data records are shown in Figure 33 for the various 3-hourly intervals (which are referred to by the start of the interval).

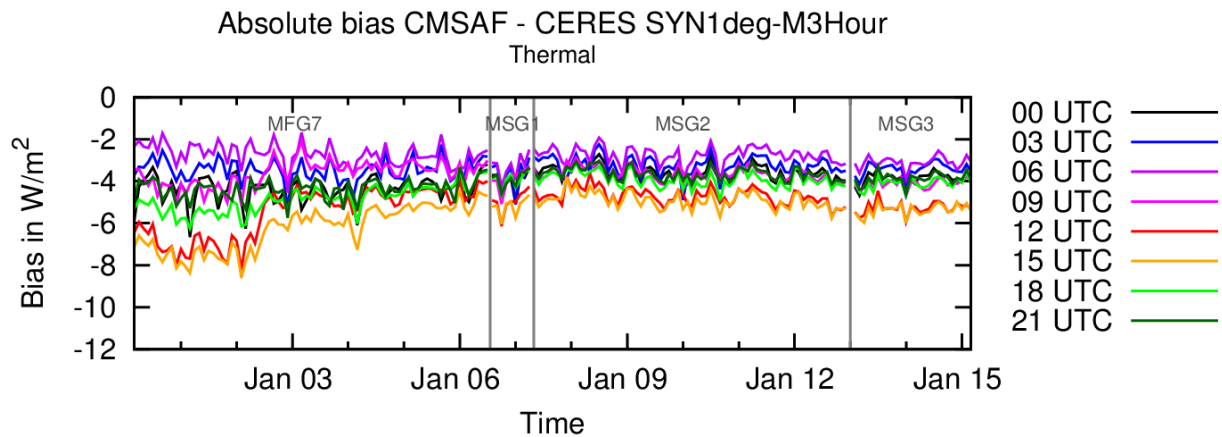


Figure 33: Time series of the bias between CM SAF MMDC and CERES SYN1deg-M3Hour TET products.

Some diurnal variation is observed in the biases which are higher during “cold” intervals (nighttime, early morning) and lower during “warm” intervals (midday and afternoon). Several causes may be responsible for this. First, it is worth remembering that the CERES thermal products are based on a difference between the total (TOT) and SW channel measurements and this can introduce a diurnal cycle in the CERES thermal level. This is the most likely cause of the change observed in July 2002 for the 12 and 15 UTC curves. Before July 2002 the CERES products are based on the FM1 instrument which shows, compared to GERB, higher thermal flux during daytime than night time (Clerbaux et al., 2009). Secondly, the Meteosat TET fluxes retrieval, based on the WV and IR bands, may be inaccurate over very

	Scientific Validation Report TOA Radiation MVIRI/SEVIRI Data Record	Doc.No.: SAF/CM/RMIB/VAL/MET_TOA Issue: 1.1 Date: 05 October 2016
---	--	---

warm deserts which are typically observed during the afternoon in the Meteosat FOV. The thermal emissivity of the desert surface can also be responsible for this.

Discarding the data before July 2002, the bias remain mostly between -2 W/m^2 and -5 W/m^2 , which fulfils the $4 \text{ W/m}^2/\text{decade}$ threshold requirement for the stability.

5.1.4 Stability wrt HIRS OLR CDR – Daily

The radiometric stability is further investigated by comparison with the HIRS OLR CDR - Daily (described in section 3.1.4), as shown in Figure 34. This CDR is especially useful as it covers the early part of the data record contrary to the CERES products. MFG2 and MFG3 data are displayed in red as the recalibration of the WV and IR channels using HIRS is not yet available for these satellites. The operational calibration is used instead (see the Algorithm Theoretical Basis Document [RD3] for details about the calibration). The mean bias, computed for MFG4 to MSG3, is -3.1 W/m^2 and is indicated by the red dotted line on Figure 34.

Generally speaking, the MFG2 and MFG3 levels agree reasonably well with the following satellites and the 4 W/m^2 stability requirements are fulfilled. However, a significant peak is observed for MFG2 from the 19th January 1987 until the 2^d April 1987. After investigation, this peak seems to be due to a sudden change of the calibration gain level happening on the 19th January 1987 at the slot 17 which may have not been properly taken into account in the operational calibration. However, no explanation was found for the return to the normal level on the 2^d April 1987 since no change of the calibration gain level occurs on this date (it should have stayed constant until the 21st April 1987). As long as a solution is not found, those DM TET products (and the corresponding MM products) should be flagged and the users should be warned not to use them.

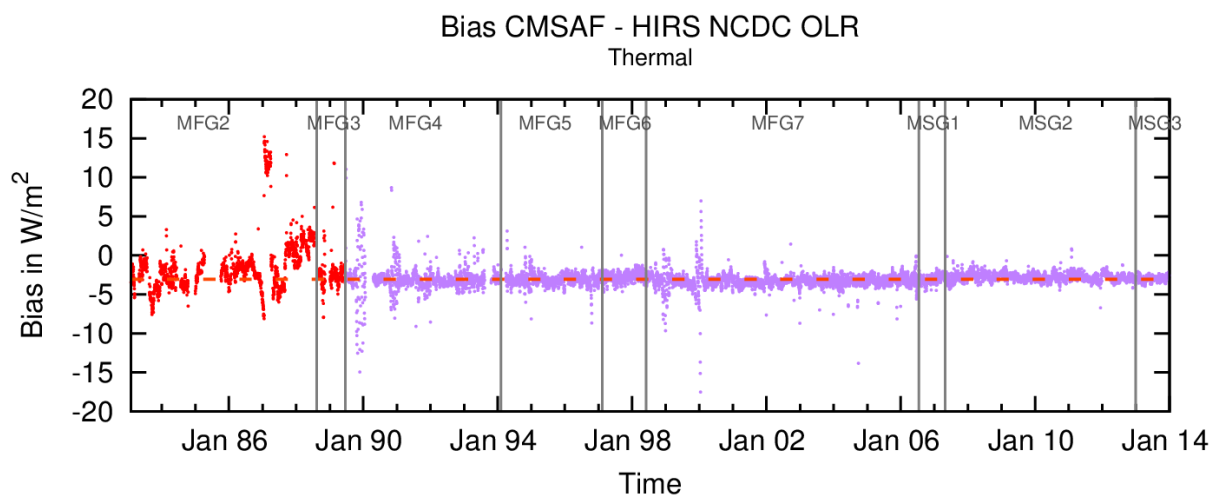


Figure 34: Time series of the bias between CM SAF TET DM and HIRS OLR CDR - Daily products. The red dotted line gives the mean bias over the time series. MET-2 and -3 data, displayed in red, use the EUMETSAT operational calibration.

5.1.5 Stability wrt HIRS OLR CDR – Monthly

Another reference useful to address the radiometric stability of the MM products is the HIRS OLR CDR – Monthly data record (described in section 3.1.5). Time series of the bias is shown in Figure 35. A really good stability in time is observed with a bias which varies quite continuously without sharp transitions or jumps between satellites and remains within the stability threshold of $4 \text{ W/m}^2/\text{decade}$, except for Meteosat-2. In particular, a significant peak is observed in the MFG2 time series during the months of January, February and March 1987.

It can be noted that the MFG3 level agrees well with the following satellites. The mean bias, computed for MFG3 to MSG3, is about -3.8 W/m^2 and is indicated by the red dotted line in Figure 35.

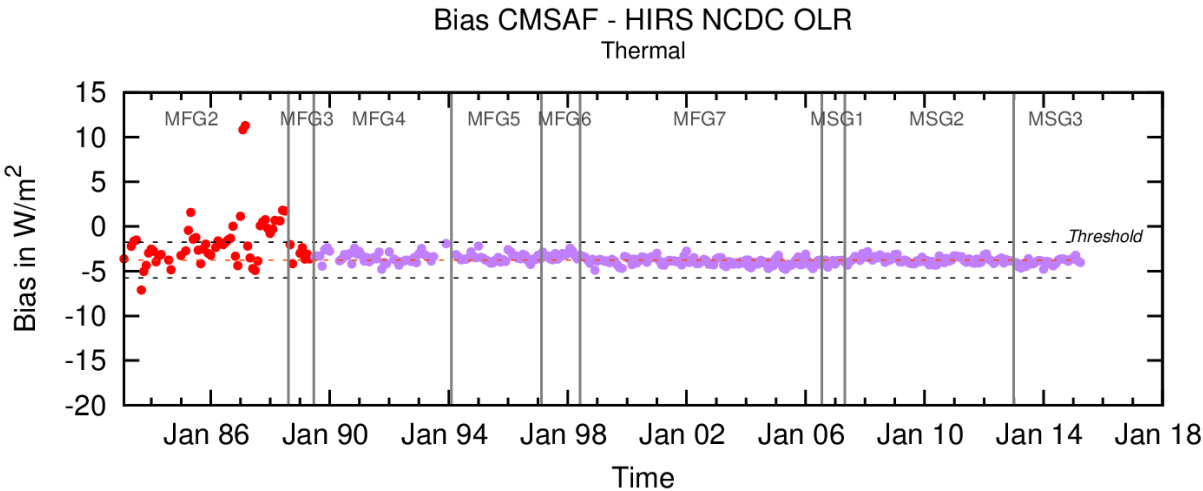


Figure 35: Time series of the bias between CM SAF TET MM and HIRS OLR CDR – Monthly products. The red dotted line gives the mean bias over the time series. MET-2 and -3 data, displayed in red, use the EUMETSAT operational calibration.

5.1.6 Stability wrt ERBS WFOV-CERES – Monthly

On Figure 36, the MM TET products are compared to the recently updated ERBS WFOV-CERES (or DEEP-C) data record over the period 1985-2015. From March 2000 onward, when CERES data are used to generate the ERBS WFOV-CERES data record, a very good stability in time is observed with no apparent change between satellites and the stability threshold of 4 W/m^2 is met. Prior to 2000, however, when the MM radiative fluxes are reconstructed, the variability of the bias is much larger and widely exceeds the threshold. The mean bias, computed from March 2000 onward, is about -4.7 W/m^2 and is indicated by the red dotted line. It is interesting to mention that the jump at end of Meteosat-2 observed with HIRS OLR CDR – Monthly is not present in this comparison. As with the previous comparison, the bias is higher during three months in 1987.

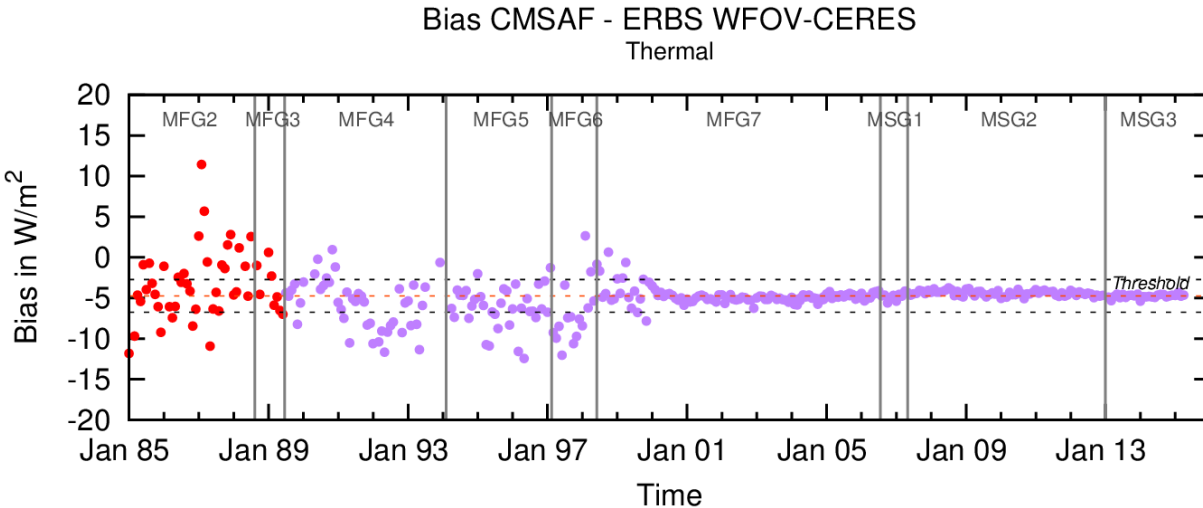


Figure 36: Time series of the bias between CM SAF MM and ERBS WFOV-CERES (or DEEP-C) TET products. The red dotted line gives the mean bias over the time series. MET-2 and -3 data, displayed in red, use the EUMETSAT operational calibration.

	Scientific Validation Report TOA Radiation MVIRI/SEVIRI Data Record	Doc.No.: SAF/CM/RMIB/VAL/MET_TOA Issue: 1.1 Date: 05 October 2016
---	--	---

5.1.7 Stability wrt ISCCP FD

The radiometric stability of the early part of the MVIRI/SEVIRI data record is also addressed with respect to the ISCCP FD data record from July 1983 to December 2004, as shown in Figure 37. Stability issues are mainly observed for MFG2 while MFG3 seems to agree well with the following MFG satellites. Again a significant peak is observed for the months of January, February and March 1987. The mean bias, computed for MFG4 to MFG7, is about 0.6 W/m^2 and is indicated by the red dotted line.

The decreases of the bias observed around 1994 and at the end of 2001 are not supported by similar variations wrt the CERES, HIRS or ERBS WFOV-CERES data records. These decreases of the bias are therefore attributed to an increase of the OLR in the ISCCP FD data record. Concerning the discontinuity at the end of 2001, it is worth noting that a similar change is observed wrt the ISCCP FD TRS fluxes (see Figure 8).

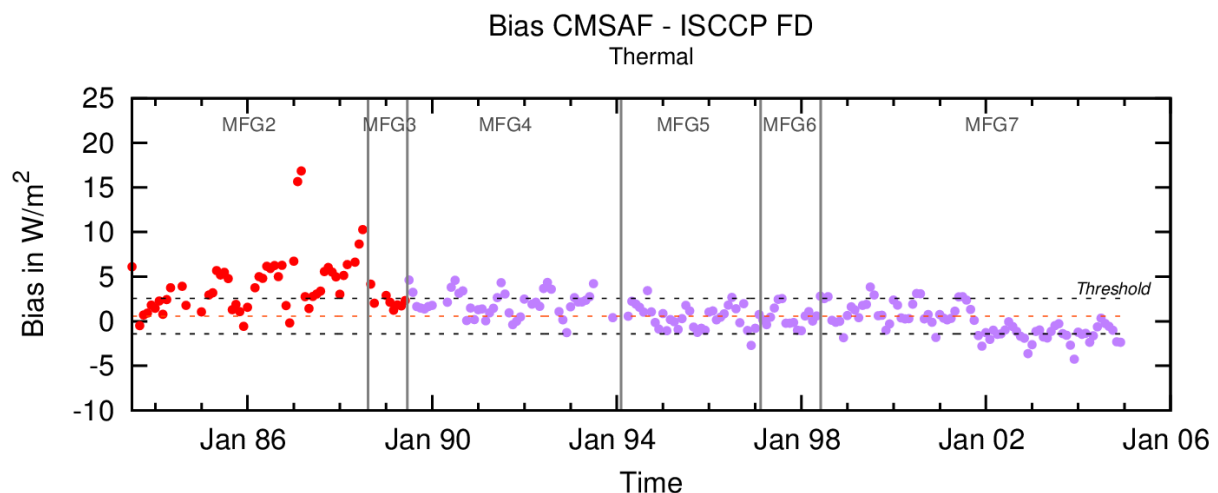


Figure 37: Time series of the bias between CM SAF MM and ISCCP FD TET products. The red dotted line gives the mean bias over the time series. MET-2 and -3 data, displayed in red, use the EUMETSAT operational calibration.

5.1.8 Stability of FOV-averaged TET fluxes

Figure 38 shows the time series of the TET instantaneous fluxes at 12 UTC over the whole data record and averaged over the 5 already mentioned surface types (see section 4.1.6), while Figure 39 shows the anomalies for these time series. Again, the displayed time series have first been deseasonalised to remove the seasonal cycle and then been locally smoothed (from inside a moving window of 60 days) to reduce the variations due to changes in the cloud cover. In general, a good stability in time is observed for each surface type with a limited change between satellites and generations of instruments. A significant peak is observed during the year 1987 in the MFG2 time series for all surface types. As explained before this peak is attributed to a change in the calibration gain level that may have not been properly taken into account in the operational calibration. This results in a significant jump in the TET values around this date.

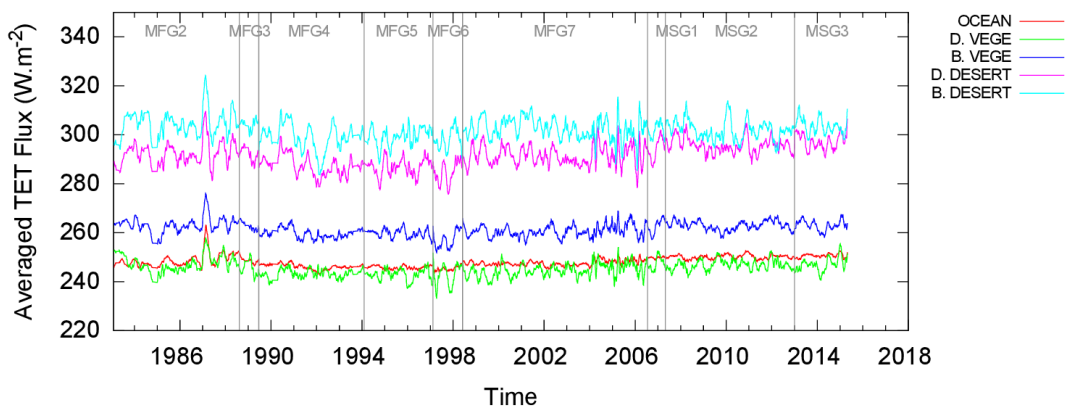


Figure 38: Time series of averaged TET fluxes according to various surface types.

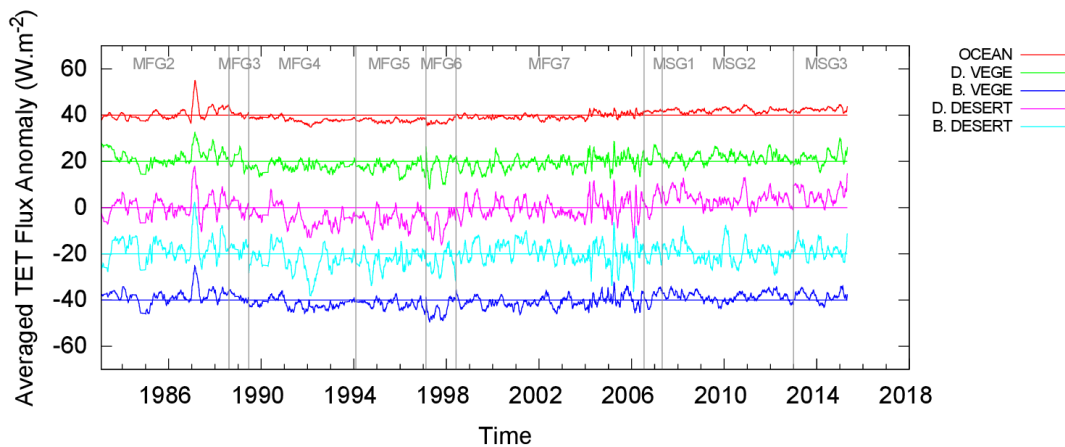


Figure 39: Time series of anomalies for the averaged TET fluxes according to various surface types. The anomalies are obtained by subtracting the average TET flux (straight lines) from the time series. An additional shift of -40 W/m^2 , -20 W/m^2 , 0 W/m^2 , $+20 \text{ W/m}^2$, $+40 \text{ W/m}^2$ is done to improve the readability of the graph.

Figure 40 shows the time series of the TET instantaneous fluxes at 12 UTC averaged over the full Meteosat disk without any surface type distinction, while Figure 41 shows the anomalies for this time series. Again, the time series has first been deseasonalised and locally smoothed over a moving window of 60 days before investigating its stability in time. The same peak as before is observed in the MFG2 time series during the year 1987. In general, a good stability is observed with a limited change between satellites and generations of instruments.

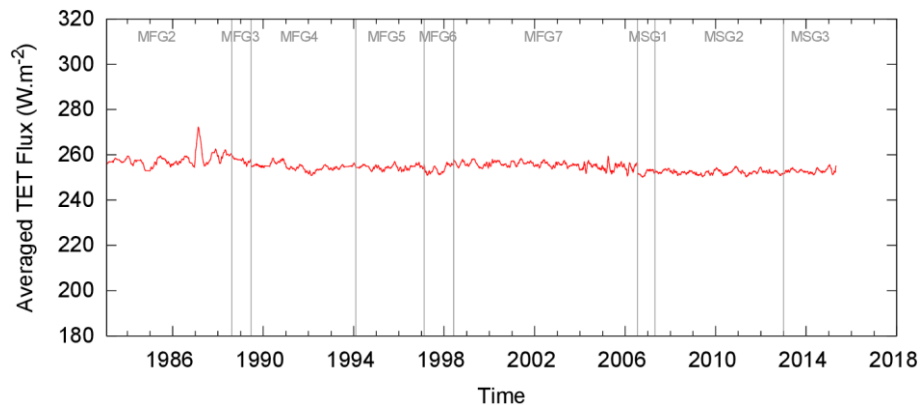


Figure 40: Time series of TET fluxes averaged over the whole Meteosat disk.

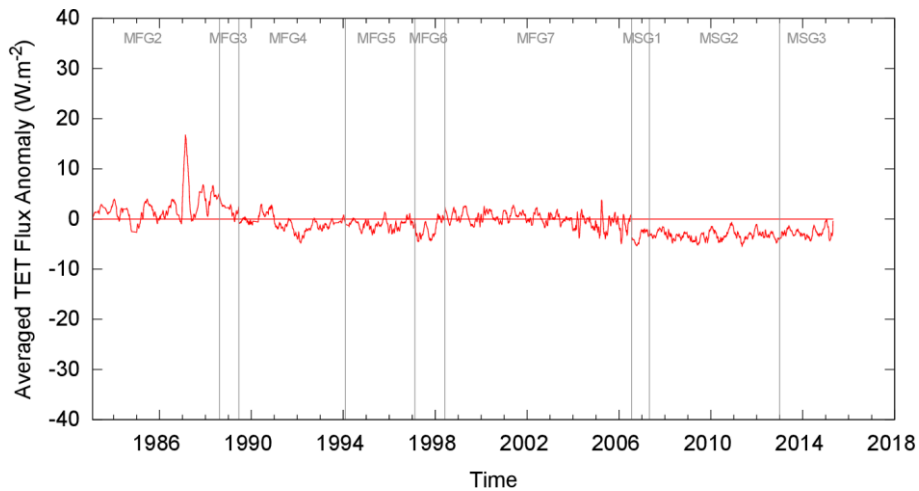


Figure 41: Time series of anomalies for the TET fluxes averaged over the whole Meteosat disk. The anomalies are obtained by subtracting the average TET flux (straight line) from the time series.

5.1.9 Discussion of TET stability results and absolute level

From the (somewhat contradicting) results presented in the previous sections it is not possible to provide a single value that would represent the stability of the TET products over the full data record extend. It is however obvious that the stability is far from the optimal and target requirements (0.3 and 0.6 W/m²/decade, resp.). On the other hand, most of the results are consistent with a stability better than the threshold value of 4 W/m²/decade (for the MM products). The main argument in support of this is the comparison of the DM and MM products with the HIRS OLR CDR (Daily/Monthly).

Table 6 gives a summary of the averaged biases, expressed in W.m⁻², of the MM TET products per satellite wrt to several data records as well as the difference between the maximum and minimum values.

Table 6 : Averaged biases (in W.m⁻²) of the MM TET products per satellite.

	CERES EBAF	HIRS OLR CDR (Monthly)	ERBS WFOV CERES	ISCCP FD	Averaged all-sky flux anomaly
MFG2	-	-1.6	-3.2	4.2	3.1
MFG3	-	-3.2	-3.9	2.3	2.4
MFG4	-	-3.4	-5.7	2.0	-0.3
MFG5	-	-3.5	-6.3	0.5	-0.4
MFG6	-	-3.2	-6.6	0.4	-1.3
MFG7	-4.9	-3.9	-4.7	-0.2	0.4

MSG1	-4.8	-4.0	-4.8	-	-1.9
MSG2	-4.4	-3.7	-4.4	-	-1.9
MSG3	-4.8	-4.0	-4.8	-	-1.3
(max-min)	0.5	2.4	3.4	4.4	5.0

Concerning the absolute level, the TET fluxes are significantly lower than the EBAF (-4.9 W/m²), SYN1deg-Day (-4.3 W/m²) and the HIRS OLR CDR - Daily (-3.1 W/m²). This is the consequence of using the GERB thermal fluxes as reference for the NB to BB regressions.

5.2 Accuracy of the monthly mean TET products

5.2.1 Comparison with CERES EBAF

To estimate the accuracy of the MM TET products, the RMS difference (bias corrected) with respect to CERES EBAF is computed for each month from March 2000 to March 2015. As it can be seen in Figure 42, the RMS difference, indicated by the red dotted line, is about 2.6 W.m⁻² which lies between the target (2 W.m⁻²) and threshold (4 W.m⁻²) accuracies.

Most of the outliers in Figure 42 can be attributed to missing input Meteosat data (see section 5.2.3). However, some EBAF products are biased by extensively missing CERES observations during specific periods (Lee, 2014): August 2000, June 2001 and March 2002.

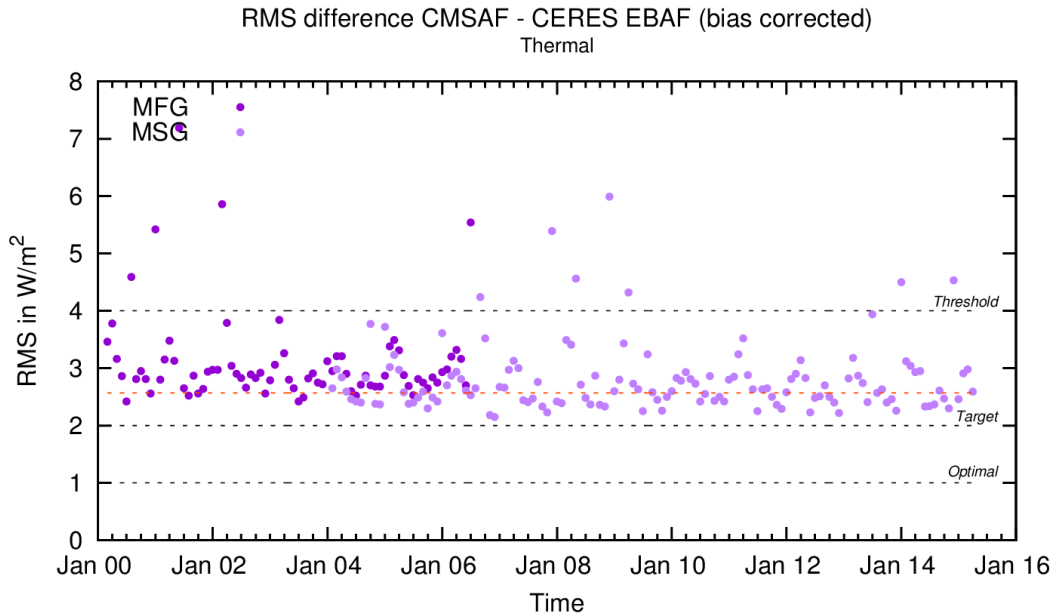


Figure 42: Time series of the RMS difference (bias corrected) between CM SAF MM and CERES EBAF TET products. The red dotted line gives the mean RMS over the time series. The optimal, target and threshold accuracies are indicated in black dotted lines.

Figures 43 and 44 show the products comparison for the best and the worst months in terms of RMS difference, respectively December 2006 and June 2001. The best case (Figure 43) does not show obvious regional error patterns in the VZA < 60° region. For grazing observations, a significant underestimation of the thermal flux is found over a large part of the tropical Indian Ocean which is attributed to underestimation of the anisotropy of the thermal radiance field. A high anisotropy is expected there due to semi transparent clouds

over warm ocean surface. In Figure 43, the mean RMS difference (bias corrected) is about 2 W/m^2 which is the target accuracy. In June 2001, the high RMS difference (7.2 W/m^2) is not due to missing Meteosat data but instead to extensively missing CERES observations biasing the EBAF product for this month.

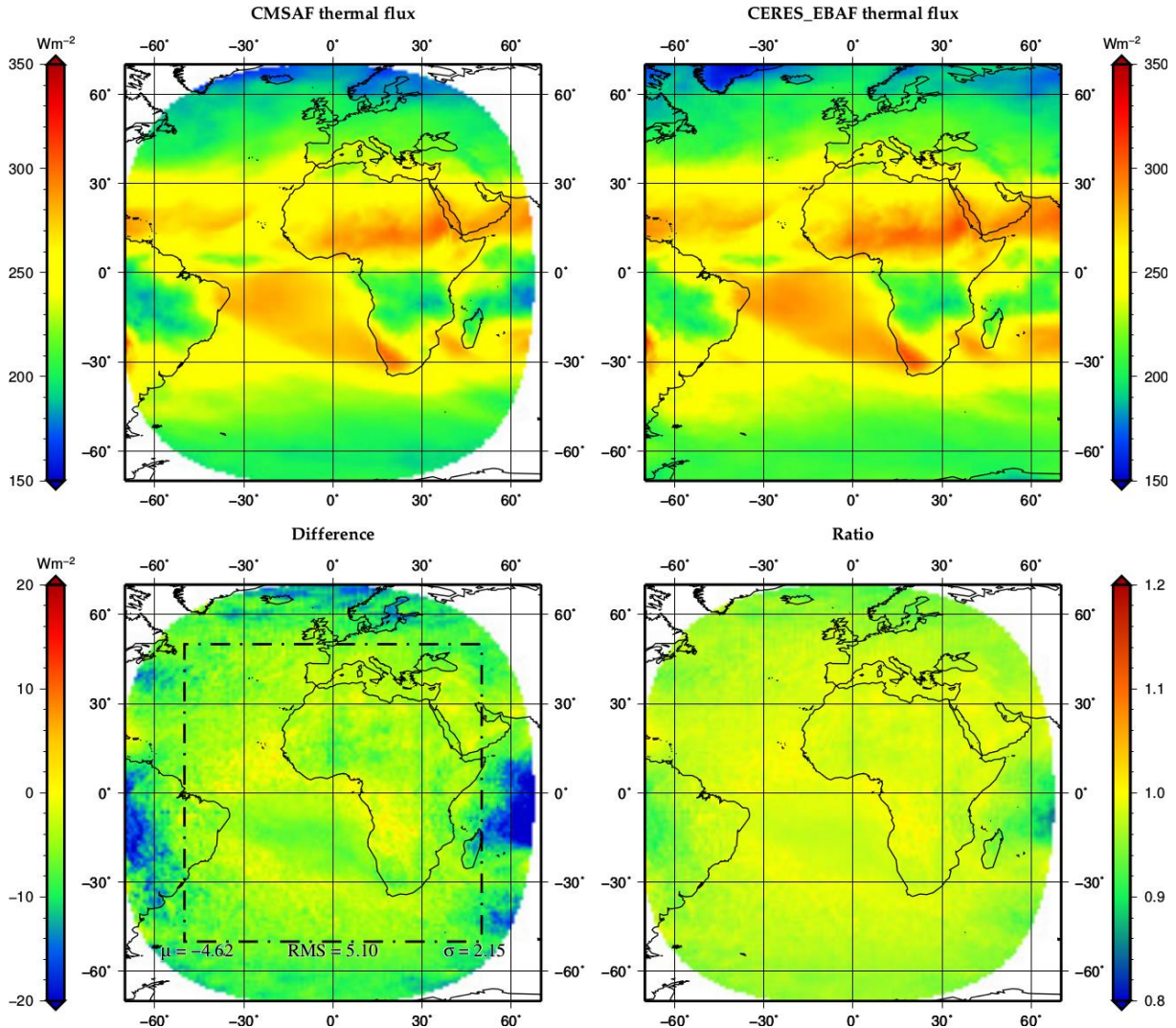


Figure 43: Comparison of CM SAF MM and CERES EBAF TET products for December 2006 (MSG1). Upper panels show the CM SAF (left) and CERES EBAF (right) products. Bottom images show the difference (left) and the ratio (right) of these products.

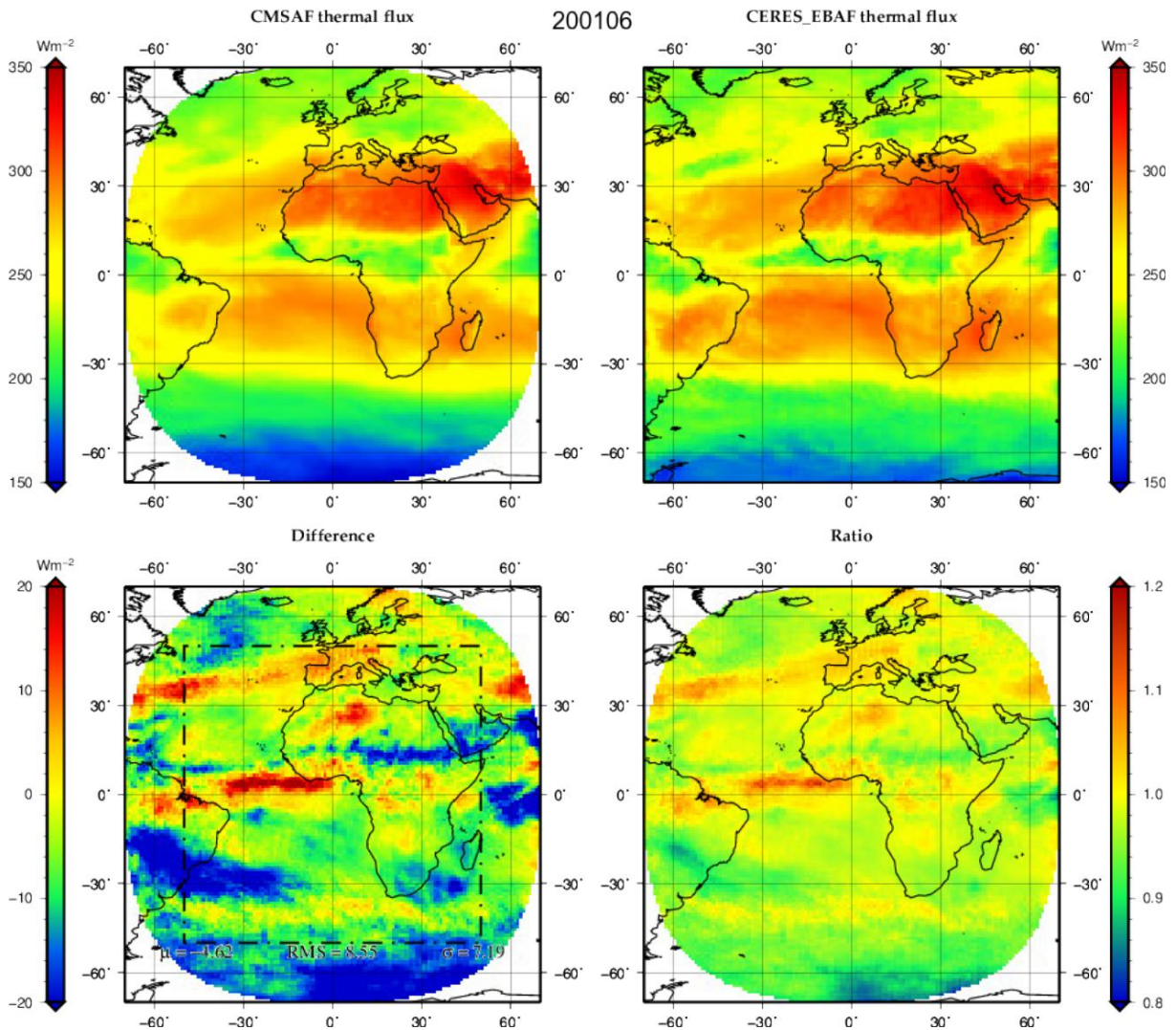


Figure 44: Comparison of CM SAF MM and CERES EBAF TET products for June 2001 (MFG7). Upper panels show the CM SAF (left) and CERES EBAF (right) products. Bottom images show the difference (left) and the ratio (right) of these products.

5.2.2 Comparison with HIRS OLR CDR

Figure 45 shows the time series of the RMS difference (bias corrected) with respect to the HIRS OLR CDR - Monthly. The mean RMS difference (about 3.1 W/m^2) is slightly higher than compared with CERES. The time series shows that the characteristics of the error remain constant over the data record extend with only 2 months violating the threshold requirements. These months are April and October 1986 which are biased by extensively missing input Meteosat observations (respectively 13 and 16 missing days).

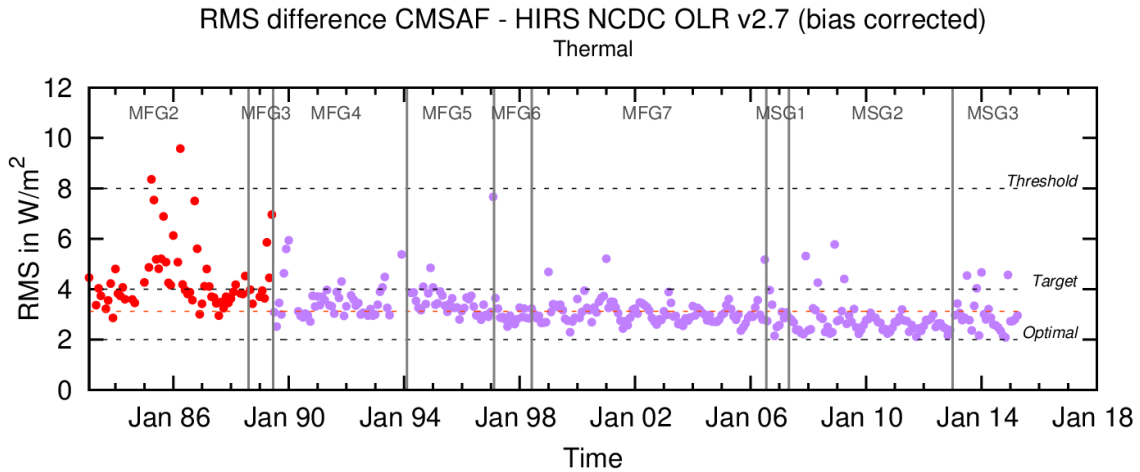


Figure 45: Time series of the RMS difference (bias corrected) between CM SAF MM TET and HIRS OLR CDR - Monthly products. The red dotted line gives the mean RMS over the time series. The optimal, target and threshold accuracies are indicated in black dotted lines.

Figures 46 and 47 show the products comparison for the best and the worst months in terms of RMS difference wrt the HIRS OLR CDR, respectively August 1997 and April 1986. In August 1997, only a few regional patterns are visible except a slight overestimation of the TET in the centre of the FOV (probably due to high semi-transparent clouds observed by Meteosat close to the nadir). The large RMS difference for the April 1986 products is explained by the 13 missing days affecting the CM SAF data record for this month.

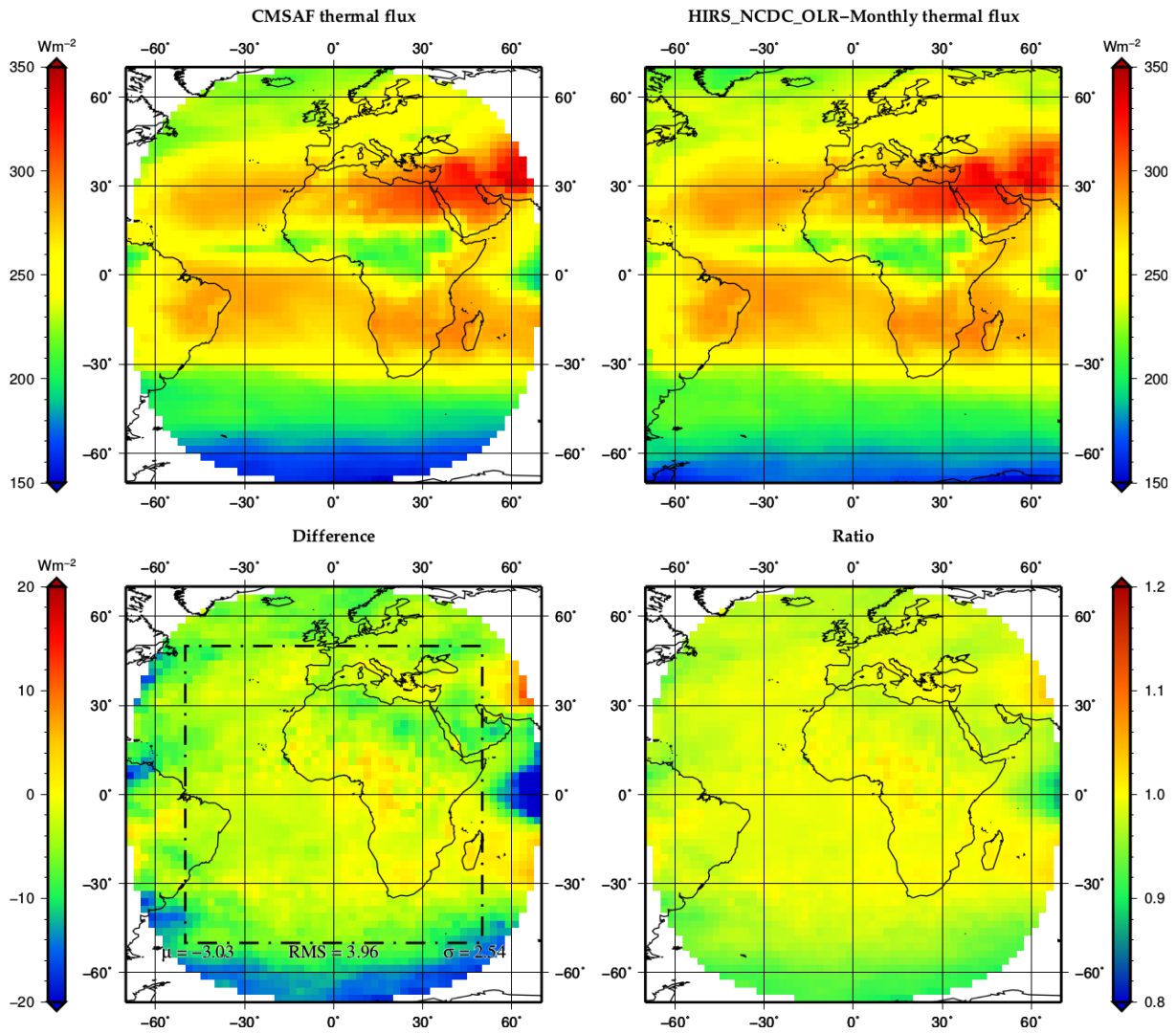


Figure 46: Comparison of CM SAF MM TET and HIRS OLR CDR - Monthly products for August 1997 (MFG6). Upper panels show the CM SAF (left) and HIRS OLR CDR (right) products. Bottom images show the difference (left) and the ratio (right) of these products.

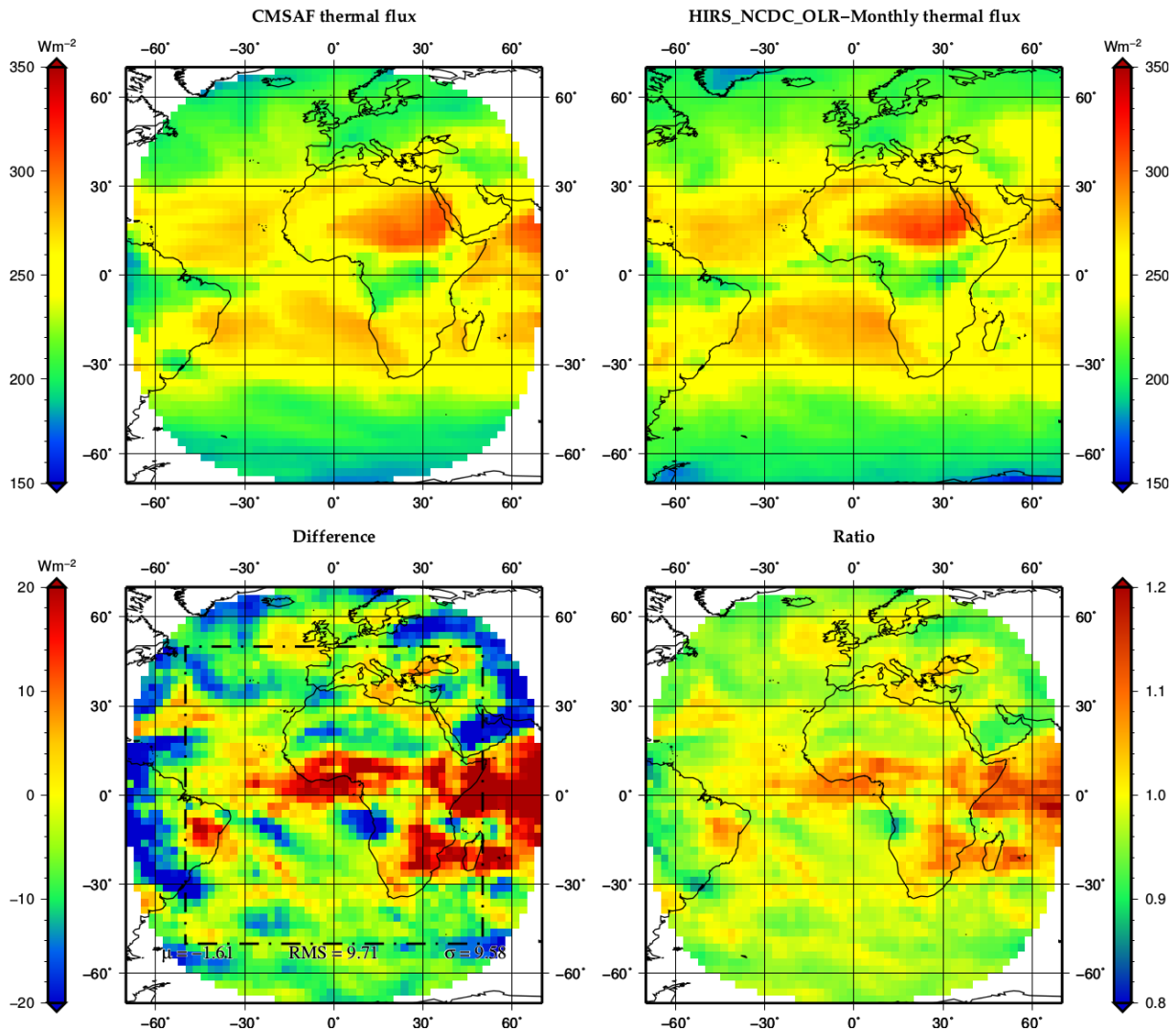


Figure 47: Comparison of CM SAF MM TET and HIRS OLR CDR - Monthly products for April 1986 (MFG2). Upper panels show the CM SAF (left) and HIRS OLR CDR (right) products. Bottom images show the difference (left) and the ratio (right) of these products.

5.2.3 Effect of missing data

Figure 48 shows the bias (left panel) and the RMS difference (right panel, bias corrected) of the CM SAF - EBAF comparison as a function of the number of days without Meteosat TET observations within the month (for instance due to decontamination or satellite failure). As observed in the right panel, the RMS difference increases more or less linearly with the number of missing days. The increase of RMS error in the MM TET products due to missing data is estimated to $0.2 \text{ W/m}^2/\text{day}$. This value is lower than the $0.3 \text{ W/m}^2/\text{day}$ observed for the TRS products.

	Scientific Validation Report TOA Radiation MVIRI/SEVIRI Data Record	Doc.No.: SAF/CM/RMIB/VAL/MET_TOA Issue: 1.1 Date: 05 October 2016
---	--	---

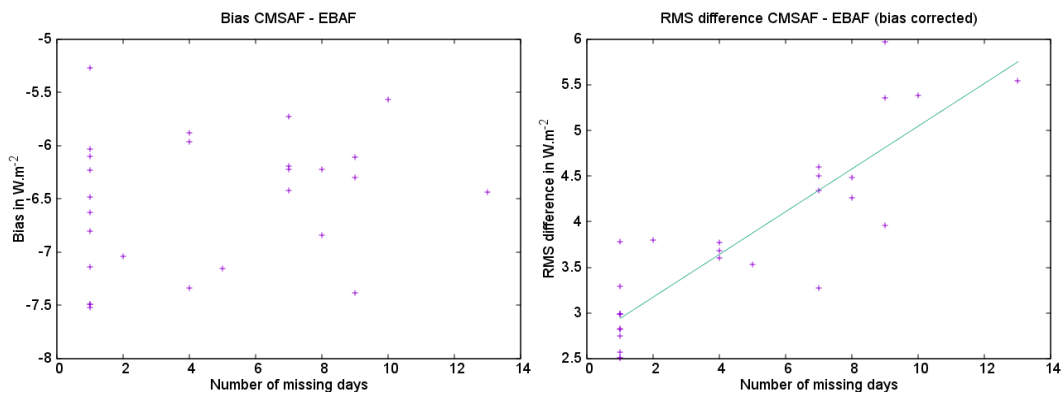


Figure 48: Bias (left) and RMS difference (right) of the CM SAF - EBAF comparison as a function of the number of days without Meteosat TET observations.

5.2.4 Discussion

From the comparison with EBAF, the accuracy on the MM TET is estimated at 2.6 W/m^2 , both for the MFG and MSG eras. This accuracy is consistent with the one of the MM TET products in the GERB data record (estimated at 2.0 W/m^2 , [RD5]), given the need of the additional NB to BB step in the MVIRI/SEVIRI datasets. The comparison with the HIRS OLR CDR provides evidence that this error level can be expected over the full data record extend.

The 2.6 W/m^2 error value, and the $0.2 \text{ W/m}^2/\text{day}$ increase in case of missing inputs, are reported in Table 8, in the summary.

5.3 Accuracy of the daily mean TET products

5.3.1 Comparison with CERES SYN1deg-Day

The RMS difference (bias corrected) with respect to CERES SYN1deg-Day for each day from March 2000 to March 2015 is shown in Figure 49. As for the MM products, the data before July 2002 (pre-Aqua) have slightly higher RMS values. Discarding this period, the RMS difference, indicated by the red dotted line, is about 5.0 W/m^2 which is between the target (4 W.m^{-2}) and threshold (8 W.m^{-2}) accuracies for this product [RD1]. Looking at the MFG/MSG overlap period (2004-2006) shows that the error characteristics are not dependent on whether MVIRI or SEVIRI is used as input. It should be noted that most of the days that are exceeding the threshold accuracy in 2000-2001 can be explained by extensively missing CERES observations biasing the SYN1deg-Day products for these days (Lee, 2014). In particular, it is the case for the periods: 6-18 August 2000, 15-30 June 2001 and 19-27 March 2002.

	Scientific Validation Report TOA Radiation MVIRI/SEVIRI Data Record	Doc.No.: SAF/CM/RMIB/VAL/MET_TOA Issue: 1.1 Date: 05 October 2016
---	--	---

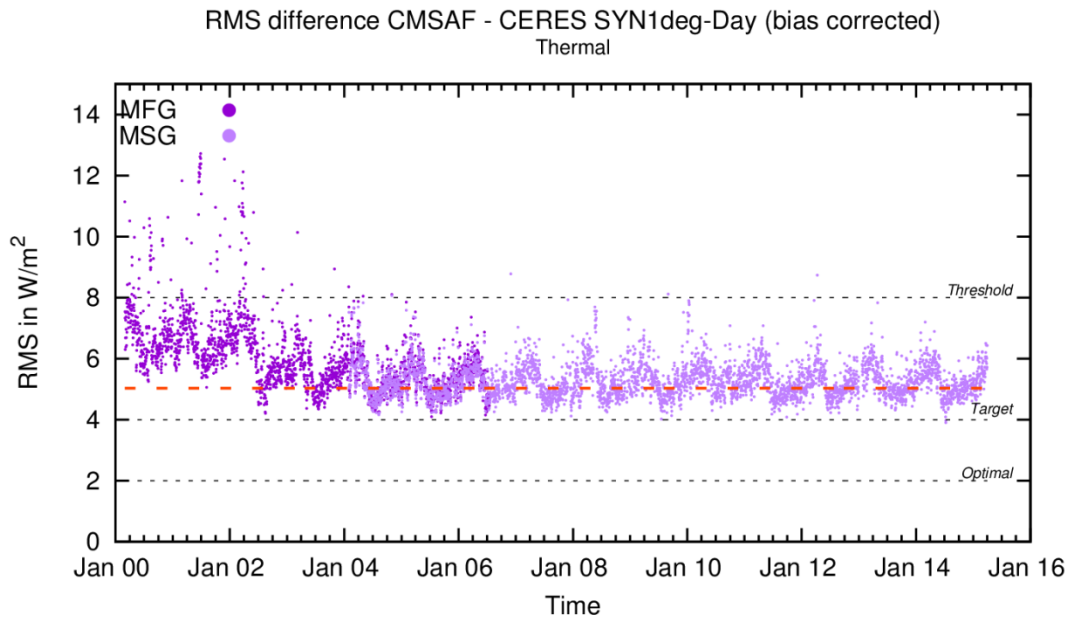


Figure 49: Time series of the RMS difference (bias corrected) between CM SAF DM and CERES SYN1deg-Day TET products. The red dotted line gives the mean RMS over the time series. The optimal, target and threshold accuracies are indicated in black dotted lines.

Figures 50 and 51 show the DM TET products comparison for the best and the worst days in terms of RMS difference, respectively the 10th July 2014 and the 13th March 2002. Figure 50 does not show obvious regional patterns of error. The mean RMS difference for this “best case” is 3.9 W/m² which is consistent with the 4 W/m² accuracy target. On the other hand, Figure 51 shows obvious artefacts that can be attributed to the CERES SYN1deg-Day product for this specific day.

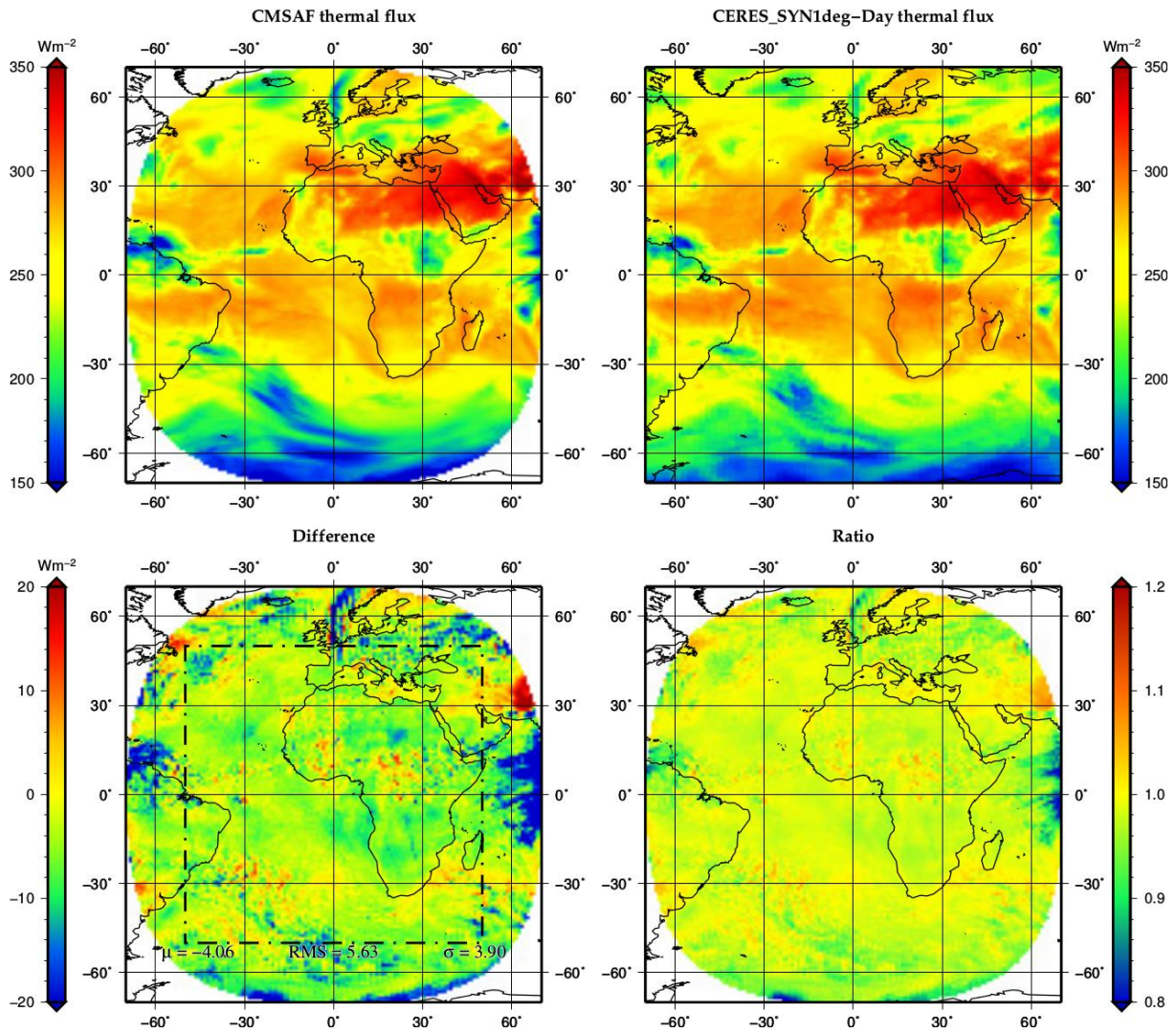


Figure 50: Comparison of CM SAF DM and CERES SYN1deg-Day TET products for the 10th July 2014 (MSG3). Upper panels show the CM SAF (left) and CERES SYN1deg-Day (right) products. Bottom images show the difference (left) and the ratio (right) of these products.

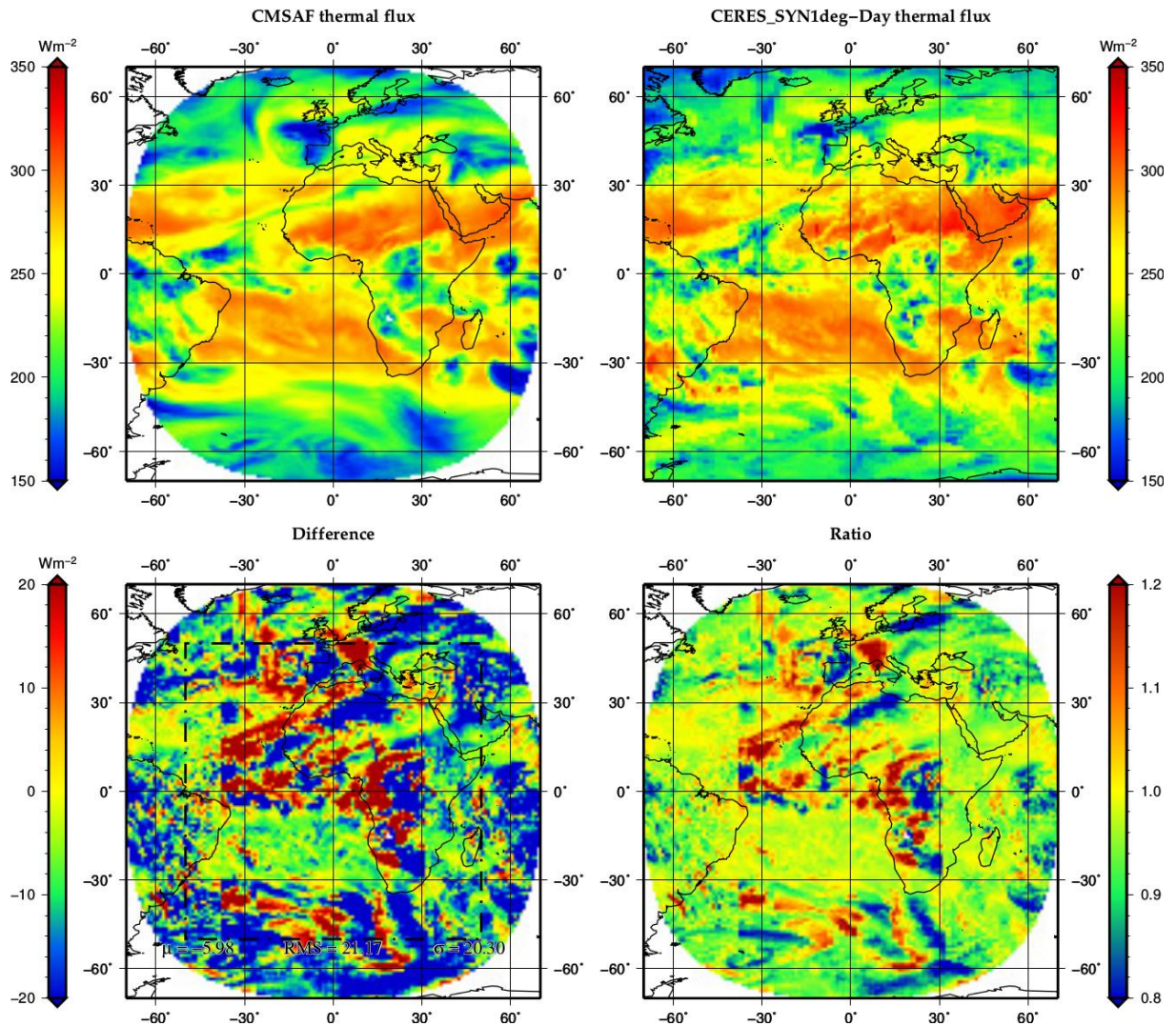


Figure 51: Comparison of CM SAF DM and CERES SYN1deg-Day TET products for the 13th March 2002 (MFG7). Upper panels show the CM SAF (left) and CERES SYN1deg-Day (right) products. Bottom images show the difference (left) and the ratio (right) of these products.

5.3.2 Comparison with HIRS OLR CDR - Daily

Figure 52 shows the time series of the RMS difference (bias corrected) between the CM SAF TET DM products and the daily HIRS OLR CDR. The RMS difference is about 4.2 W/m² which is significantly better than in the comparison with CERES SYN1deg-Day (5.0 W/m²). In addition, the time series shows that the characteristics of the error remain constant over the data record extend, except an increase of the error during the MFG2 period (but still fulfilling generally the threshold requirements).

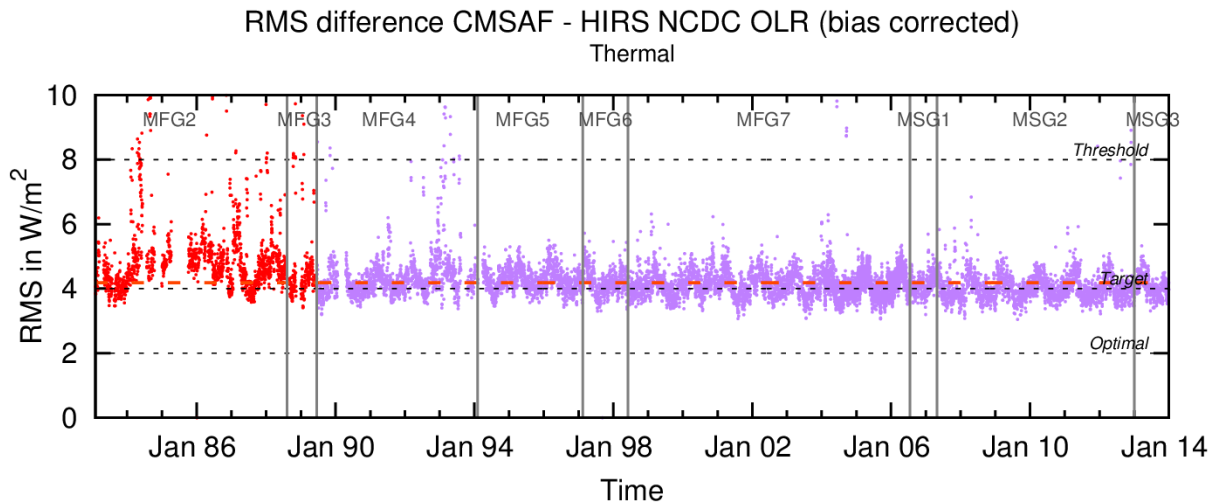


Figure 52: Time series of the RMS difference (bias corrected) between CM SAF DM and HIRS OLR CDR - Daily products. The red dotted line gives the mean RMS over the time series.

5.3.3 Effect of missing data

The methodology described in section 3.2.3 is followed to quantify the (additional) error that can affect the DM product when some input Meteosat observations are missing. Figure 53 shows the bias (left panel) and RMS (right panel, bias corrected) of the differences with respect to the CERES SYN1deg-Day products as a function of the number of missing MVIRI repeat cycles of acquisition. It should be noted that the days with more than 5 (MVIRI) or 11 (SEVIRI) successive missing input data were not considered because the interpolation of missing data can not exceed 3 hours in the daily processing. No DM product is issued in the data record in these cases.

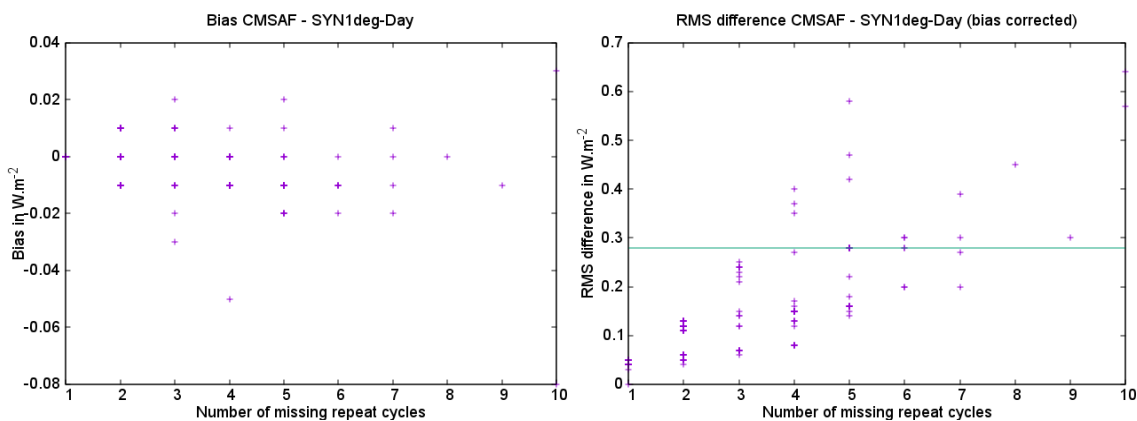


Figure 53: Bias (left) and RMS (right, bias corrected) of the CM SAF - SYN1deg-Day comparison as a function of the number of repeat cycles of acquisition without Meteosat TET observations.

The maximum RMS error introduced in the DM products is 0.64 W/m^2 while the bias remains negligible for a varying number of missing images. For a large majority (0.9 percentile) of the cases, the increase of RMS error due to missing data is less than 0.3 W/m^2 and it is proposed to adopt this value as representative of the effect of missing images on the DM TET products. Obviously, most of the days in the data record do not have any missing input and have therefore no associated error.

	Scientific Validation Report TOA Radiation MVIRI/SEVIRI Data Record	Doc.No.: SAF/CM/RMIB/VAL/MET_TOA
		Issue: 1.1
		Date: 05 October 2016

5.3.4 Discussion

From the comparison with the HIRS OLR CDR - Daily, the accuracy on the DM TET is estimated at 4.2 W/m^2 both for the MFG and MSG eras (with slightly higher values during the MFG2 period). This accuracy is consistent with the one of the DM TET products in the GERB data record (estimated at 3.6 W/m^2 , [RD5]), given the need of the additional NB to BB step in the MVIRI/SEVIRI data records. The 4.2 W/m^2 error value, and the 0.3 W/m^2 increase in case of missing inputs, are reported in Table 8, in the summary.

5.4 Accuracy of the monthly mean diurnal cycle TET products

5.4.1 Comparison with CERES SYN1deg-M3Hour

The overall accuracy of the CM SAF MMDC products is estimated by computing the RMS difference (bias corrected) against the CERES SYN1deg-M3Hour products for each monthly diurnal cycle, in 3-hours intervals, from March 2000 to March 2015. As it can be seen in Figure 54, the overall mean RMS difference for each time interval lies under the target accuracy of 4 W.m^{-2} . The 3 peak values reaching the threshold accuracy of 8 W.m^{-2} that are observed in the beginning of the time series, are due to extensively missing CERES observations biasing the CERES SYN1deg-M3Hour products for these months (i.e. August 2000, June 2001 and March 2002; Lee, 2014). The other peaks are mainly due to a high number of missing Meteosat images. For example, the following months are affected by numerous missing data: September 2006 (8 missing days), December 2007 (10 missing days), May 2008 (7 missing days), December 2008 (9 missing days) and April 2009 (7 missing days). The time series shows that the error characteristics remain stable during the July 2002 – 2015 period and are similar for the MFG and MSG satellites. A higher RMS is observed when the CERES SYN1deg-M3Hour products are based on Terra only. Discarding this period, an averaged RMS error of 3.5 W/m^2 is observed for this product.

The magnitude of the error is (slightly) higher for the “warm” intervals (e.g. 12 and 15 UTC) than for the “cold” intervals (nighttime, early morning). This is explained by a higher spatial and temporal variability of the OLR in the afternoon due to surface warming and convection. During the night, the OLR is more constant in space and time.

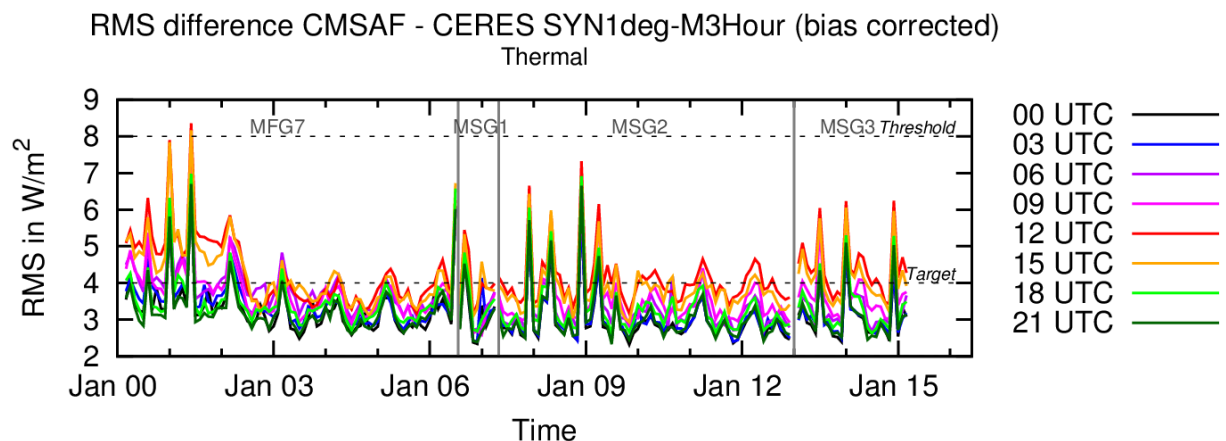


Figure 54: Time series of the RMS difference (bias corrected) between CM SAF MMDC and CERES SYN1deg-M3Hour TET products. The target and threshold accuracies are indicated in black dotted lines.

Figures 55 and 56 show the 12 UTC (i.e. the 3-hours interval [12-15] UTC) comparison for the best and the worst months in terms of RMS difference, respectively November 2004 and June 2001. Figure 55 does not show any obvious regional pattern of error. The bias-

corrected RMS difference for the “best case” is 3.1 W.m^{-2} which is well within the targeted accuracy of 4 W.m^{-2} . The large RMS value (about 8.4 W.m^{-2}) for June 2001 (see Figure 56) is due to a high number of missing CERES observations biasing the CERES SYN1deg-M3Hour product for this month.

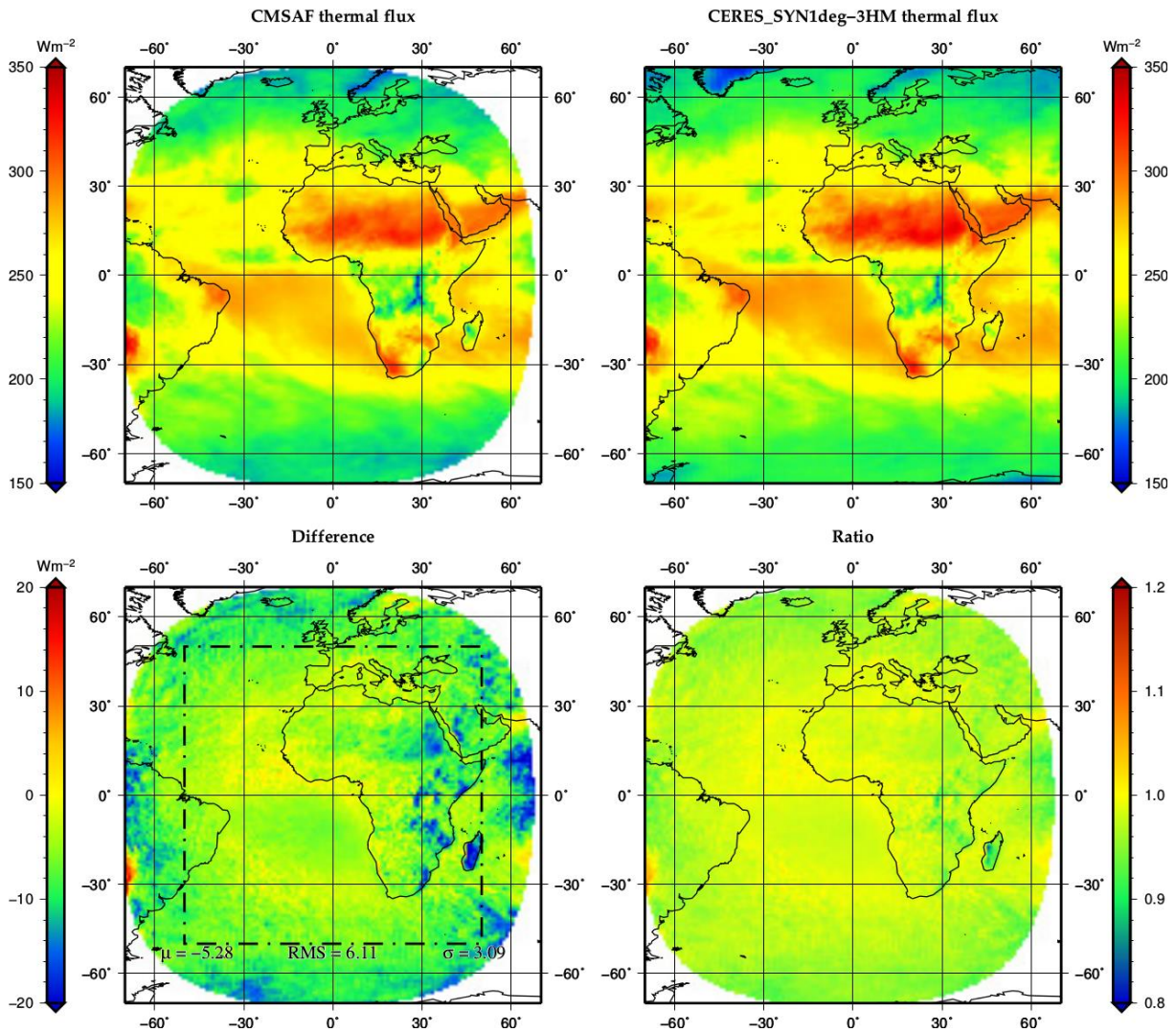


Figure 55: Comparison of CM SAF MDMC and CERES SYN1deg-M3Hour TET products for November 2004 (MSG1) at [12-15] UTC. Upper panels show the CM SAF (left) and CERES SYN1deg-M3Hour (right) products. Bottom images show the difference (left) and the ratio (right) of these products.

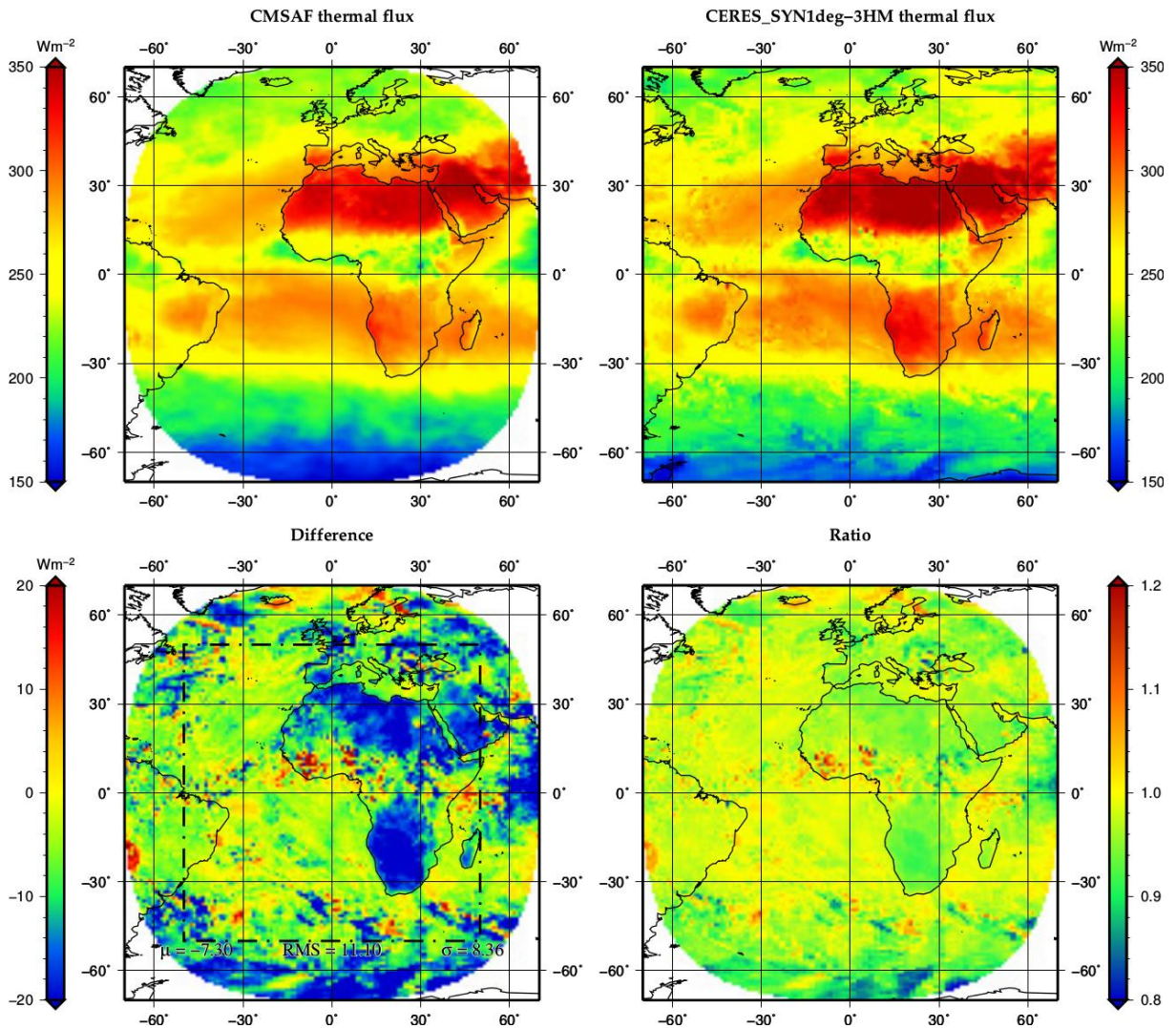


Figure 56: Comparison of CM SAF MDC and CERES SYN1deg-M3Hour TET products for June 2001 (MFG7) at [12-15] UTC. Upper panels show the CM SAF (left) and CERES SYN1deg-M3Hour (right) products. Bottom images show the difference (left) and the ratio (right) of these products.

5.4.2 Effect of missing data

Figure 57 shows the bias (left panel) and the RMS difference (right panel, bias corrected) of the CM SAF - SYN1deg-M3Hour comparison as a function of the number of days without Meteosat TET observations within the month (for instance due to decontamination or satellite failure). The various monthly 3-hourly averaged fluxes are shown in different colours. As observed in the right panel, the RMS difference between CM SAF and CERES SYN1deg-M3Hour increases more or less linearly with the number of missing days within the month.

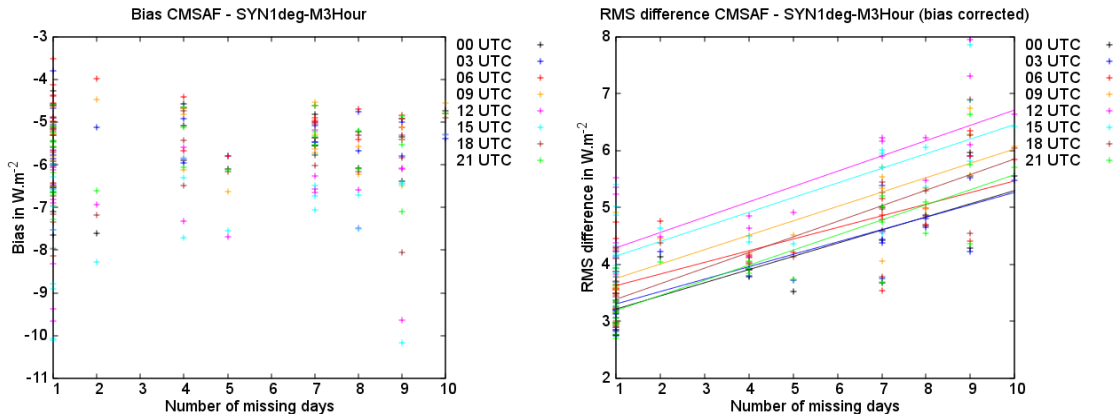


Figure 57: Bias (left) and RMS difference (right, bias corrected) of the CM SAF - SYN1deg-M3Hour comparison as a function of the number of days without Meteosat TET observations.

Table 7 gives the individual values of the increase of the RMS error as a function of the number of missing days and the intercept values. In the worst case, the increase of RMS error due to missing data in the MMDC TET product is estimated at $0.3 \text{ W/m}^2/\text{day}$.


Table 7: Increase of the RMS error of the CM SAF - SYN1deg-M3Hour TET comparison as a function of the number of missing days and intercept values, for each 3-hours time interval.

3-hourly interval	RMS error increase ($\text{W/m}^2/\text{day}$)	Intercept (W/m^2)
00 UTC	0.2	3.0
03 UTC	0.2	3.1
06 UTC	0.2	3.4
09 UTC	0.3	3.5
12 UTC	0.3	4.0
15 UTC	0.3	3.9
18 UTC	0.3	3.1
21 UTC	0.3	2.9

5.4.3 Discussion

The accuracy on the MMDC TET products is estimated as about $3.5 + 0.3 N_{\text{day}} \text{ W.m}^{-2}$ both for the MFG and MSG eras. Those values are reported in Table 8, in the summary.

This accuracy is not the one of the products at full spatial (0.05° lat-lon) and temporal (1-hourly interval) resolution but instead of the products averaged in 1° spatial grid boxes and for 3-hourly intervals.

	Scientific Validation Report TOA Radiation MVIRI/SEVIRI Data Record	Doc.No.: SAF/CM/RMIB/VAL/MET_TOA
		Issue: 1.1
		Date: 05 October 2016

6 Summary of the errors

Three sources of error have been identified in section 3.2 as affecting the MVIRI/SEVIRI data record: the stability error, the processing error and the missing data error. Table 8 gives a summary of the estimated errors for each of these sources respectively for the monthly mean (MM), daily mean (DM) and monthly mean diurnal cycle (MMDC) products.

Table 8: Errors affecting the monthly mean, daily mean and monthly mean diurnal cycle products in CM-23311 (TRS) and CM-23341 (TET).

Error sources	MM		DM		MMDC	
	TRS	TET	TRS	TET	TRS (midday) (3)	TET
Stability error	Stability of all the products better than 4 W/m^2 (max-min) except for the TET during a given period in 1987 (MFG2) (4) <i>(see § 4.1 (TRS) and 5.1 (TET))</i>					
Processing error (at 1 std. dev.)	3.6 W/m^2 <i>(see § 4.2)</i>	2.6 W/m^2 <i>(see § 5.2)</i>	6.5 W/m^2 <i>(see § 4.3)</i>	4.2 W/m^2 <i>(see § 5.3)</i>	11.0 W/m^2 <i>(see § 4.4)</i>	3.5 W/m^2 <i>(see § 5.4)</i>
Additional error due to missing input data (1)(2)	$0.3 \text{ W/m}^2/\text{day}$ <i>(see §4.2.4)</i>	$0.2 \text{ W/m}^2/\text{day}$ <i>(see §5.2.3)</i>	0.5 W/m^2 <i>(see §4.3.2)</i>	0.3 W/m^2 <i>(see §5.3.3)</i>	$0.7 \text{ W/m}^2/\text{day}$ <i>(see §4.4.2)</i>	$0.3 \text{ W/m}^2/\text{day}$ <i>(see §5.4.2)</i>

Remarks

1. The reported errors due to missing data do not affect the products without missing data. For the DM products, the missing data error is the 0.9 percentile of the error over days affected by missing repeat cycles of image acquisition.
2. The missing data error must be added to the processing error (not a root mean summation of these errors).
3. The reported errors for the MMDC of the TRS are estimated for the time intervals with the highest illumination of the Meteosat FOV (e.g. [11-12] and [12-13] UTC).
4. Those months are January, February and March 1987.

	Scientific Validation Report TOA Radiation MVIRI/SEVIRI Data Record	Doc.No.: SAF/CM/RMIB/VAL/MET_TOA Issue: 1.1 Date: 05 October 2016
---	--	---

7 Conclusion

Validation of the CM-23311 and CM-23341 data records is mainly performed by intercomparison with the CERES products. The quality of the early part of the data records is verified against other data records such as the HIRS OLR CDR (Daily and Monthly), the ERBS WFOV-CERES (DEEP-C) and the ISCCP FD data record. The comparison with multiple sources allows attributing differences, such as stability problems, to one of these sources.

The validation process indicates that the CM SAF MVIRI/SEVIRI data records fulfil the threshold requirements defined in the Product Requirement Document (PRD, [AD2]). Moreover, the target requirements are fulfilled for most of the products and periods in the data records.

The radiometric stability of the products has been verified by computing the time series of the bias against several data records over the full data record extent. In general, the systematic error (i.e. the absolute calibration error) shows a relatively good stability in time without sharp transition between satellites and generations of instruments, for both TRS and TET fluxes. In addition, no instrumental drift (i.e. ageing effect) is apparent. Almost all the products fulfil the threshold requirements in terms of stability that were defined in the PRD. As exception, 3 months of Meteosat-2 TET fluxes, from January to March 1987, show a radiometric level that is likely to differ from the remaining of the data record by more than the 4 W/m² threshold requirement. These months will be flagged and the users will be warned via the PUM.

The accuracy of the different products is also investigated and proved to remain stable over the full data record extent. From comparison with CERES EBAF, the RMS error of the monthly mean TRS and TET fluxes is estimated at 3.6 W/m² and 2.6 W/m², respectively. From comparison with the CERES SYN1deg-Day products, the RMS error of the daily mean TRS is estimated at 6.5 W/m². From comparison with the HIRS OLR CDR - Daily, the RMS error of the daily mean TET is estimated at 4.2 W/m². For both these products (MM and DM), the targeted accuracy is met for the TRS fluxes while the threshold accuracy is met for the TET fluxes. For the MMDC products, the accuracy is estimated at 11.0 W/m² for the TRS (daytime) and at 3.5 W/m² for the TET. This time, the targeted accuracy is met for the TET fluxes while the threshold accuracy is met for the TRS fluxes.

	Scientific Validation Report TOA Radiation MVIRI/SEVIRI Data Record	Doc.No.: SAF/CM/RMIB/VAL/MET_TOA Issue: 1.1 Date: 05 October 2016
---	--	---

8 References

- Allan, R.P., Liu, C., Loeb, N.G., Palmer, M.D., Roberts, M., Smith, D., & Vidale, P.L. (2014). Changes in global net radiative imbalance 1985–2012. *Geophysical research letters*, 41(15), 5588-5597.
- N. Clerbaux, J.E. Russell, S. Dewitte, C. Bertrand, D. Caprion, B. De Paepe, L. Gonzalez Sotelino, A. Ipe, R. Bantges, H.E. Brindley (2009): Comparison of GERB instantaneous radiance and flux products 2 with CERES Edition-2 data, *Remote Sensing of Environment*, 113, 102-114.
- Dewitte, S., Gonzalez, L., Clerbaux, N., Ipe, A., & Bertrand, C. (2008). The Geostationary Earth Radiation Budget Edition 1 data processing algorithms. *Advances in Space Research*, 41, 1906-1913.
- Doelling, D.R., Young, D.F., Wielicki, B.A., Wong, T., & Keyes, D.F. (2006). The newly released 5-year Terra-based monthly CERES radiative flux and cloud product. *In Preprints, 12th Conf. on Atmospheric Radiation, Madison, WI, Amer. Meteor. Soc* (Vol. 9).
- Doelling, D. R., Loeb, N. G., Keyes, D. F., Nordeen, M. L., Morstad, D., Nguyen, C., ... & Sun, M. (2013). Geostationary enhanced temporal interpolation for CERES flux products. *Journal of Atmospheric and Oceanic Technology*, 30(6), 1072-1090.
- Ellingson, R.G., Lee, H.-T., Yanuk, D., & Gruber, A. (1994). Validation of a technique for estimating outgoing longwave radiation from HIRS radiance observations. *Journal of Atmospheric and Oceanic Technology*, 11(2), 357-365.
- Harries, J., Russell, J., Hanafin, J., Brindley, H., Futyran, J., Rufus, J., Kellock, S., Matthews, G., Wrigley, R., Last, A., Mueller, J., Mossavati, R., Ashmall, J., Sawyer, E., Parker, D., Caldwell, M., Allan, P., Smith, A., Bates, M., Coan, B., Stewart, B., Lepine, D., Cornwall, L., Corney, D., Ricketts, M., Drummond, D., Smart, D., Cutler, R., Dewitte, S., Clerbaux, N., Gonzalez, L., Ipe, A., Bertrand, C., Joukoff, A., Crommelynck, D., Nelms, N., Llewellyn-Jones, D., Butcher, G., Smith, G., Szewczyk, Z., Mlynczak, P., Slingo, A., Allan, R., & Ringer, M. (2005). The Geostationary Earth Radiation Budget projet. *Bulletin of the American Meteorological Society*, 86(7), 945- 960.
- Lee, H.-T., Gruber, A., Ellingson, R.G., & Laszlo, I. (2007). Development of the HIRS outgoing longwave radiation climate dataset. *Journal of Atmospheric and Oceanic Technology*, 24(12), 2029-2047.
- Lee, H.-T. (2014). HIRS Daily OLR Climate Data Record Development and Evaluation, *CERES Science Team Meeting, April 22-24, 2014 Hampton, VA*.
- Lee, H.-T., Schreck, C. J., & Knapp, K. R. (2014). Generation of the Daily OLR Climate Data Record. *2014 EUMETSAT Meteorological Satellite Conference, 22–26 September 2014, Geneva, Switzerland*.
- Loeb, N.G., Wielicki, B.A., Doelling, D.R., Smith, G.L., Keyes, D.F., Kato, S., Smith, N.M., & Wong, T. (2009). Towards optimal closure of the earth's top-of-atmosphere radiation budget. *Journal of Climate*, 22, 748-766.
- Loeb, N.G., Lyman, J.M., Johnson, G.C., Allan, R.P., Doelling, D.R., Wong, T., Soden, B.J., & Stephens, G. L. (2012). Observed changes in top-of-the-atmosphere radiation and upper-ocean heating consistent within uncertainty. *Nature Geoscience*, 5(2), 110-113.
- Loveland, T.R., Reed, B.C., Brown, J.F., Ohlen, D.O., Zhu, Z., Yang, L.W.M.J., & Merchant, J.W. (2000). Development of a global land cover characteristics database and IGBP

	Scientific Validation Report TOA Radiation MVIRI/SEVIRI Data Record	Doc.No.: SAF/CM/RMIB/VAL/MET_TOA Issue: 1.1 Date: 05 October 2016
---	--	---

DISCover from 1 km AVHRR data. *International Journal of Remote Sensing*, 21(6-7), 1303-1330.

Minnis, P., Harrison, E. F., Stowe, L. L., Gibson, G. G., Denn, F. M., Doelling, D. R., & Smith, W. L. (1993). Radiative climate forcing by the Mount Pinatubo eruption. *Science*, 259(5100), 1411-1415.

Schmetz, J., Pili, P., Tjemkes, S., & Just, D. (2002). An introduction to Meteosat second generation (MSG). *Bulletin of the American Meteorological Society*, 83(7), 977.

Townshend, J., Justice, C., Skole, D., Malingreau, J.P., Cihlar, J., Teillet, P., Sadowski, F., & Ruttenberg, S. (1994). The 1-km AVHRR global data set: needs of the International Geosphere Biosphere Program. *International Journal for Remote Sensing*, 15, 3319-3332.


Wielicki, B.A., Barkstrom, B.R., Harrison, E.F., Lee III, R.B., Smith, G.L., & Cooper, J.E. (1996). Clouds and the Earth's Radiant Energy System (CERES): An Earth Observing System Experiment. *Bulletin of the American Meteorological Society*, 77, 853-868.

Wielicki, B.A., Wong, T., Allan, R.P., Slingo, A., Kiehl, J.T., Soden, B.J., Gordon, C.T., Miller, A.J., Yang, S.K., Randall, D.A., Robertson, F., Susskind, J., & Jacobowitz, H. (2002). Evidence for large decadal variability in the tropical mean radiative energy budget. *Science*, 295(5556), 841-844.

Wild, M., Folini, D., Schär, C., Loeb, N., Dutton, E. G., & König-Langlo, G. (2013). The global energy balance from a surface perspective. *Climate dynamics*, 40(11-12), 3107-3134.

Wong, T., Wielicki, B. A., Lee III, R. B., Smith, G. L., Bush, K. A., & Willis, J. K. (2006). Reexamination of the observed decadal variability of the earth radiation budget using altitude-corrected ERBE/ERBS nonscanner WFOV data. *Journal of Climate*, 19(16), 4028-4040.

Zhang, Y., Rossow, W.B., Lacis, A.A., Oinas, V., & Mishchenko, M.I. (2004). Calculation of radiative fluxes from the surface to top of atmosphere based on ISCCP and other global data sets: Refinements of the radiative transfer model and the input data. *Journal of Geophysical Research: Atmospheres*, 109(D19).

	Scientific Validation Report TOA Radiation MVIRI/SEVIRI Data Record	Doc.No.: SAF/CM/RMIB/VAL/MET_TOA Issue: 1.1 Date: 05 October 2016
---	--	---

9 Glossary

AD	Applicable Document
ADM	Angular Dependency Model
ATBD	Algorithm Theoretical Basis Document
AVHRR	Advanced Very High Resolution Radiometer
BB	Broadband
BSRN	Baseline Surface Radiation Network
CDOP	Continuous Development and Operations Phase
CDR	Climate Data Record
CERES	Cloud and the Earths Radiant Energy System
CLAAS	CLoud property dAtAset using SEVIRI
CM SAF	Satellite Application Facility on Climate Monitoring
CS	Clear-Sky
DEEP-C	Diagnosing Earth's Energy Pathways in the Climate system
DGCDD	Dataset Generation Capability Description Document
DM	Daily Mean
DWD	Deutscher Wetterdienst (German MetService)
EBAF	Energy Balanced And Filled
ECMWF	European Centre for Medium Range Forecast
ECV	Essential Climate Variable
ERA-Interim	European Centre for Medium-range Weather Forecasts Interim reanalysis
ERB	Earth Radiation Budget
ERBE	Earth Radiation Budget Experiment
ERBS	Earth Radiation Budget Satellite
EUMETSAT	European Organisation for the Exploitation of Meteorological Satellites
FCDR	Fundamental Climate Data Record
FMI	Finnish Meteorological Institute
FOV	Field Of View
GERB	Geostationary Earth Radiation Budget instrument
GISS	Goddard Institute for Space Studies
GSICS	Global Space-based Inter-Calibration System

GSIP	GOES Surface and Insolation Products
HIRS	High-resolution Infrared Radiation Sounder
IGBP	International Geosphere Biosphere Program
IOP	Initial Operations Phase
IR	Infrared
ISCCP	International Satellite Cloud Climatology Project
KNMI	Koninklijk Nederlands Meteorologisch Instituut
LW	Longwave
MeteoSwiss	Meteorological Service of Switzerland
MFG	Meteosat First Generation
MM	Monthly Mean
MMDC	Monthly Mean Diurnal Cycle
MSG	Meteosat Second Generation
MVIRI	Meteosat Visible and InfraRed Imager
NB	Narrowband
NCDC	National Climatic Data Center
NCEI	National Centers for Environmental Information
NMHS	National Meteorological and Hydrological Services
NOAA	National Oceanic and Atmospheric Administration
OLR	Outgoing Longwave Radiation
PRD	Product Requirement Document
PUM	Product User Manual
RD	Reference Document
RMIB	Royal Meteorological Institute of Belgium
RMS	Root Mean Square
SAF	Satellite Application Facility
SARAH	Surface Solar Radiation DataSet - Heliosat
SEVIRI	Spinning Enhanced Visible and Infrared Imager
SMHI	Swedish Meteorological and Hydrological Institute
SW	Shortwave
SZA	Solar Zenith Angle
TET	TOA Emitted Thermal
TOA	Top Of the Atmosphere

TIS	Top of the Atmosphere Incoming Solar
TOA	Top Of the Atmosphere
TOT	Total
TRS	Top of the Atmosphere Reflected Solar
UKMO	UK Met-Office
VIS	Visible
VZA	Viewing Zenith Angle
WFOV	Wide Field Of View
WV	Water Vapour